CASE STUDY OF BIRD STREAMER CAUSED TRANSIENT EARTH FAULTS ON A 275 KV TRANSMISSION GRID

by

Paul Taylor

This thesis was submitted to the University of Natal in fulfilment of the requirements for a Master's degree in Electrical Engineering.

DECLARATION

I, Paul Taylor, declare that the work contained in this thesis is my own and has not been submitted, in part or otherwise, to another university.

Paul Taylor

25 May 2001

ABSTRACT

This thesis discusses the results of an investigation that was initiated in January 1996 to determine the root cause of the increasing fault trend in respect of transient earth faults on the 275 kV transmission grid in KwaZulu-Natal, South Africa. Historically it was thought that the persistently poor performance of this network was caused by pollution faults. This network was reinsulated with silicone composite insulators, and cane fire as well as veld fire management programmes were introduced. These projects did not result in a consistently decreasing fault trend on this 275 kV transmission grid.

The burn marks caused by the power arcs, which were identified in this study, appeared to indicate that air gap breakdown was occurring. Birds were also observed in close proximity to the faulted towers. Consequently it was thought that bird streamers caused the transmission line faults. Welded rod bird guards designed to prevent bird streamer faults were installed on eighteen 275 kV transmission lines. The accumulative length of these transmission lines is 932 km. The implementation of this initiative coincided with a 73% reduction in the total number of transient earth faults. This improvement in performance indicates a strong statistical correlation showing that a large number of the transient earth faults on the transmission grid are related to bird streamers.

Bird streamer induced faults were identified by means of the following diagnostic techniques:

- Burn mark analysis
- Time-of-day analysis

Bird streamer line faults have been observed on I string, V string and strain jumper assemblies on the 275 kV power lines. However, on the 400 kV power lines bird streamer faults have only been observed on V string assemblies.

Experimental work involved simulated bird streamers and determining the minimum flashover distance for AC system voltages. Electric field measurements by means of a capacitive probe were undertaken at the ground plane. The electric field measurements at the ground plane under bird streamer intrusion confirm that if the streamer is moved away from the live tower hardware, the electric field enhancement at the ground plane decreases below the background streamer propagation field.

This case study determined that in order to prevent bird streamer faults the bird streamer must be moved away from the live tower hardware. The distance it must be moved is at least 900 mm for 275 kV power lines and 1 100 mm for 400 kV lines.

ACKNOWLEDGEMENTS

I would like to thank my wife and family for their constant support of this project.

Special thanks to my project mentors, Mr P Naidoo, Mr AC Britten, Mr M Booysen and Mrs R Gamede, as well as Dr H Geldenhuys, for their contributions to this project.

The hallmark of this project was the excellent cooperation received from the University of Natal. Special thanks to Dr Derek Hoch for his enthusiastic supervision of this study. I would also like to thank Mr T Roos and Mr B Alexander for their technical assistance, which is greatly appreciated.

Special thanks also to all those in Eskom who supported this work - especially to those involved in the KwaZulu-Natal bird guard project.

Finally, I think it is fitting to acknowledge that all good things come from heaven. I want to thank my Lord and Saviour Jesus for the insight and abilities He has given me.

TABLE OF CONTENTS

DECLARATION 2

ABSTRACT 3

ACKNOWLEDGEMENTS 5

LIST OF TABLES 9

LIST OF FIGURES 10

Ckapter 1. INTRODUCTION 12

1.1. Historical context of current investigation 12

1.2. Thesis objective 17

1.3. Thesis layout 19

Ckapter 2. AC AIR GAP BREAKDOWN IN SMALL AIR GAPS 20

2.1. Other power utilities' experience 21

2.2. Air gap breakdown mechanisms for uniform and nonuniform electric field distributions 22

2.2.1. Uniform field distributions 23

2.2.2. Nonuniform field distributions 24

2.3. Streamer propagation characteristics and streamer-to-leader transition in air 25

2.3.1. Streamer propagation characteristics of small air gaps 25

2.3.2. Streamer-to-leader transition 27

2.3.3. AC breakdown characteristics 28

2.4. Switching surge clearances: gap factor 30

2.5. Bird streamer fault mechanism hypothesis 31

2.6. Conclusion 33

Ckapter3. STATISTICAL ANALYSIS OF GEORGEDALE-VENUS PERFORMANCE 34

3.1. Kstorical information on the 275 kV Georgedale-Venus 1 and 2 lines 34

3.1.1. Discussion of the Georgedale-Venus 1 and 2 line route 35

3.1.2. Measurements of tower window clearances 36

3.1.3. Post-line-fault investigations 37

3.1.4. Georgedale-Venus technical summary 38

3.1.5. Identification of bird streamer fault mechanism 40

3.2. Twelve-month moving average as a progression of the bird guard project 42

3.3. Total number of faults versus time of day 44

3.4. Total number of faults per month versus average rainfall 47

3.5. Total number of faults per month versus average humidity 49

3.6. Discussion of fault correlation 51

3.7. Conclusion 52

Ckapter 4. EXPERIMENTAL INVESTIGATION INTO AC BREAKDOWN BEHAVIOUR OF SMALL DIVERGING FIELD AIR GAPS. 53

4.1. Experimental hypothesis 53

4.1.1. Experimental setup 55

4.1.2. Experimental procedure 56

4.2. Rod-to-plane AC breakdowns versus electrode type and rod diameter 56

4.2.1. Experimental setup 57

4.2.2. Results of AC breakdown voltage versus electrode tip type rod-to -plane configuration 58

4.3. Investigation into the effects of a corona ring on bird streamer intrusion 59

4.3.1. Experimental setup 60

4.3.2. Results of corona ring investigation 60

4.4. Electrode position versus AC air gap breakdown for V string insulator assemblies 62

4.4.1. Experimental setup 62

4.4.2. Experimental results 64
4.5. Electrode position versus AC air gap breakdown for I string configurations 67
4.5.1. Experimental setup 67
4.5.2. Experimental results 67
4.6. Effect of wet string resistivity on AC breakdowns 69
4.7. Final summary of V string AC voltage trends for various electrodes 70
4.8. Final summary of I string AC voltage trends for various electrodes 71
4.9. Discussion and conclusion of results 72

Cliapter 5. ELECTRIC FIELD MEASUREMENTS AT THE GROUND PLANE 74

5.1. Block diagram of a capacitive probe 74
5.2. Introduction to electric field measurements 75
5.3. Experimental setup 77
5.3.1. Capacitive probe calibration - parallel plane geometry 77
5.3.2. Capacitive probe calibration - sphere plane geometry 79
5.4. Electric field measurement under bird streamer intrusion 80
5.4.1. Experimental setup 80
5.4.2. Experimental procedure 81
5.4.3. Results of electric field measurements under simulated bird streamer intrusion 81

CLapter 6. BIRD GUARD PROJECT IMPLEMENTATION. 83

6.1. Identification of suitable bird guards and test sites respectively 83
6.2. Bird guard designs for field test 84
6.3. Summary of bird guard field tests and results 86
6.4. Discussion of field results, 1996-1997 (December) 87
6.5. Discussion of field results, 1998-1999 91
6.6. Conclusion 95

Ckapter 7. CONCLUSION 96

Chapter 8. RECOMMENDATIONS FOR FURTHER WORK 97

References 98

APPENDIX 1: All KwaZulu-Natal 275 kV Line Faults in 1996 102

APPENDIX 2: Georgedale-Venus Performance Summary, 1996-1998 108

APPENDIX 3: Suspected Bird Streamer Faults, 1993-1998 111

APPENDIX 4: AC Voltage Flashover Results 114

APPENDIX 5: Bird Streamer Poster 123

LIST OF TABLES

Table 1. 275 kV transmission line performance summary 13

Table 2. 275 kV transmission line fault causes in 1996 - chart derived from data contained in Appendix 1 15

Table 3. Summary table of streamer propagation criteria 28

Table 4. Summary of Georgedale-Venus performance, 1990-1999 41

Table 5. Line faults summary, 1996-1998 42

Table 6. Summary of bird guard work on the Georgedale- Venus lines 43

Table 7. Distribution summary of bird streamer faults 45

Table 8. Faults versus wet and dry months 48

Table 9. Faults caused by vultures at Griffins Hill 48

Table 10. Summary of AC breakdown voltage versus variation in streamer resistivity ... 69

Table 11. Summary results of air gap breakdown clearances - V string 71

Table 12. Calibration of capacitive probe 77

Table 13. Results of capacitive probe saturation properties 78

Table 14. Sphere plane electric field measurements 79

Table 15. Field test results on the Georgedale-Venus 1 line 86

Table 16. Field test results on the Georgedale-Venus 2 line 87

Table 17. Line 1 performance summary, 1997 88

Table 18. Line 2 performance summary, 1997 89

LIST OF FIGURES

Figure 1. Map of South Africa indicating the relative position of KwaZulu-Natal 12
Figure 2. Florida Power & Light time of day versus fault mechanism correlation 21
Figure 3. Streamer current evolution, primary streamer 25
Figure 4. Streamer current evolution from primary streamer to transient arc 25
Figure 5: Rod-plane illustration 29
Figure 6. Bird streamer illustration 31
Figure 7. Geographic location of the Georgedale-Venus power lines - line length 140 km 35
Figure 8. AIV tower illustration of live hardware electrical clearances 36
Figure 9. Left: Burn marks on live corona ring, Right: Burn marks on centre of tower steelwork 38
Figure 10. 12 MMA summary of the Georgedale-Venus lines 43
Figure 11. Number of suspected bird streamer faults per time of day 44
Figure 12. Bird streamer faults versus time of day - sample size 90 45
Figure 13. Bird streamer profile of the Georgedale-Venus lines 46
Figure 14. Faults per month versus average humidity 50
Figure 15. Experimental setup 55
Figure 16. Rod-plane experimental layout 57
Figure 17. Illustration of rod electrode tips 57
Figure 18. Rod-plane AC breakdown trends versus electrode tip type 58
Figure 19. Rod-plane AC breakdown trends versus electrode diameter 58
Figure 20. T string assembly illustrating the different air gap lengths with and without corona rings 60
Figure 21. AC breakdown trends versus corona ring application 61
Figure 22. V string configuration indicating the electrode positions for vertical bird streamer intrusion 63

Figure 23. V string configuration indicating the electrode position for across-the-string bird streamer intrusion 63
Figure 24. V string configuration indicating horizontal bird streamer intrusion 64
Figure 25. AC breakdown trends versus electrode position - silicone V string 65
Figure 26. AC breakdown trends versus electrode position - glass V string 65
Figure 27. I string bird streamer simulations indicating vertical and horizontal intrusion positions 67
Figure 28. AC breakdown trends versus electrode position - silicone I string 68
Figure 29. AC breakdown trends versus electrode position - glass I string 68
Figure 30. V string AC voltage trends summary 70
Figure 31. Summary of I string AC voltage trends for various electrodes 71
Figure 3 2. Summary of air gap breakdown clearance results -1 string 72
Figure 33. Capacitive probe block diagram 75
Figure 34. Absolute % error versus applied electric field of the capacitive probe 78
Figure 35. Electric field experimental setup 80
Figure 36. Results of electric field measurements under bird streamer intrusion 81
Figure 37. Welded rod bird guard design 84
Figure 38. Application of welded rod bird guard 85
Figure 39. Application of whirely bird with bird runways 85
Figure 40. Map of 275 kV network in KwaZulu-Natal 90
Figure 41. KwaZulu-Natal bird guard project results 91
Figure 42. Bird guard performance summary of the Bloukrans lines 92
Figure 43. Bird guard performance summary of the Georgedale lines, 1998-9 93
Figure 44. Bird guard performance summary of the Avon lines, 1998-9 94

Chapter 1

INTRODUCTION

1.1. Historical context of current investigation

The South African transmission network comprises a total of 25 000 km of transmission lines, as illustrated in Figure 1.

Figure 1. Map of South Africa indicating the relative position of KwaZulu-Natal

The KwaZulu-Natal transmission network comprises 2 573 and 1 541 kilometres of 400 kV and 275 kV transmission lines respectively. The national performance target for the 275 kV transmission lines within this network is 5.8 faults/100 km/pa (Bell, 1999). The performance of the 275 kV network in KwaZulu-Natal for the period between 1993 and 1999 is summarised in Table 1.

Year	Number of line faults pa	Line faults: faults/100 km/pa	Target: faults/100 km/pa
1993	102	6.62	**5.8**
1994	126	8.12	**5.8**
1995	**81**	5.26	**5.8**
1996	125	**8.11**	**5.8**
1997	**94**	6.10	**5.8**
1998	**78**	5.06	**5.8**
1999	**49**	3.11	**5.8**

Table 1. 275 kV transmission line performance summary

The fault performance of the 275 kV network from 1993 to the end of 1995 displayed a decreasing trend. This reduction in line faults was associated with the effectiveness of the various transmission line projects in KwaZulu-Natal implemented during that period. However, this trend was reversed in 1996.

Prior to 1996 several projects had been implemented to improve the transmission network performance, including the reinsulation of power lines that were within 50 km of the coast with silicone composite insulators and the implementation of sugar cane fire and veld fire management programmes. The objective of these projects was to reduce the outages caused by pollution flashovers, cane fires and veld fires respectively. Details of the projects are discussed briefly below:

- **Reinsulation of transmission lines with silicone composite insulators**

  Between 1993 and 1996 most coastal transmission lines (ie within 50 km of the coast) were reinsulated with siiicone rubber composite insulators, with a specific creepage of 31 mm/kV, and this proved very effective in mitigating line faults related to marine pollution. This project was suspended when there was a dramatic increase in the number of line faults on the two Georgedale-Venus 275 kV lines in 1996. Of note is

that all the silicone composite insulators were fitted with corona rings as specified by the manufacturer.

- **Sugar cane fire management programme**

  Cane fire faults evolve when the heat and smoke emitted by a cane fire are of a sufficient quantity to compromise the air insulation of a transmission line (Evert, 1993). On the 275 kV network most of the faults occur from midspan to ground. In order to reduce faults caused by cane fires, the cane fire management programme was introduced. This programme coordinated planned sugar cane burns with transmission line outages for the duration of the cane burns. The scope of this programme was recently extended to establish cane-free power line servitudes.

- **Veld fire management programme**

  Veld fire faults occur in the same way as cane fire faults. However, their occurrence is restricted to areas where there are grasslands. Because of its length and topography, the 400 kV network is susceptible to veld fire faults. These faults are currently managed by grass cutting programmes, in which the veld is cut immediately after the growing season.

To account for the increasing trend of transient earth faults during 1996 there had to be another earth fault mechanism besides those of pollution flashovers, cane fires, veld fires and lightning, which were already known. Investigation into the line faults occurring in 1996 revealed that 51% of the faults could be attributed to bird pollution. The 275 kV line fault data is tabulated in Appendix 1.

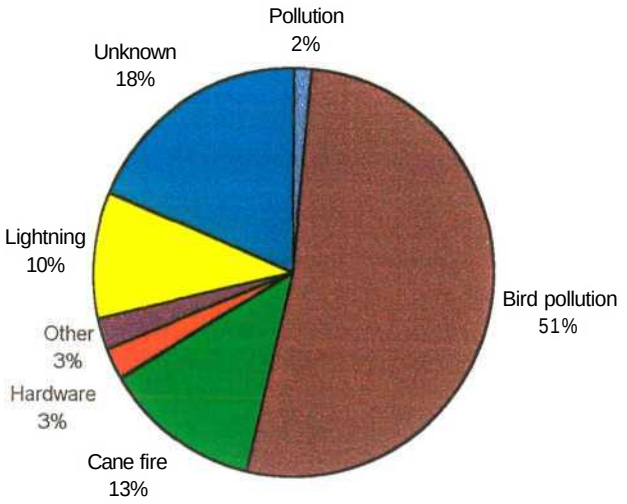

Table 2. 275 kV transmission line fault causes in 1996 - chart derived from data contained in Appendix 1

Table 2 summarises the 275 kV transmission line faults that occurred in KwaZulu-Natal in 1996. The line fault causes are discussed below:

- **Pollution faults**

  The transmission lines that are located near Durban and Richards Bay (see Figures 1 and 7) are exposed to marine pollution and consequently experienced numerous faults (Schneider et al, 1978). However, since these lines were reinsulated with silicone composite insulators no recurring pollution faults have occurred.

- **Unknown faults**

  When a transmission line trips and the cause of the transmission line fault cannot be determined, that fault is classified as an unknown fault. Generally faults are classified as unknown if the burn marks caused by the power arc are not located. In this investigation travelling wave fault locators were installed on the transmission lines to determine the location of the line faults. This assisted in establishing the causes of the

unknown faults, as the location of each fault could be accurately determined. This made it possible for each unknown fault on the Georgedale-Venus power lines to be located by a post-fault line patrol. In addition the location and nature of the power arc, bum marks were also documented. Britten (Britten, 1998) is investigating a light pollution light wetting earth fault mechanism which could also be a possible mechanism of the "unknown" faults. This work is still under way.

- **Lightning faults**

  The CSIR has profiled the lightning density of KwaZulu-Natal and found that it varies from 4 to 10 strikes per square kilometre per annum. Durban has a lightning density of 4, Pietermaritzburg of 7 and Ladysmith of 9 strikes per square kilometre per annum. All the faults caused by lightning have been correlated with the lightning position and tracking system (LPATS).

- **Other faults**

  "Other" faults are **the** line faults that are caused by protection malfunction, bird nest infringement on the air gap clearances of the transmission lines, veld fires beneath the lines, or trees growing into the phase conductors. In northern KwaZulu-Natal crows build nests on the transmission towers. These nests are constructed with fencing wire and they encroach on the electrical air gap clearances when they become dislodged by strong winds.

- **Hardware faults**

  These are line faults caused by mechanical failure of the transmission line hardware. They usually result in permanent outages.

- **Cane fire faults**

  These are line faults that result from controlled burning of cane fields underneath **the** transmission lines. The utility has introduced a cane fire management programme **that** coordinates the burning of the cane with power line outages. This programme **has**

been very effective in preventing the line faults caused by cane fires; but it does not prevent faults during runaway cane fires. It is possible to manage the latter scenario by implementing a cane-free servitude policy.

- **Bird pollution faults**

  Post-line-fault patrols often observed bird pollution on the faulted transmission tower and its insulator hardware. These faults were classified as bird pollution faults.

  Although some of the transmission lines were selectively reinsulated with silicone composite and new glass insulators respectively, these projects did not reduce the total number of flashovers per annum.

This thesis details the results of an investigation in which a solution was found to the faults attributed to bird pollution. Because of their persistently poor performance, the 275 kV Georgedale-Venus 1 and 2 lines were identified as test lines for this investigation. These two lines accounted for 45 line trips during 1996.

This thesis discusses:

1. The cause of the earth faults
2. Possible solutions
3. Small air gap (0-0.5 metre) breakdown characteristics under AC voltages
4. Field results of solutions implemented

1.2. Thesis objective

Historically the bird-related faults were thought to be caused by bird excreta accumulating on the insulators. When these excreta were wetted by mist or condensation it resulted in leakage current activity, and dry band arcing could then develop and evolve into insulation breakdown. This viewpoint was further substantiated by the observations of field staff

that the line faults coincided with mist and occurred between the hours of 22:00 and 06:00.

Although some of the line faults attributed to the above are a pollution mechanism, this investigation proposed that many of these faults were caused by a direct bridging out of the air gap as a result of the intrusion of a bird streamer. This mechanism was postulated because of the correlation of bird activity within the power line servitude at the time of faults.

This investigation also correlated weather data with that of the bird streamer fault mechanism. This was done in order to determine possible bird streamer fault trend characteristics.

The bird streamer fault mechanism was modelled in the High Voltage Laboratory of the University of Natal. These laboratory simulations attempted to determine the required electrical air gap insulation levels to prevent bird streamer faults from evolving. Electric field measurements at the ground plane were also recorded to confirm the proposed air gap clearances.

1.3. Thesis layout

Chapter 2 details the findings of a literature survey of air gap breakdown mechanisms and their application to air gap breakdown for an applied AC voltage, and also reviews published data on other utilities' experience with bird-related outages.

Chapter 3 records the Georgedale-Venus transmission line history and the associated design specifications. The bird streamer faults identified are correlated with average rainfall, humidity and time of day to determine bird streamer fault characteristics.

Chapter 4 records the High Voltage Laboratory air gap breakdown results as a function of electrode tip and diameter type, insulators with or without corona rings, insulator assembly type and streamer resistivity of liquid streamers.

Chapter 5 records electric field measurements at the ground plane under bird streamer intrusion. These results are used to determine the probability of flashover once the bird streamer has been moved away from the high-voltage transmission line hardware.

Chapter 6 details the post-line-fault patrol findings. This chapter discusses the bird streamer mechanism and the prevention of bird streamer faults. The field results of the KwaZulu-Natal bird project are also presented.

apter 2

AC AIR GAP BREAKDOWN IN SMALL AIR GAPS

This thesis postulates that the bird streamer earth fault mechanism is essentially an air gap breakdown phenomenon. The findings of the literature survey discussed below focus on work with respect to unknown flashovers and air gap breakdown of small air gaps. This study investigated:

1. Other power utilities' experience
2. Air gap breakdown mechanisms for uniform and nonuniform electric field distributions
3. Streamer propagation characteristics and streamer-to-leader transition
4. Switching surge clearances
5. Bird streamer fault hypothesis

Numerous researchers have been involved in developing models to explain air gap breakdown characteristics under various high-voltage applications. Models have been proposed for air gap breakdown under AC conditions. These models are used to determine AC air gap breakdown characteristics when a bird streamer intrudes into a transmission tower air gap clearance.

2.1. Other power utilities' experience

Burnham (Burnham, 1995) investigated lightning, pollution and bird streamer fault mechanism characteristics on the Florida Power & Light (FP&L) 138 kV, 230 kV and 500 kV networks. This investigation examined the number of line faults versus the time of day of the occurrence of the line faults. The observations on Florida Power & Light are summarised in Figure 2 (Burnham, 1995).

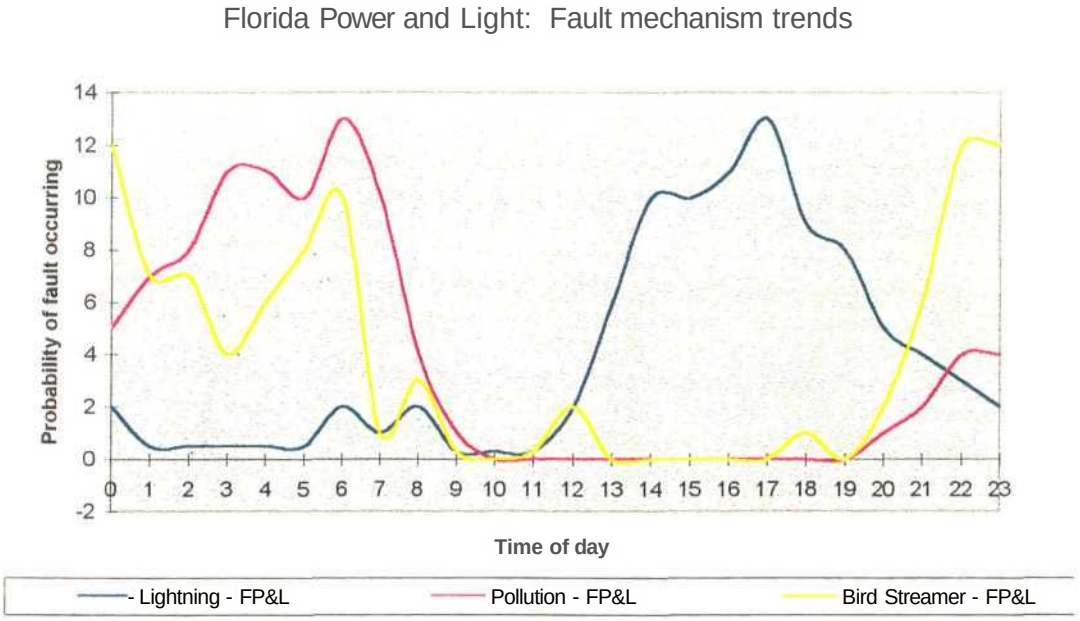

Figure 2. Florida Power & Light time of day versus fault mechanism correlation

The correlation of fault type versus time-of-day analysis, as illustrated in Figure 2, could prove to be a very effective method of determining the cause of power line faults. The Burnham model indicates that faults caused by pollution and faults caused by bird streamers occur at a similar time of day, ic in the period between 22:00 and 06:00 hours. Burnham speculated that this could be the reason why faults caused by bird streamers had **not** been identified as a major cause of transmission **line** outages **on** other networks. Burnham proposed that the time-of-day fault distribution could differentiate between

pollution and the bird streamer fault mechanisms since the profiles of the two curves were different. The bird streamer profile was bimodal and the pollution profile unimodal.

Bonneville Power Administration (West et al, 1971) demonstrated that bird streamers were able to initiate flashover on 320 kV AC and 400 kV DC transmission lines. West (West et al, 1971) determined that large birds could excrete a volume of 60 cm^3. The resistivity of these streamers varied between 30 and 120 Qcm.

EPRI (EPRI, 1988) also conducted investigations into unexplained transmission line outages. EPRI concluded that the faults they observed could not be attributed to bird streamers but were caused by a pollution mechanism.

Bird streamer faults in the South African context have been correlated with time of day under section 3.3. A bird streamer model leading to flashover is discussed in sections 2.2 to 2.4. These models are used to develop a hypothesis in respect of the flashover mechanism and techniques for identifying and preventing bird streamer faults.

2.2. Air gap breakdown mechanisms for uniform and nonuniform electric field distributions

For uniform and nonuniform electric field distributions the development of the electron avalanche and the consequent breakdown mechanisms have been well documented by Raether (Raether, 1964), Loeb (Loeb, 1955) and Meek (Meek & Craggs, 1978) among others. The subsequent discussion of this work represents a summary of their findings with respect to the expected breakdown characteristics of uniform and nonuniform air gaps.

2.2.1. Uniform field distributions

Townsend (Kuffel et al, 1984) investigated the growth of current as a function of the applied voltage across an air gap. Townsend proposed that for uniform fields the growth of charge carriers in the air gap is summarised by equation 1.

$$N = Noe'^{*1} \qquad \textbf{Equation 1}$$

where N is the number of charge carriers

a is Townsend's first ionisation coefficient

Equation 1 quantifies the growth of ions in the air gap, either by electron collisions or by photoionisation, as an exponential function. The phenomenon is termed an electron avalanche. Equation 1 was later modified to include the effect of electron attachment in the process of charge carrier multiplication. This relationship is summarised in equation 2.

$$N = N_o e^{(a-n)d} \qquad \textbf{Equation 2}$$

where r| is the attachment coefficient and (a - r|) is known as the effective ionisation coefficient (A,).

Raether (Kuffel et al, 1984) observed that when the number of charge carriers was greater than 10^6 but smaller than 10^8 the growth of the electron avalanche was weakened. When the number of charge carriers exceeded 10^8 the growth of the charge carriers was exponential and breakdown followed. At this point the electric field in the air gap was 31 kV/cm. In a uniform field the start of the electron avalanche ensures that the entire air gap will break down.

Raether attributed this weakening of the avalanche growth to the space charge effect of the ion concentrations on the head of the electron avalanche. In uniform fields, the space charge effects on the growth of the electron avalanche are negligible. However, in nonuniform fields the space charge effects play an important role in the mechanism of corona discharge and subsequent air gap breakdown.

Townsend's electron avalanche model hypothesised that the breakdown time for the air gap should be at least the time taken for an electron to cross the air gap. Experimental evidence proved that the time to spark was quicker than this. This observation led to the establishment of the streamer breakdown model.

2.2.2. Nonuniform field distributions

In a nonuniform electric field distribution the electric field in the air gap varies across the air gap as a function of electrode geometry and distance. The relationship between the applied voltage and the electric field is summarised in equation 3.

$$V = \int \pounds . dx \qquad \textbf{Equation 3}$$

At low pressures Townsend's equation takes the form of equation 4

$$N = N_o \exp[\int /l(x)dx] \qquad \textbf{Equation 4}$$

Corona inception will occur when the electric field at the high-voltage electrode approaches 31 kV/cm. However, this will not lead to complete air gap breakdown but to sustained corona discharges.

In investigations into nonuniform electric field distributions it has been observed that the time of development of sparks in the gap is much shorter - one order of magnitude less - than the average time taken by an electron to cross the air gap. Moreover, for rod-plane geometries electric field enhancement is only high enough at the anode for ionisation to occur. Ionisation can only occur near the cathode with the aid of space charge distortion. These observations have illustrated the important role that space charge distortion plays in nonuniform air gap breakdown and have given rise to the development of the streamer breakdown mechanism.

2.3. Streamer propagation characteristics and streamer-leader transition in air

Streamer propagation characteristics of small air gaps have been investigated extensively by Marode (Marode, 1975), Waters (Waters et al, 1968), Goldman (Goldman, 1981) and Gallimberti (Gallimberti, 1972) among others. Their findings are discussed below.

2.3.1. Streamer propagation characteristics of small air gaps

Marode (Marode, 1975) determined that immediate breakdown does not result when the streamer arrives at the cathode, but it appears that electron attachment is dominant.

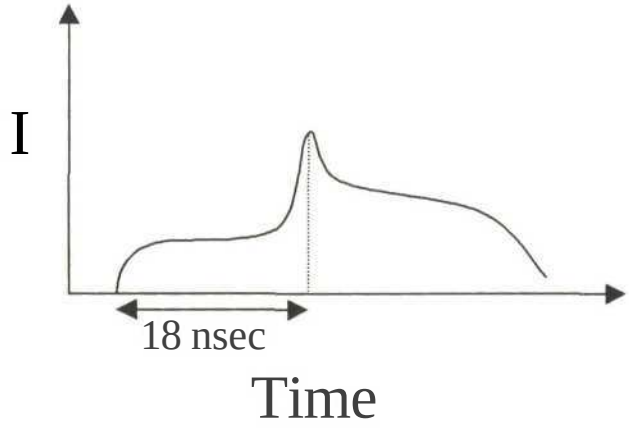

Figure 3. Streamer current evolution, primary streamer

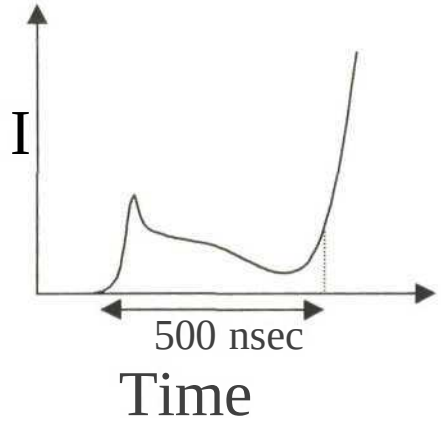

Figure 4. Streamer current evolution from primary streamer to transient arc

Figure 3 illustrates the current evolution of a streamer that crosses the air gap but does not cause breakdown. Marode (Marode, 1975) also determined that the streamer channel has an electric field gradient of about 4-5 kV/cm. As the streamer reaches the cathode, a return wave propagates towards the anode at a velocity of 10^9 cm/s. This return wave is correlated with a decrease in current flowing in the air gap, as indicated in Figure 4.

Marode (Marode, 1975) concluded that electron attachment is dominant in the conductive channel. The streamer channel will be transformed into a hot arc channel when the ion density exceeds 10^{17} electrons/cm^3. Consequently rapid thermalisation of the channel must occur due to detachment and joule heating within the streamer channel. Marode also determined that streamer pulses have a rise time of the order of 18 ns in air.

Goldman (Goldman, 1981) investigated corona discharges prior to sparkover as a function of electrode geometry, air pressure and humidity. Goldman determined that corona discharges have current/volt characteristics similar to those of a glow discharge. This implies that there is a current magnitude dependency before self-sustained streamer discharges evolve into an arc.

Waters (Waters, 1968) investigated the measurements of the electric field at the ground plane under streamer propagation in the air gap. He determined that the electric field at the ground plane could be as high as 8 kV/cm. Waters used a field mill to determine the electric field intensity at the ground plane. Field mills are instruments that are able to measure the electric field at the ground plane by measuring the charge induced on a plane. This induced charge is a function of the electric field exposed to the plane. The field mills have been used extensively to measure electric fields in the study of atmospheric electricity, including lightning, and in high-voltage measurements (Waters, 1968; and Kuffel et al, 1984). The principle of relating electric field at a plane to the charge induced on that plane is discussed in section 5.2.

The model of streamer propagation proposed by Gallimberti (Gallimberti, 1972) determined that new electron avalanches would occur where the electric field was greater than 26 kV/cm. A streamer would be initiated where the electric field was greater than 26 kV/cm and would propagate into the air gap until the electric field was reduced to less than 7 kV/cm.

2.3.2. Streamer-to-leader transition

The role of streamer propagation in large air gaps has also been investigated in detail by Rizk (Rizk, 1997), Jones (Jones et al, 1978), Hutzler (Hutzler et al, 1978) and Waters (Waters, 1981) among others.

An important distinction between corona streamers and leader transition is that when streamers bridge an air gap, voltage collapse does not result immediately, whereas a leader channel is sufficiently conductive to initiate a final arc after bridging an air gap (Jones et al, 1978). As the charge conducted by the streamer increases, there is sufficient energy available to increase the core temperature of the streamer channel (via collisions and joule heating). When the temperature reaches 3 000 °K a stable leader channel is formed. The leader channel has been observed to progress in stepped growth, at a velocity of 20 mm/(is, behind the streamer discharges (Jones et al, 1978).

Rizk (Rizk, 1989) proposed that a continuous leader would begin propagation where the electric field exceeded 31 kV/cm. At this point the leader gradient would start at 4 kV/cm and approach 0.5 kV/cm when a cumulative charge injection of 45 μC/m into the leader channel is maintained. This work concerned switching surges. Rizk's work quantified the difference in electric field gradient between streamers and leaders.

Hutzler (Hutzler et al, 1978) suggested that the streamer gradient is about 4-5 kV/cm. Thus a streamer would tend to propagate until the average electric field is 4 kV/cm. This value is sensitive to space charge in the air gap, as the streamer would not be propagating into a space charge free air gap. This work was published in respect of switching surges.

Geldenhuys (Geldenhuys, 1986) also investigated the electric field at the earth plane. He determined that the streamer would propagate to the earth plane when the field at the earth plane was 5-6 kV/cm. A summary of streamer propagation criteria is set out in Table 3.

Reference	Voltage application	Air gap size	Electric field threshold for streamer propagation: kV/cm peak
Waters	Positive switching	20 cm	8 kV/cm
Gallimberti	Positive switching	1 cm	6.8 kV/cm
Hutzler	Positive switching	1 m	4 kV/cm
Geldenhuys	Positive switching	0.5 m	5-6 kV/cm

Table 3. Summary table of streamer propagation criteria

The above models are not consistent in determining the background field where streamers will stop propagating but a minimum of 4 to 5 kV/cm seems reasonable.

2.3.3. AC breakdown characteristics

Alternating current corona has been investigated by Boulet (Boulet et al, 1966), Trinth (Trinth et al, 1968), Rizk (Rizk, 1997) and Goldman (Hirsh et al, 1978) amongst others. Their findings are discussed below.

Trinth (Trinth et al, 1968) investigated both direct current and alternating current corona modes from corona inception until the onset of breakdown streamers. Trinth (Trinth et al, 1968) summarised the relationships between the corona modes and explained why the negative corona modes are suppressed under normal condition during alternating current excitation.

Boulet (Boulet et al, 1966) investigated the effects of conductor gradient changes caused by atmospheric conditions above and below freezing point. This work calculated the increase in corona loss and also the increase of radio interference levels attributed to these atmospheric conditions.

Rizk (Rizk, 1997) investigated AC breakdown characteristics at AC voltages with a frequency of 60 Hz. He determined that for air gaps of less than 1 metre there is no significant difference between the sparkover voltages in the presence of fog and dry air.

Under AC voltage application streamer ionisation of the air gap is expected to result. Of note is the fact that the space charge generated in the air gap is essentially generated ahead of the electron avalanche (once the electron avalanche has reached its critical size). Observations during experiments show a luminous discharge near the anode that tends to propagate towards the cathode, as illustrated in Figure 5.

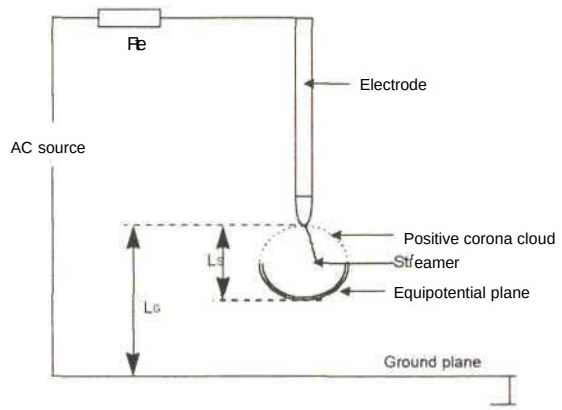

Figure 5: Rod-plane illustration

As the streamer reaches the cathode, an injected current is observed, which is a function of the external circuit capacitance. It can also be deduced that there are charge carriers outside the luminous glow (corona cloud). Consequently it is not possible to conclude that streamers will always emanate from the electrode and propagate into the air gap. A streamer can be initiated anywhere in the air gap where there is a charge carrier and sufficient electric field gradient. This is more apparent with respect to lightning and switching surge applications.

Goldman (Hirsh et al, 1978) has investigated streamer growth as a function of applied voltage and current flowing into the air gap. Under AC voltages the role that ions play in each half cycle is reversed. It is also expected that the ions left in the air gap during the

previous half cycle will tend to reduce streamer propagation during the next half cycle until the electric field has swept the ions from the previous discharges away.

Goldman (Hirsh et al, 1988) documented that for a point-to-plane electrode geometry the electric field distribution along the x axis of the air gap can be determined as:

$$E_x = \frac{2V}{(r+2x)\ln[(r+2d)/r]} \qquad \textbf{Equation 5}$$

where r is the point radius, V is applied voltage, d is air gap length and E is the electric field in the air gap axis x.

This relationship will be useful to model the above rod-plane gap and aid in any electric field measurements at the ground plane (discussed in Chapter 5).

2.4. Switching surge clearances: gap factor

This discussion presents a switching surge model to substantiate the findings that the current air gap clearances on the transmission lines are sufficient to withstand switching surges. Gallet (Gallet et al, 1973) proposed a model for air gap breakdown under switching surges:

$$V_{50} = \frac{k^* 3450}{1 + \frac{8}{d}} \text{ kV} \qquad \textbf{Equation 6}$$

where k is the gap factor =1.2 and d is distance in metres.

This gap factor has been detennined experimentally for rod-rod (in the vertical plane) geometry (Kuffel et al, 1984; Les Renardienes group, 1972; and Lloyd, 1981) among others.

For an air gap clearance of 1.97 metres, the application of equation 6 for a gap factor of 1.2 would require a switching surge magnitude of 818 kV for air gap breakdown. Georgedale-Venus 2 has a minimum air gap clearance of 1.97 metres. There have been no line faults correlated with switching operations on the transmission grid. This observation appears to be consistent with Gallet's model.

2.5. Bird streamer fault mechanism hypothesis

On the basis of the above discussion it is postulated that for an AC flashover to occur some conductive or partially conductive object has to be introduced into the tower window such that it encroaches the live tower hardware. The most logical source of such an intrusion would be a bird streamer. The proposed bird streamer mechanism is defined as:

> *A liquid streamer excreted from a bird, which bridges the entire distance between tower steelwork (earth plane) and the nearest live hardware point, or a sufficient part thereof. This streamer then acts as a fuse and as the current through the streamer increases, it vaporises due to joule heating and an electrical arc is established.*

This mechanism is illustrated in Figure 6 (a bird streamer is illustrated in Appendix 5).

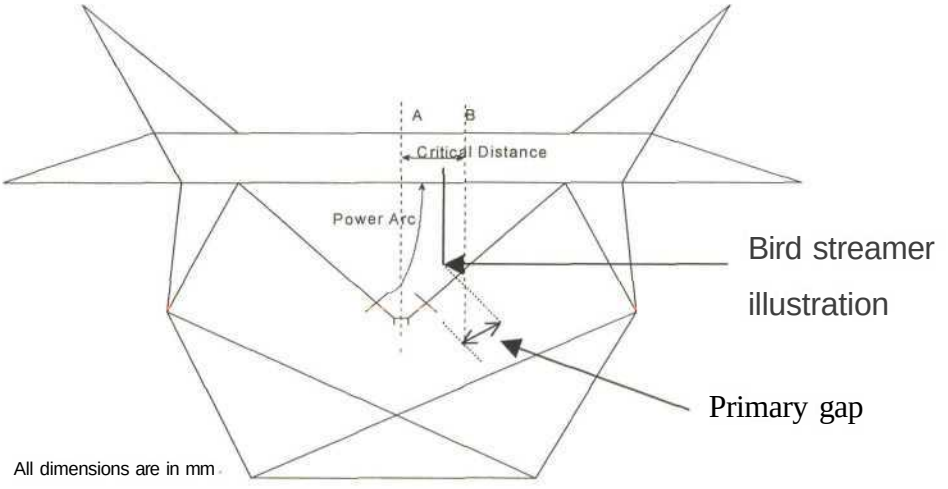

Figure 6. Bird streamer illustration

As the bird streamer encroaches the tower air gap clearances, the necessary (but not sufficient) condition for breakdown will occur, ie the primary gap between the live hardware and the approaching streamer will break down. This event is not necessarily sufficient for a transient earth fault to evolve. The resistance of the bird streamer will initially limit the amount of current flowing in this dynamic circuit. The sufficient condition for a transient arc to evolve would be the current flowing in this circuit being sufficient to vaporise the bird streamer (due to joule heating) and then to drive a power arc, which would evolve, to bridge out the entire transmission tower's air gap clearance.

Figure 6 shows that if the bird streamer is moved laterally away by more than a 'critical distance', from position A to B, no flashover will result as the primary gap clearance will be sufficient to insulate the now intruding ground electrode of the bird streamer. This thesis proposes to determine the required air insulation to fulfil this condition and in so doing prevent a transient arc from developing by ensuring that a bird streamer is not able to meet the necessary and sufficient criteria established in the above model.

If, however, a pollution mechanism were responsible for the earth faults experienced, the trip incidence would remain unchanged. The pollution mechanism referred to here is not the classical dust or salt deposit buildup over a period of time, but rather one where bird excreta pollute the insulators. The insulators would be polluted as birds are not discouraged from perching above the entire insulator string. If this bird streamer hypothesis is feasible, burn marks caused by the power arc could be used to identify bird streamer faults. The burn marks caused by the power arc when the streamer bridges the transmission tower air gap clearances should be vertically above one another, ie the power arc should be initiated on the live hardware and terminate vertically above the live hardware on the tower steelwork. The power arc termination should be a few metres away from the dead end insulators (on a 275 kV, V string configuration). Burn mark analysis applied to fault cause identification is discussed in detail in Chapter 3.1.3 and further illustrated in Appendix 5 (for strain towers, I strings and V strings).

2.6. Conclusion

Research has been initiated into air gap breakdown phenomena relating to lightning and switching surges. These voltage impulses were thought to be the most stressful design contingency for transmission line insulation. However, this work will have to be applied to AC voltage application to determine air gap clearances for bird streamer intrusion.

As discussed in section 2.2, various authors have extensively investigated streamer propagation and its role in air gap breakdown. This thesis will make use of their models to model the breakdown of the primary air gap under bird streamer intrusion. According to the published literature there appears to be a large range for the electric field magnitudes at which a streamer propagation will stop propagating. These magnitudes range from 4 to 8 kV/cm. This investigation will determine the electric field magnitude at the ground plane under AC voltage application. Rizk (1997) has also determined the AC breakdown voltage versus air gap length for both dry and mist conditions. These results indicated that air humidity does not play a crucial role at 158 kV phase to earth. Consequently this investigation will consider only dry air conditions.

Burnham's time-of-day analysis (as discussed in section 2.1.) will be correlated with the Georgedale-Venus faults. This correlation could prove a useful diagnostic tool in determining the cause of power line outages by means of historical performance data. West (1971) also demonstrated that bird streamers cause transient earth faults on 320 kV AC systems.

A model of bird streamer faults and a possible solution have been proposed. This model indicates that to prevent line faults caused by bird streamers the bird streamers should be moved laterally away from the high-voltage hardware. This model also proposes that it is possible to identify bird streamer caused line faults by visually observing the location of the burn marks caused by a power arc after a line fault. These burn marks should indicate that the flashover is in a vertical plane, ie across the transmission tower air gap clearances.

Chapter 3

STATISTICAL ANALYSIS OF GEORGEDALE-VENUS PERFORMANCE

The purpose of this chapter is to determine the statistical fault characteristics of the bird streamer faults. To achieve this, the following data has been investigated:

1. Historical information on the Georgedale-Venus lines
2. The twelve-month moving average (12 MMA) performance statistics
3. Total number of faults versus time of day
4. Total number of faults per month versus average rainfall
5. Total number of faults per month versus average humidity

3.1. Historical information on the 275 kV Georgedale-Venus 1 and 2 lines

Post-line-fault investigations of the Georgedale-Venus transmission lines by operations and maintenance staff have laid the foundation from which the bird streamer fault mechanism was identified. This chapter discusses:

1. The Georgedale-Venus 1 and 2 line route
2. Measurement of tower window clearances
3. Post-line-fault investigations
4. Identification of the bird streamer fault mechanism

3.1.1. Discussion of the Georgedale-Venus 1 and 2 line route

Figure 7 shows the geographic location of the Georgedale-Venus lines. The power lines traverse the KwaZulu-Natal Midlands of South Africa. This area is prime agricultural land stretching south of the Mooi River to Baynesfield and 15 km north of the Mooi River to Griffins Hill. North of Griffins Hill the climate is noticeably drier and the vegetation is predominantly thorn-veld. Bird activity has always been observed in the servitude during routine line patrols. Commonly sighted birds include vultures, ibis and cranes.

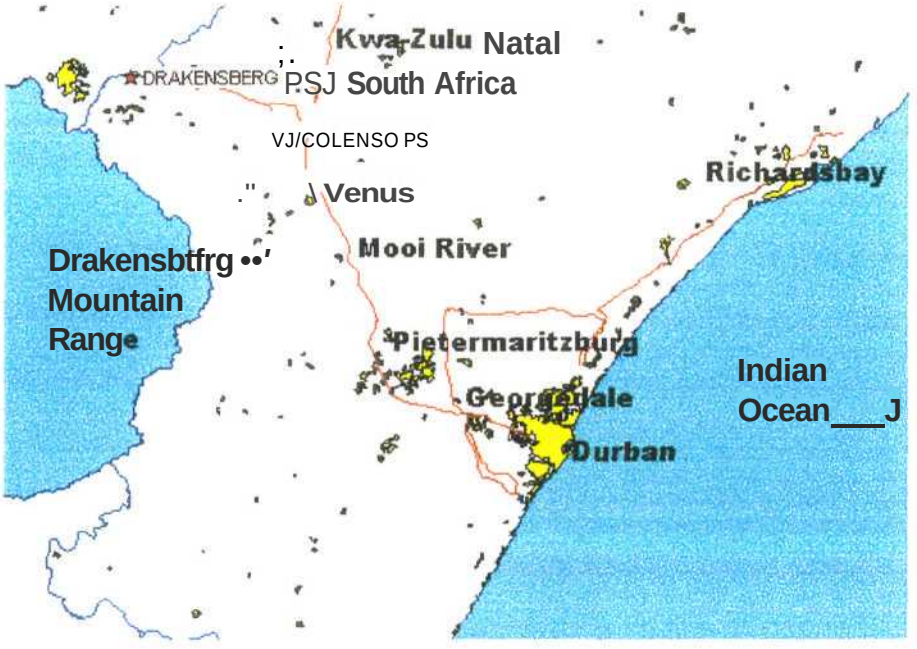

Figure 7. Geographic location of the Georgedale-Venus power lines - line length 140 km

These observations also implicated the birds as the primary cause of the earth faults, but no conclusive fault mechanism had been determined. Previous experiments proved that bird streamers could initiate an air gap breakdown (Burger et al, 1995). However, this investigation did not conclude that bird streamers were a dominant fault mechanism.

3.1.2. Measurements of tower window clearances

The IVI suspension towers of the Georgedale-Venus power lines are of the AIV tower type. The minimum air gap clearance on the Georgedale-Venus lines is 2.1 metres for the glass insulator string assemblies. This clearance was measured in the centre of the V string assembly on tower 61 of Georgedale-Venus 1. The electrical clearance of tower 61 is summarised in Figure 8.

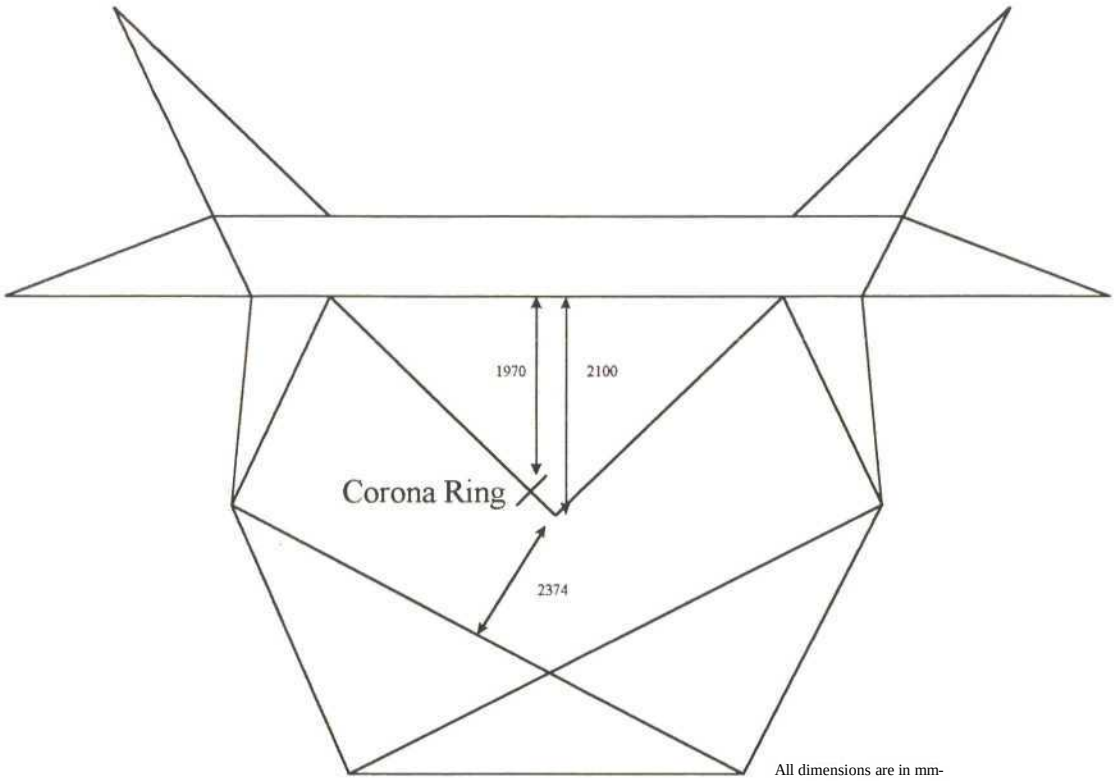

Figure 8. Illustration of live hardware electrical clearances for the AIV tower type

However, after the IVI towers were reinsulated with silicone composite insulators, the minimum air gap clearance was measured as 1.97 metres. This decrease in air gap clearance was caused by the installation of the corona ring fitted on the live end of the silicone composite insulators. The reduction in air gap clearance would certainly increase the probability of air gap breakdown under bird streamer intrusion, as experienced in the sudden increase in line 2 earth fault trip incidence during 1996. Theoretically these

clearances should withstand switching surges in excess of 818 kV (refer to equation 6, Chapter 2).

Rizk (Rizk, 1997) and Takasu (Takasu et al, 1981) reported rms phase-to-earth breakdown voltages of approximately 500 kV (rms, phase-to-earth voltage under dry conditions) and 460 kV (rms, phase-to-earth voltage under fog conditions) for 2 m air gaps. Rizk's results confirm that the air gap clearances of the Georgedale-Venus lines should not influence the line's electrical performance under either wet or dry conditions. In practice no earth faults coinciding with transmission switching operations have been observed. Most of the lightning faults occur on the outer phases (Appendix 2).

3.1.3. Post-line-fault investigations

Post-line-fault patrols on the Georgedale-Venus lines revealed the following data:

- The majority of faults occurred on the centre phase of the towers. The centre phase is electrically denoted as the white phase on these lines.
- The majority of faults occurred on the V strings, although faults have been observed on I strings as well as on strain tower jumpers.
- The faults appeared to start on the live end corona ring and terminate directly above the live hardware on the tower steelwork, as depicted in Figure 8. Strain towers exhibited similar flash marks - burn marks on the jumpers and directly above the jumpers on the tower steelwork, as illustrated in Appendix 5. On glass insulation the yoke plate and usually the first disc were burnt, and there was a corresponding burn mark directly above the V string on the tower steelwork.
- Faults appeared to coincide with mist or rainy periods.
- The lightning position and tracking system (LPATS) confirmed that lightning was responsible for 30% of the faults (5-6 faults pa).

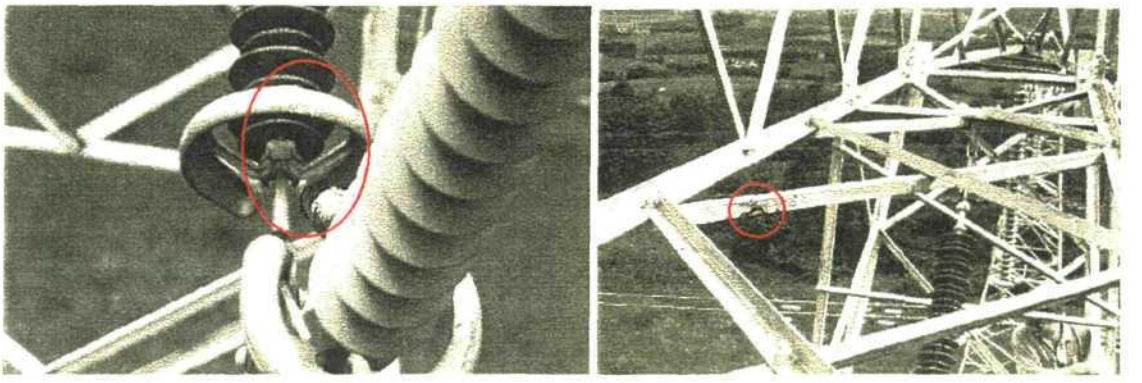

Figure 9. Left: Burn marks on live corona ring **Right: Burn marks on centre of tower steelwork**

3.1.4. Georgedale-Venus technical summary

The 275 kV Georgedale-Venus 1 and 2 lines were among the poorest performing 275 kV transmission lines in KwaZulu-Natal. Steynberg (Steynberg et al, 1993) initiated an investigation to determine the cause of this poor performance. The historical information pertaining to these two lines is summarised below:

- The Georgedale-Venus lines were commissioned in the 1960's, using the A1V tower type. The term A1V refers to a particular tower manufactured by Powerlines and now supported locally by ABB (Pty) Ltd.
- The length of each line is 140 km and the lines were initially insulated with glass discs (U70 and U120 glass insulators) with a specific creepage of 14.9-15.9 mm/kV.

The insulation coordination specifications are:

- One minute power frequency withstand of 460 kV, rms.
- Switching impulse withstand of 850 kV.
- Lightning impulse withstand of 1 050 kV.

- The lightning density on the line route is high: 7-8 strokes per km^2 pa.
- Pollution levels on the line are very light: ESDD 0.03-0.06 mg $NaCl/cm^2$ (IEC 815,1986; Steynberg et al, 1993).
- Bird pollution was identified as a fault mechanism, but its impact was limited to two known vulture restaurants, one at Griffins Hill (still operational today) and the other 10 km south of Griffins Hill at Mooi River (which was closed down after 1993). Vulture restaurants are areas where animal carcasses are placed with the express purpose of feeding vultures to prevent species extinction. Special precautions are taken to ensure that no other animals can eat the carcasses.
- The fault performance of these lines exceeded 10 faults/100 km/pa.

As a result of Steynberg's investigation (Steynberg et al, 1993) both transmission lines were reinsulated.

- Line 1: This line was selectively reinsulated with glass disc U120 insulators. The term selective reinsulation means that only the glass insulator assemblies, which had either pin corrosion or extensive pollution, were replaced. Insulator assemblies in the area of Mooi River were observed to have moss growing on the sheds of the I string assemblies. All these insulators were replaced. These insulator assemblies had no corona rings. This project was completed in 1994.
- Line 2: All suspension towers (III, IVI) between Georgedale Substation and tower 306 (100 km from Georgedale Substation) were reinsulated with silicone composite insulators with a specific creepage of 31 mm/kV. All silicone composite insulators were fitted with 12 inch diameter corona rings, as specified by the manufacturer. The application of corona rings reduced the minimum air gap clearances from 2.1 m to 1.97 m. This project was completed at the end of 1995.

3.1.5. Identification of bird streamer fault mechanism

After the Georgedale-Venus lines had been reinsulated the performance of these lines was radically altered. Line 2 had 70% of its suspension towers fitted with silicone composite insulators. Silicone composite insulators had previously proved to eliminate pollution-related trips in KwaZulu-Natal. Historically most unexplained earth faults on these lines were attributed to a pollution type breakdown mechanism. After reinsulating the Georgedale-Venus 2 power line with silicone composite insulators (in 1995) the occurrence of pollution faults was thought to be very unlikely. As a result of the accumulation of data supporting bird streamers as the dominant fault mechanism, a decision was taken to identify suitable bird guards that would prevent bird streamer faults and implement them at various test sites. This philosophy was adopted to prove the hypothesis, based on the experience of Florida Power & Light (Burnham, 1995), that a bird streamer fault mechanism could be a dominant earth fault mechanism.

A detailed list of the line faults is tabulated in Appendix 2. The performance of the two lines is summarised as a progression of the bird guard project in Table 4.

	Georgedale-Venus 1 (275 kV)		Georgedale-Venus 2 (275 kV)	
Year	Action taken	Fault trips pa	Action taken	Fault trips pa
Jun-Dec 1990	None	10	None	9
1991	None	9	None	14
1992	None	13	None	16
1993	First investigation complete	12	First investigation complete	7
1994	Reinsulated with glass	18	None	16
1995	None	7	Reinsulated with composites	16
1996	None	15	Experimentation with WRBGs	29
1997	Installation of WBs	9	Installation of WRBGs	9
1998	Initial installation of WRBGs (centre phase only)	6	WRBG installation continued (centre phase only)	9
1999	Completion of WRBG installation (centre phase only)	1	Completion of WRBG installation (centre phase only)	3

Table 4. Summary of Georgedale-Venus performance, 1990-1999

During 1994 both Georgedale-Venus lines (1 and 2) faulted excessively. The performance of both lines exceeded 11 faults/100 km/pa. However, after line 1 had been reinsulated (with glass) its fault performance improved dramatically, and it was decided to continue with the reinsulation of line 2 (with silicone composite insulators) in 1995. During 1996 both lines continued faulting excessively, and the number of faults on line 2 doubled.

The line fault performance data in respect of the two Georgedale-Venus 275 kV lines between 1996 and 1998 was used in the statistical analysis that would determine the bird streamer earth fault characteristics. With the acquisition of a travelling wave fault locator after November 1996, fault location on the Georgedale-Venus lines was greatly enhanced. This allowed consistent fault cause identification. The causes of the line faults in the period of 1996 to 1998 are summarised in Table 5.

Fault cause	Line 1. Number of faults, 1996-1998	Line 2. Number of faults 1996-1998	TOTAL
Fires (cane and veld)	1	2	3
Pollution	2	0	2
Storm (lightning)	3	11	14
Bird streamer	19	23	42
Unknown	2	6	8
TOTAL	27	42	69

Table 5. Line fault summary, 1996-1998

The Georgedale-Venus 1 and 2 transmission lines share the same servitude. If the known fault causes (storms, cane and veld fires) are excluded, it can be assumed that the rest of the fault sample could be caused by bird streamers. This would result in a fault sample of 52 faults (ie 42 bird streamer, 2 pollution and 8 unknown) for 1996 to 1998.

The bird streamer faults were also correlated with the weather parameters. It was hoped that these correlations would aid in determining the bird streamer fault trends as a function of weather parameters.

3.2. Twelve-month moving average as a progression of the bird guard project

The effectiveness of the bird guard project in reducing line faults is summarised in the twelve-month moving average (12 MMA) statistic. The 12 MMA statistic is determined as:

$$12\ \text{MMA} = \frac{\sum_{1}^{12} (number\_of\_line\_faults)}{12}$$

The 12 MMA is the cumulative sum of all the faults experienced by each of the transmission lines over the past 12 months. The 12 MMA, normalised to faults/100 km/pa, is presented in Figure 10.

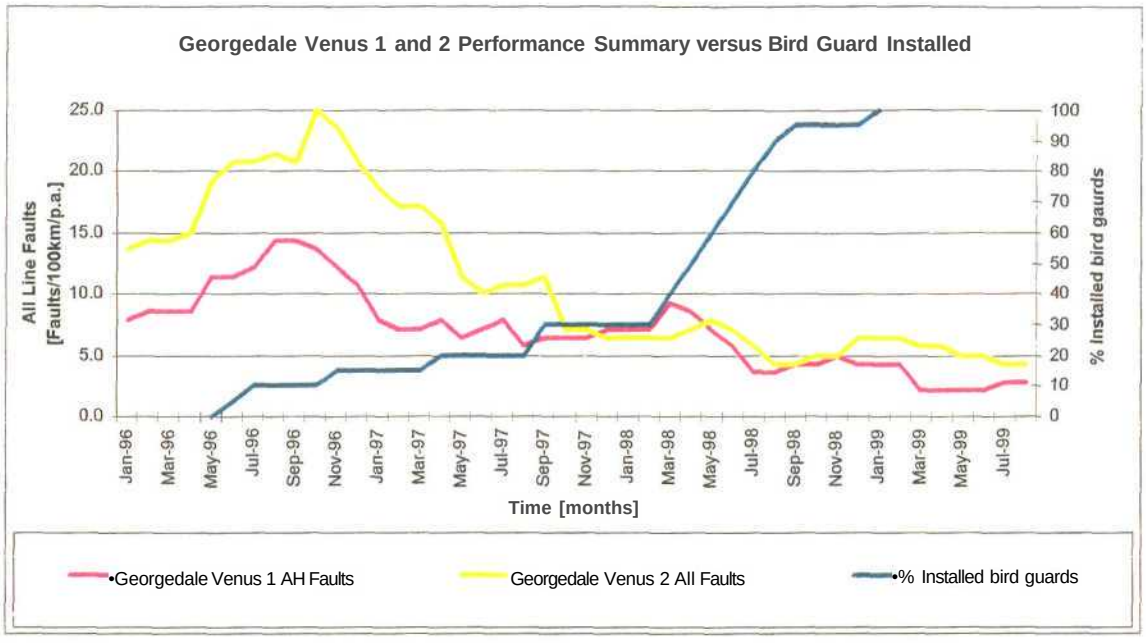

Figure 10. 12 MMA summary of the Georgedale-Venus lines

The effectiveness of the welded rod bird guards (WRBGs) is clearly illustrated by the significant improvement in both transmission lines' performance (see section 6.2). Table 6 details the action taken in installing bird guards on the two Georgedale-Venus power lines. Since the application of the bird guards the performance summary of the power lines shows a decrease from more than 15 faults/100 km/pa to less than 5 faults/100 km/pa.

Time	Action taken
Jan 96	Investigation into poor performance started
Aug96	WRBGs, type 1, installed at Griffins Hill - line 2
Sep96	WRBGs installed at Midmar Dam on line 2 / shade cloth on line 1
Nov96	WRBGs, type 1, installed on T 18-100, line 2
April 97	WRBG installation started on line 1
May 98	WRBGs, type 2, installation continued on line 2
May 98	WRBGs, type 2, installation continued on line 1
Feb99	Installation of WRBGs on lines 1 and 2 completed

Table 6. Summary of bird guard work on the Georgedale-Venus lines

3.3. Total number of faults versus time of day

Further verification (if needed) that birds were the cause was obtained by performing time-of-day analysis on the line faults (sample size 52) highlighted in Table 5. The time-of-day analysis for the Georgedale-Venus 1 and 2 transmission lines is presented in Figure 11.

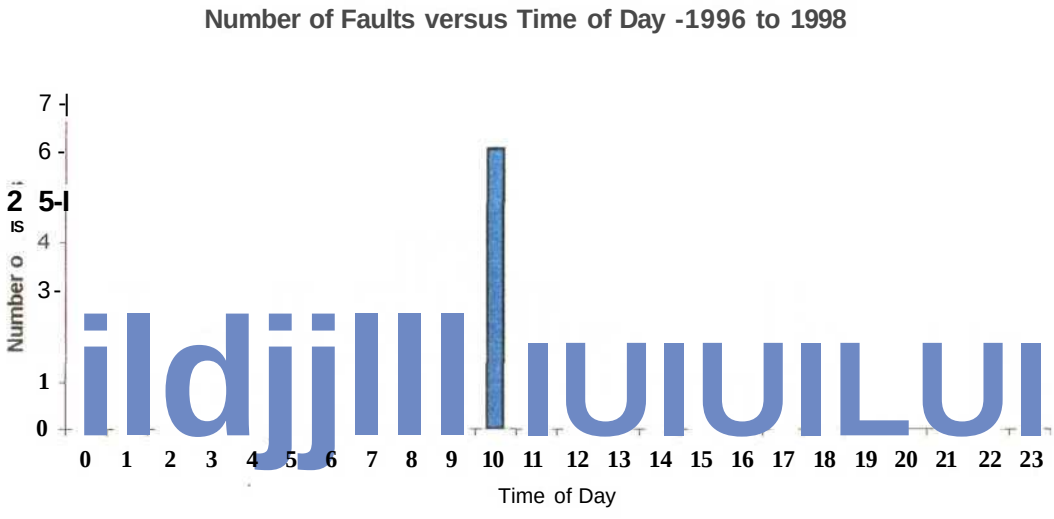

Figure 11. Number of suspected bird streamer faults per time of day

The bird streamer faults on the Georgedale-Venus transmission lines appear to have three dominant peaks. The majority of bird streamer faults occur during the morning hours of 05:00-12:00. A substantial number of faults also occur during the late night and early morning hours. This is a noteworthy trend as one might assume that bird activity would decrease in the evening. Apparently this hypothesis is not conclusive.

This distribution shows significant differences from those published by Florida Power & Light (Burnham, 1995). The bird streamer fault distributions of FP&L (sample size of 145 faults) indicate that that the majority of the faults reported occurred during the hours of 20:00 to 06:00 and no significant faulting activity between 10:00 and 19:00.

If the characteristics of the Georgedale-Venus lines prior to reinsulation are considered, the sample size is increased to 90 faults, excluding all storm- (lightning-) and fire-related faults. A detailed listing of these faults is in Appendix 3 and presented in Figure 12.

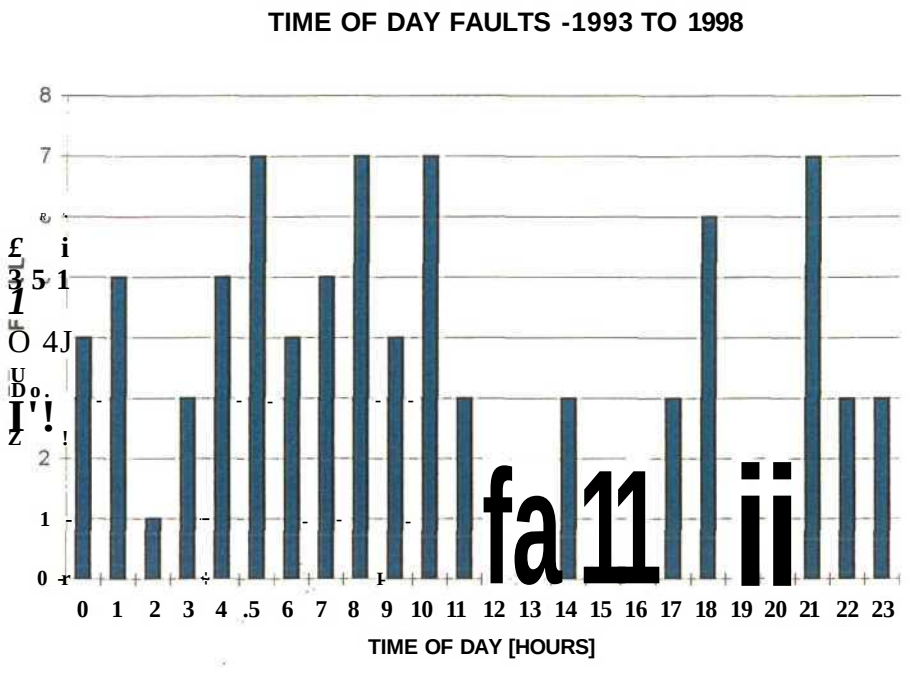

Figure 12. Bird streamer faults versus time of day for a sample size of 90 faults

It is noticeable that the faults occur over the entire 24-hour period. The distribution is summarised in Table 7.

	Time of peak	Bird streamer faults, 1996-1998 (52)	Bird streamer faults, 1993-1998(90)
Peak 1	04:00-12:00 .	54%	49%
Peak 2	21:00-03:00	25%	29%
Peak 3	16:00-20:00	12%	17%
Peak 4	14:00	2%	3%
Other	Rest of day	7%	2%

Table 7. Distribution summary of bird streamer faults

The time-of-day analysis on these two lines indicates that the bird activity occurs all day and all night, with 70% of the faults occurring between 21:00 and 12:00.

The time-of-day analysis by Burnham (Burnham, 1995) indicates that the profile of the time-of-day analysis and time of line faults are two parameters that can be used to differentiate between line faults caused by pollution and those caused by bird streamers. However, when the bird streamer faults were correlated with this model there were no noticeable similarities between the Florida Power & Light pollution correlation and the Georgedale-Venus bird streamer faults. A direct application of this model to the Georgedale-Venus power lines may therefore have resulted in the wrong conclusion being drawn. The correlation is presented in Figure 13. Clearly the profile of the Georgedale-Venus lines is significantly different from that of Florida Power & Light (Burnham, 1995). Although this analysis is extremely interesting, it clearly needs more detailed investigation before it can be accepted as conclusive.

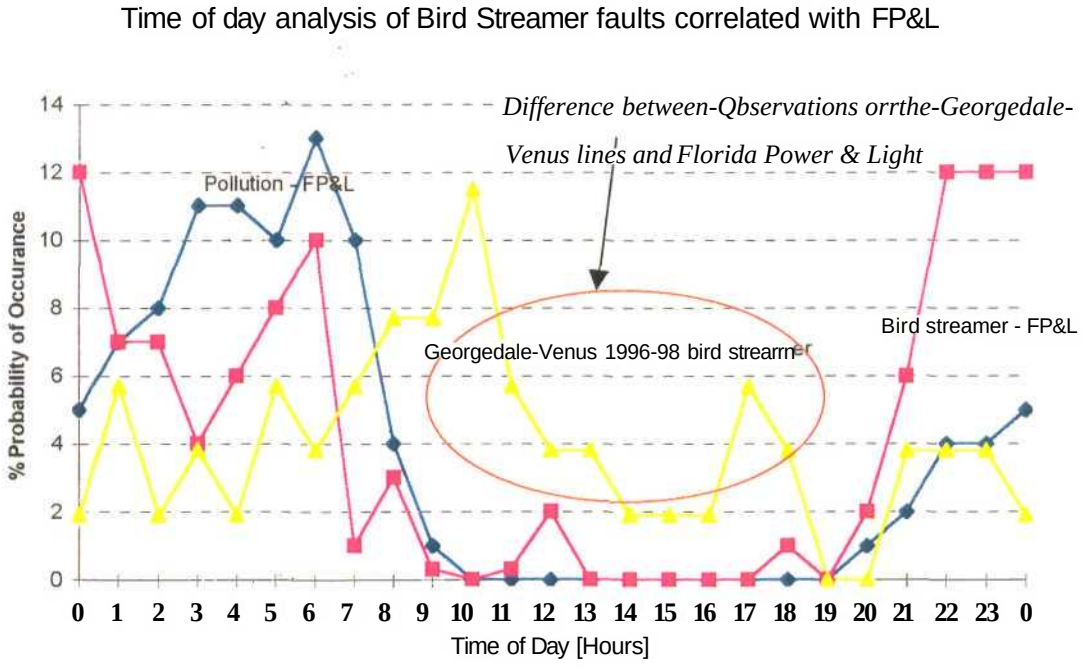

Figure 13. Bird streamer profile of the Georgedale-Venus lines

The only similarity between the Florida Power & Light (Burnham, 1995) and the Georgedale-Venus lines is the shape of the time-of-day analysis as opposed to the time of

the dominant peaks. To elaborate, both curves have a peak at 22:00, after which the curve drops off at 02:00. The curves then peak again at 06:00. This double peak characteristic is in stark contrast with the pollution single peak characteristic as proposed by Florida Power & Light (Burnham, 1995).

3.4. Total number of faults per month versus average rainfall

The bird streamer faults were also correlated with rainfall to determine whether there was any direct relationship between bird streamer faults and rainfall patterns. The rainfall data was obtained from two weather stations - Cedara and Estcourt. These weather stations are located 20 km from the power lines. A detailed listing of this data is tabulated in Appendix 2.

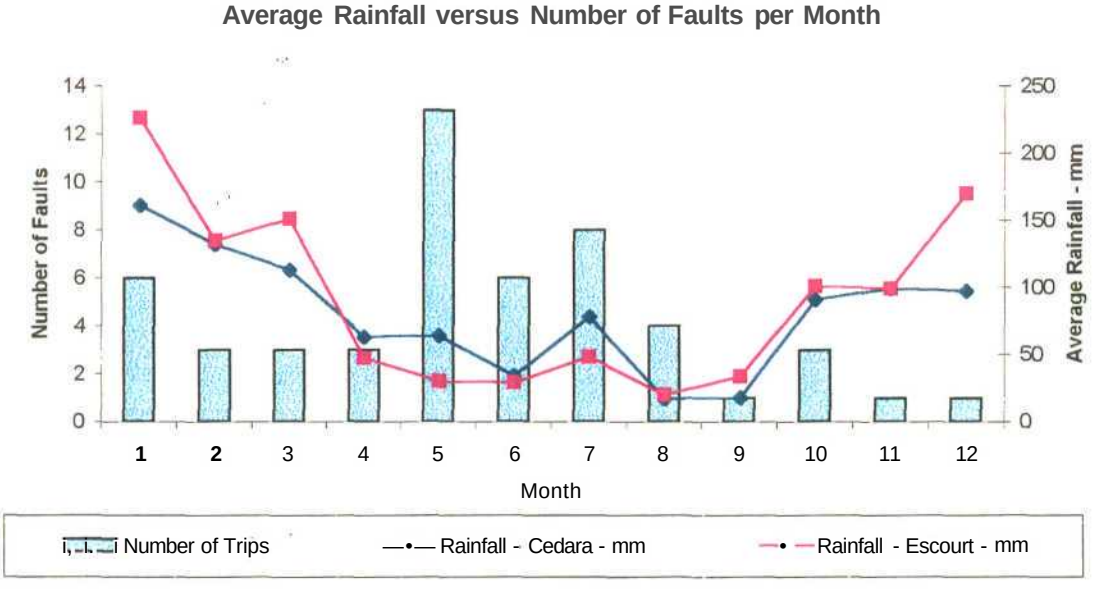

Graph 4: 1996-1998 faults per month versus average rainfall

The results presented in Graph 4 appear to indicate that most of the bird streamer faults occur during dry weather conditions (the winter months). For the purposes of this discussion, the dry months are defined as May, June, July and August and the wet months as the rest of the year. The results of this correlation are summarised in Table 8.

Wet months		Dry months	
Ave rainfall	**# of faults**	Ave **rainfall**	**# of faults**
97 mm (Cedara)	**19**	48 mm (Cedara)	**31**
120 mm(Estcourt)	**19**	32 mm (Estcourt)	**31**

Table 8. Faults versus wet and dry months

Table 8 shows that 62% of all faults on the Georgedale-Venus lines occur during the winter months. Burnham (Burnham, 1995) also documented that the statistical characteristics of faults caused by bird streamers and faults caused by pollution are very similar. In order to understand this winter trend it will be useful to extract the number of faults caused by vulture activity at Griffins Hill. These faults are summarised in Table 9.

	Date	Time	Line name	Cause	Phase	Line fault locators - distance [Georgedale/Venus] km
1	11.07.97	0.54	Georgedale-Venus 1	Birds	White	117.7/23.3
2	09.05.96	1.55	Georgedale-Venus 1	Birds	White	100.4
3	09.05.96	3.25	Georgedale-Venus 1	Birds	White	101.3
4	09.05.96	4.41	Georgedale-Venus 1	Birds	White	103
5	06.05.96	4.59	Georgedale-Venus 1	Birds	White	94
6	22.04.97	5.07	Georgedale-Venus 1	Birds	Blue	94/18.56
7	29.0796	5.51	Georgedale-Venus 1	Birds	White	106.2
8	22.08.96	6.33	Georgedale-Venus 1	Birds	White	101.4
9	21.06.97	16.43	Georgedale-Venus 1	Birds	White	110/18.26
10	06.06.96	18.19	Georgedale-Venus 1	Birds	White	94
11	28.07.96	22.12	Georgedale-Venus 1	Birds	White	107.7
12	20.06.97	22.25	Georgedale-Venus 1	Birds	Blue	112/14.47
13	31.05.97	8.21	Georgedale-Venus 1	Unknown	White	131.6/8.8
14	06.05.96	1.16	Georgedale-Venus 2	Birds	White	115.8
15	07.06.96	2.47	Georgedale-Venus 2	Birds	White	94.11
16	23.05.96	6.51	Georgedale-Venus 2	Birds	White	103
17	07.06.96	7.31	Georgedale-Venus 2	Birds	White	83
18	18.07.97	10.25	Georgedale-Venus 2	Birds	White	126.1/15.2
19	22.05.96	17.56	Georgedale-Venus 2	Birds	White	103
20	27.05.96	20.42	Georgedale-Venus 2	Birds	White	100
21	22.05.96	22.46	Georgedale-Venus 2	Birds	White	98.3
22	22.07.97	11.09	Georgedale-Venus 2	Unknown	White	124/16
23	09.07.97	15.32	Georgedale-Venus 2	Unknown	Blue	84/?

Table 9. Faults caused by vultures at Griffins Hill

All the faults listed in Table 9 occurred at Griffins Hill, 15 km north of Mooi River. Once bird guards had been installed at Griffins Hill, the white-phase trips decreased to zero on both lines 1 and 2. Both lines are glass-insulated in this area. When this sample was sorted, it was only sorted on position of fault. However, all the line faults at Griffins Hill occurred during the months of May to August. All these line faults were associated with bird streamers caused by Cape griffin vultures eating and roosting on the power lines.

Table 9 confirms that although bird streamer faults may have similar characteristics to pollution mechanism faults they should not be confused. Burn mark analysis and bird excreta observations should be used to differentiate between the two mechanisms.

Graph 4 shows that during the wet season there is a definite increase in line faults during the months of January to April as well as in October. These faults are also interesting, as one would expect bird activity during the wet seasons to be consistent during the months of November and December. The reason why this data appears inconsistent is that it could be skewed by as much as 50% due to the installation of bird guards on both lines. The installation of bird guards had been completed by the end of November 1996.

3.5. Total number of faults per month versus average humidity

The transmission lines in KwaZulu-Natal are exposed to considerable humidity variances. EPRI (EPRI, 1987) recorded that natural wetting of insulators occurs when the relative humidity reaches 85-90%. The correlation between the number of faults per month and relative humidity is presented in Figure 14, and a detailed listing is given in Appendix 2.

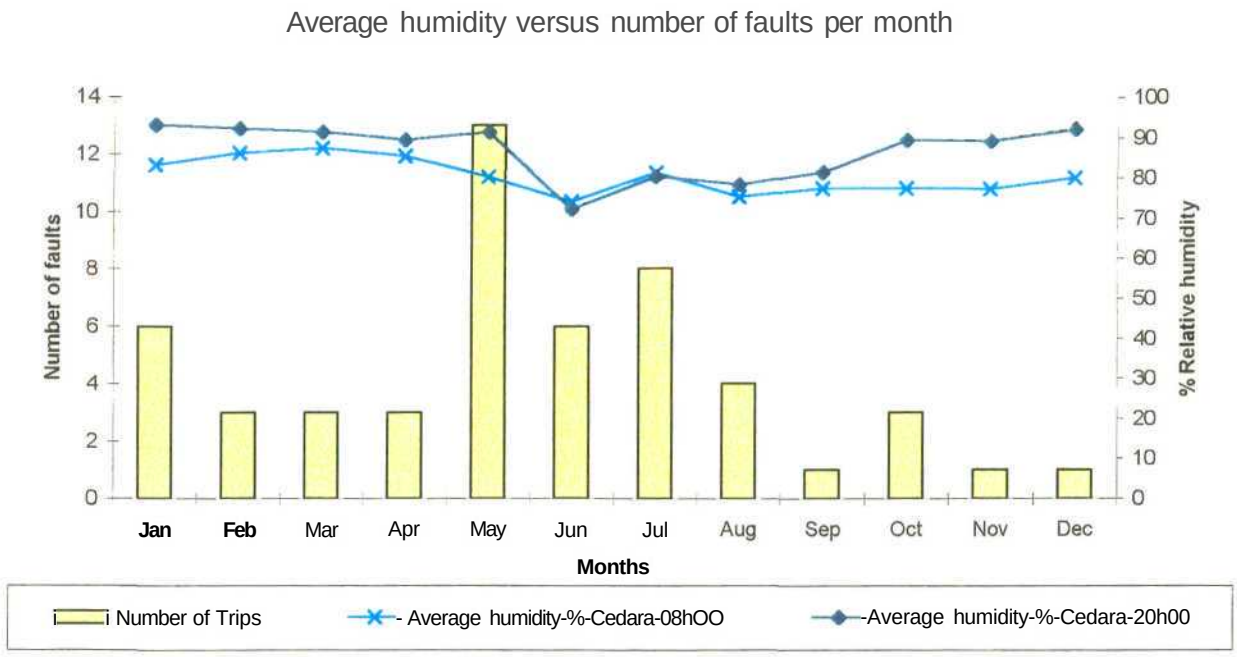

Figure 14. Faults per month versus average humidity

Figure 14 shows that natural wetting is likely to occur during most of the year, except June, July and August. During the months of April to September the average rainfall for Estcourt is less than 50 mm per month. These rainfall trends indicate that there will probably be an accumulation of pollution on the insulators and it is consequently expected that there may be pollution-related trips during this period. Figure 14 also indicates that during May and October there will probably be natural wetting of the insulators as **the** relative humidity is greater than 85%. It is interesting to note that both these months correspond with high trip incidence. This could explain why the unknown trips were historically associated with misty conditions and hence with the pollution mechanism.

However, the performance data, as summarised in Appendix 3, indicates that not many pollution trips occur on either of these power lines.

The correlation of bird streamer trips with rainfall and average humidity is not obvious. The peaks of the faults do not correspond with the traditional pollution month of August

for KwaZulu-Natal. However, what can be clearly concluded is that since the application of bird guards both lines have shown a significant decrease in faulting activity.

3.6. *Discussion of fault correlation*

Sections 3.4 and 3.5 attempted to correlate the Georgedale-Venus line faults with atmospheric conditions. However, there is no obvious correlation between the line faults and the various weather parameters. It is equally difficult to correlate the line faults with bird activity, because night-time bird habits (with respect to bird interaction with power lines) are largely unknown. However, the following bird behaviour characteristics have been observed.

The different bird species active on the Georgedale-Venus line route have complementary behavioural patterns. During the summer, spring and autumn months the majority of faults occur south of Griffins Hill. These faults can be attributed to the ibis and crane bird species. However, during the winter period most of the faults occur at Griffins Hill, while a few occur 10 km north of Griffins Hill. These faults are directly correlated with vulture activity in the area. It is interesting to note that the entire transmission network, including the 400 kV network, experiences significant faults during this period. The faults tend to occur in areas lying in an approximate 100 km arc from the Drakensberg.

The fault correlation with weather parameters showed the following trends:

1. Most faults occurred during the dry winter months.
2. The average humidity was above 85% at 20:00 for the entire year, except the winter months. This trend indicates that these lines are susceptible to natural wetting phenomena. However, no pollution-related line faults have occurred on these transmission lines.

The bird streamer faults appear to have weather characteristics very similar to those of pollution mechanism faults as recorded in the literature.

The role played by the travelling wave fault locator in fault finding cannot be overemphasised. Burn mark analysis is dependent on the location of the faulted tower being identified. Only when this is achieved, is it possible to determine the difference between pollution mechanism faults and bird streamer air gap breakdown mechanism faults.

3.7. Conclusion

This chapter attempted to identify a specific trend in the number of faults and weather parameters as an indication of a bird streamer fault mechanism. However, it has been determined that there is no obvious correlation between this fault mechanism and weather parameters. What is of interest is that during the dry periods of the year the line faults do not decrease; in certain instances they even increase.

The only successful statistical tool to differentiate between faults caused by pollution and faults caused by bird streamers is time-of-day analysis. This report suggests that further work needs to be done to develop time-of-day analysis as a conclusive tool in determining the causes of line faults.

Chapter 4

EXPERIMENTAL INVESTIGATION INTO AC BREAKDOWN BEHAVIOUR OF SMALL DIVERGING FIELD AIR GAPS

Having determined that bird streamers were the most probable cause of the poor performance of the Georgedale-Venus power lines, thought was given to quantifying the effects of bird streamer intrusion into tower window air gap clearances. The aim of these experiments was to determine the effects of the reduced air gap clearances due to the corona ring intrusion of the silicone composite insulators. Tower clearance measurements indicated that when the glass V string insulators were replaced with silicone composite insulators the air gap clearance was reduced from 2.1 to 1.97 metres.

The University of Natal High Voltage Laboratory was used to simulate the bird streamer intrusion and determine suitable air gap withstand criteria.

4.1. Experimental hypothesis

The bird streamer intrusion was initially modelled by using a brass electrode, and subsequently by using wet string soaked in a conductive salt solution. The advantage of using a brass electrode is that the effects of insulator types and corona rings can be determined more easily as the experiments are more controllable.

Eleven experiments were performed to determine the critical distance of a falling liquid streamer. The term critical distance is defined by Figure 6. These experiments investigated the effects of AC voltage breakdown as a function of:

1. Insulator types:
    a. Glass U 120 BS discs (all insulator assemblies used 16 glass discs)
    b. 275 kV silicone composite insulator
2. Insulator configurations:
    a. V string.
    b. I string
3. Effects of electrode type:
    a. Brass electrode
    b. Wet string electrode
4. All results were correlated with the classical rod-plane breakdown.

The experiments performed were:

1. Rod-plane breakdown characteristics - effects of electrode tip and rod diameter (section 4.2)
2. Effects of a corona ring (on silicone composite insulators) on breakdown characteristics (section 4.3)
3. Effects of electrode (brass) position on air gap breakdown, using a V string silicone composite insulator assembly with corona rings (section 4.4)
4. Effects of electrode (brass) position on air gap breakdown, using a glass I string with 16 U120 BS insulators (section 4.5)
5. Effects of electrode (brass) position on air gap breakdown, using silicone composite I string insulators with corona rings (section 4.5)
6. Effects of electrode (brass) position on air gap breakdown, using a glass V string insulator assembly, with 16 U120 BS insulators per string (section 4.4)

7. Effects of wet string resistivity (wet string electrode) on air gap breakdown, using a glass V string assembly (section 4.6)
8. Effects of wet string electrode on air gap breakdown, using a glass V string assembly (section 4.7)
9. Effects of wet string electrode on air gap breakdown, using a silicone composite V string assembly with corona rings (section 4.7)
10. Effects of wet string electrode on air gap breakdown, using a silicone composite I string insulator assembly with corona rings (section 4.8)
11. Effects of wet string electrode on air gap breakdown, using a glass I string insulator assembly (section 4.8)

All glass strings comprised 16 U120 BS insulators. The experimental data is documented in Appendix 3, and it includes the breakdown voltage and standard deviation.

4.1.2. Experimental setup

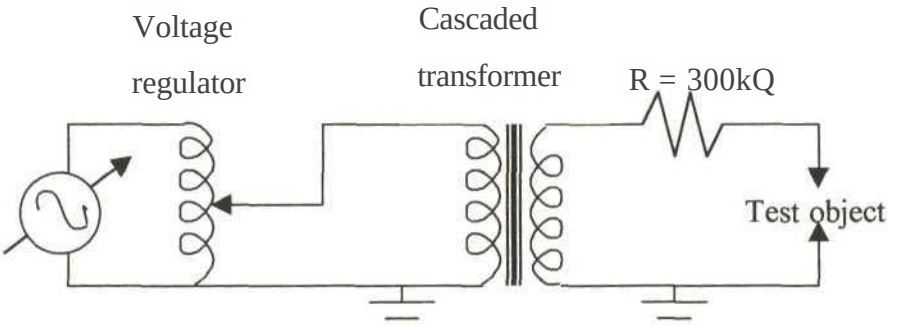

Figure 15. Experimental setup

Figure 15 illustrates the basic test circuit for all the AC experiments. A Brentford AC voltage regulator was used to increase the test voltage linearly until flashover occurred. A cascaded transformer test set of variable voltage from 0-240 kV rms was used.

Each test circuit is discussed in detail in association with the experimental results.

4.1.2. Experimental procedure

Each data point represents the mean of six applied breakdowns. The standard deviation was also computed for each data set. The results were corrected to standard temperature and pressure (STP) as per the DEC specification (DEC 60-1, 1989). All quoted voltage values are single phase-to-earth rms values.

For the purposes of this report these results will be reported under the following subsections:

1. Rod-to-plane AC breakdown voltage versus electrode type and rod diameter
2. Investigation into the effects of corona rings on bird streamer intrusion
3. Electrode position versus AC air gap breakdown for V string configurations
4. Electrode position versus AC air gap breakdown for I string configurations
5. Effects of wetted string resistivity on AC breakdowns
6. AC breakdown characteristics when using V string assemblies under various electrode type intrusions
7. AC breakdown characteristics when using I string assemblies under various electrode type intrusions

4.2. Rod-to-plane AC breakdown voltage versus electrode type and rod diameter

This experiment was conducted to determine the characteristic AC voltage breakdown relationship as a function of electrode tip type and rod diameter (d) at various primary gap lengths (l), as illustrated in Figures 16 and 17.

4.2.1. Experimental setup

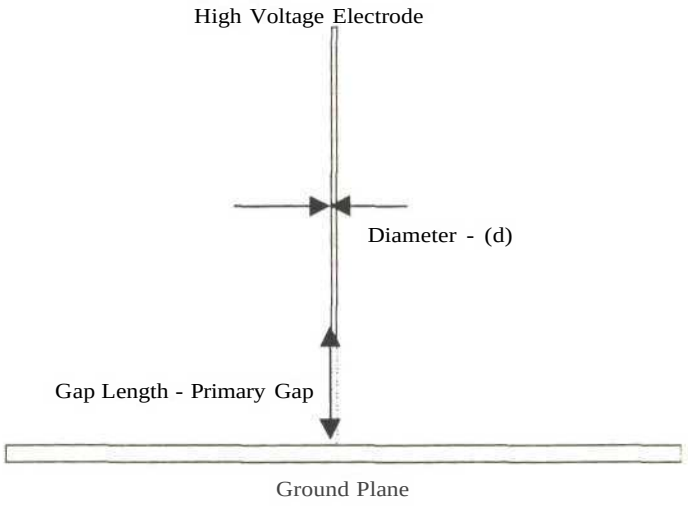

Figure 16. Rod-plane experimental layout

A brass electrode was used in this experiment and the electrode was rigged in a vertical position perpendicular to the ground plane, as illustrated in Figure 16. During these experiments the following electrode tips were investigated.

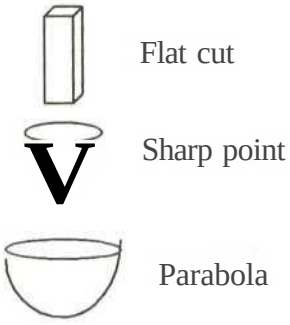

Figure 17. DIustration of rod electrode tips

4.2.2. Results of AC breakdown voltage versus electrode tip type rod-to-plane configuration

During these experiments a large amount of corona activity was observed on the live electrode. The presence of the space charge distortion produced by the corona would effectively increase the electrode radius. Consequently, as the corona cloud gets bigger the shape of the electrode tip becomes less significant.

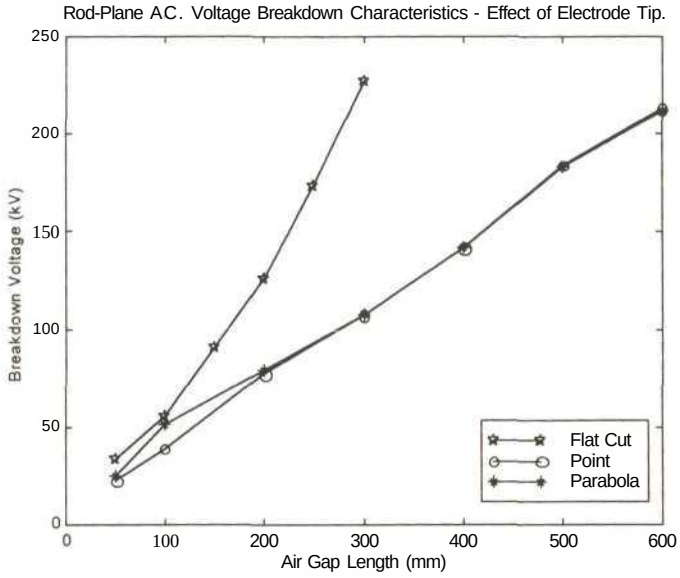

Figure 18. Rod-plane AC breakdown trends versus electrode tip type

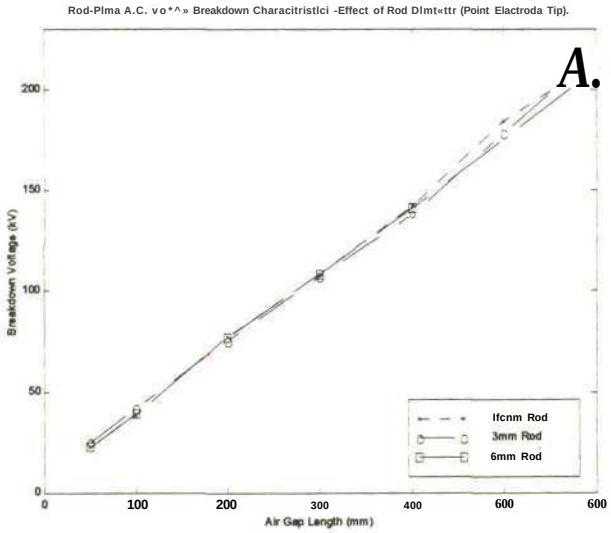

Figure 19. Rod-plane AC breakdown trends versus electrode diameter

Note: The average standard deviation for these results was less than 3%. The results obtained can be summarised as follows:

1. At low flashover voltages (< 50 kV) where no corona activity was observed, there was a variance between the AC breakdown characteristics and the different rod tips and rod diameters. However, as the applied voltage increased, the shape of the electrode tip and the rod diameter became less significant.
2. The only exception was the 12 mm flat cut electrode, which showed a drastically altered AC breakdown characteristic. This is probably due to there being no sharp edge to cause electric field enhancement near the live electrode.

These results compare favourably to Rizk (Rizk, 1997).

4.3. Investigation into the effects of a corona ring on bird streamer intrusion

The purpose of this experiment was to determine the effects of the corona ring on breakdown voltage under bird streamer intrusion. To achieve this, the primary gap breakdown voltage was correlated for the case in which there was a corona ring installed and for the case in which there was no corona ring installed.

Prior to this experiment it was thought that by installing corona rings on in-service composite insulators, this electric field grading would decrease the probability of insulation failure under bird streamer intrusion. This experiment was important considering that there is in-service silicone composite insulation without corona rings.

4.3.1. Experimental setup

The silicone composite insulators were rigged in the I string configuration. The experiment was constructed as illustrated in Figure 20. During this experiment the primary gap lengths were kept the same.

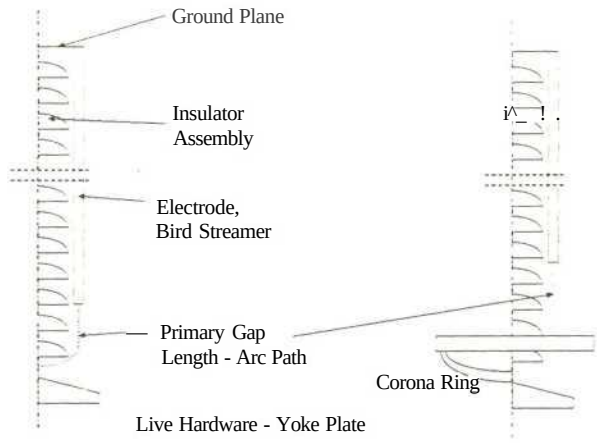

Figure 20. I string assembly illustrating the different air gap lengths with and without corona rings

4.3.2. Results of corona ring investigation

At small gap lengths (< 200 mm) the surface roughness effects of the corona rings appear to enhance the electric field as the breakdown strength is significantly less in this case than in the scenario where no corona ring was fitted. However, as the air gap spacing increases, space charge effects appear to negate the surface roughness effects of the corona rings in the breakdown process. The insulator fitted with corona rings has a greater voltage withstand (9%) than the insulator with no corona rings at 158 kV (or 275 kV service voltage).

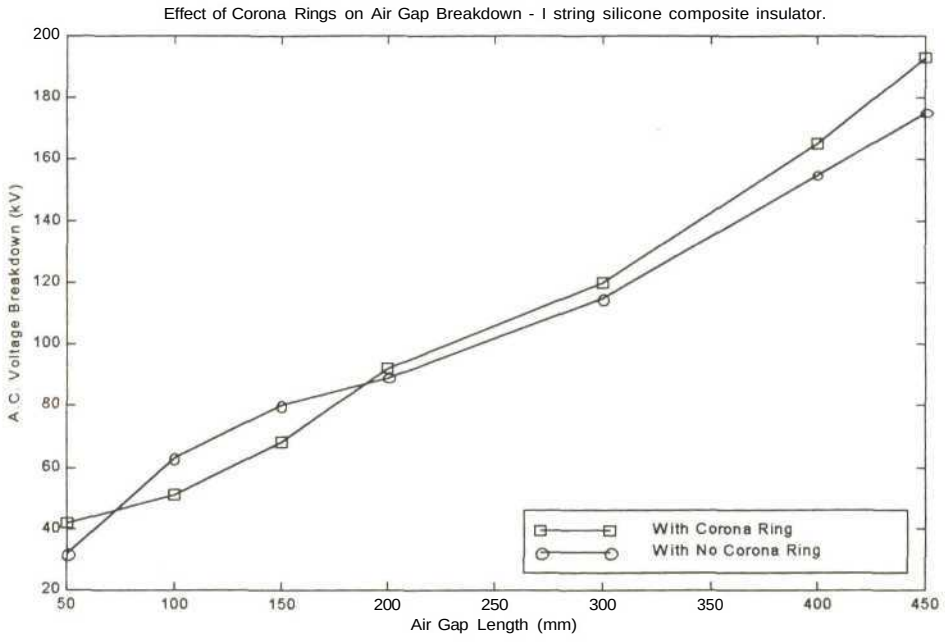

Figure 21. AC breakdown trends versus corona ring application

Note: The average standard deviation was less than 3.5%.

These results would appear to contradict the fault trip incidences incurred on the Georgedale-Venus two 275 kV powerline in 1996. A possible explanation is that the corona rings do decrease the minimum air gap clearance by 100-150 mm. This is also supported by the on-site measurement of minimum clearances of 1.97 m (silicone composite insulator with corona rings) and 2.1 m (glass insulators), although the yoke plate and conductor assemblies are not moved with respect to each insulator type. This decrease of 100 mm at service voltage potential could result in an equivalent decrease in breakdown potential from 158 kV to 120 kV for a streamer of fixed length. This amounts to a 24% decrease in insulation strength against bird streamer intrusion. This is more significant than the 9% breakdown potential gain with the use of corona rings.

This is an important requirement to consider when reinsulating glass-insulated lines with silicone composite insulators. The insulator connecting length in the latter case could be increased by as much as 200 mm to accommodate the corona ring intrusion.

4.4. Electrode position versus AC air gap breakdown for V string insulator assemblies

This experiment was implemented to determine the breakdown trends as a function of the streamer position along the V insulator configuration for both silicone composite and glass insulator assemblies. It was done to determine the minimum distance for which a bird should be moved along the tower top to prevent a falling streamer from causing air insulation breakdown.

4.4.1. Experimental setup

This experiment investigated the air gap breakdown characteristics of a bird streamer intruding into the V string assembly for three different electrode positions: vertical, across the string, and horizontal. The experimental setup is illustrated in Figures 22, 23 and 24.

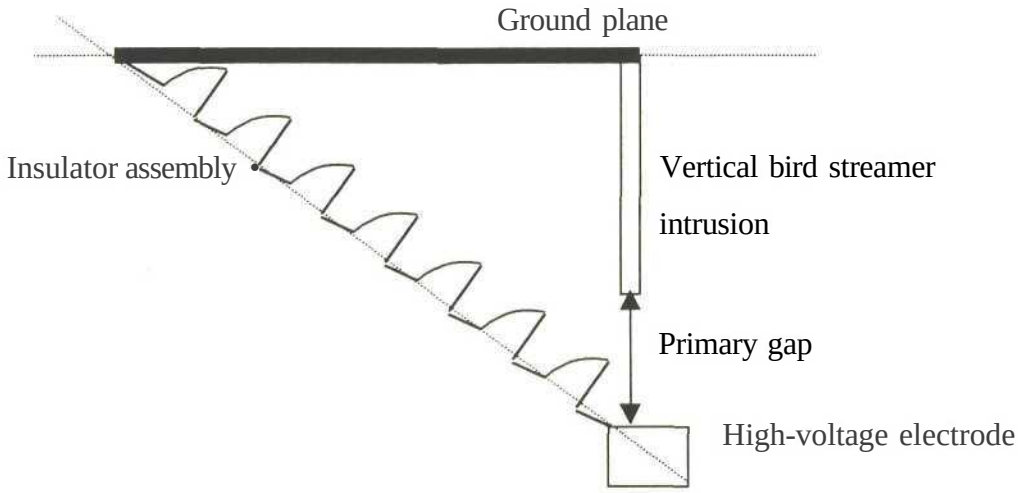

Figure 22. V string configuration - indicating the electrode positions for vertical bird streamer intrusion

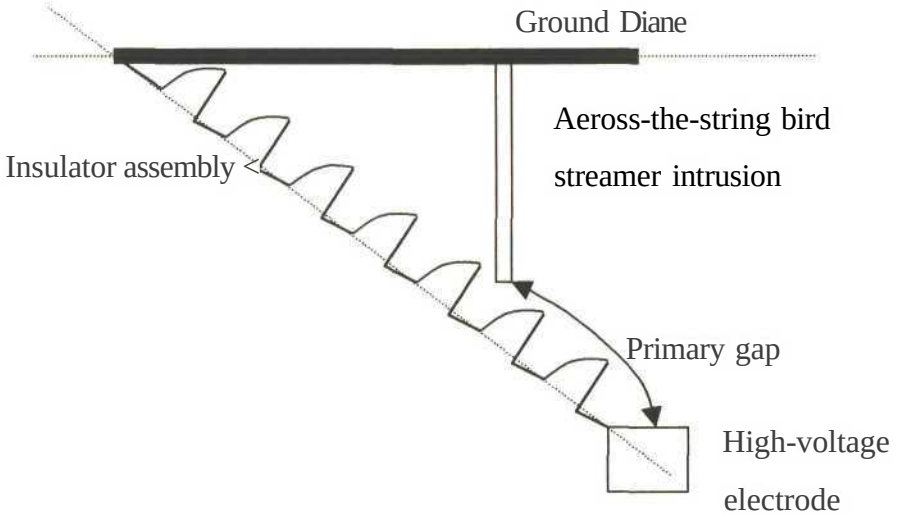

Figure 23. V string configuration - indicating the electrode position for across-the-string bird streamer intrusion

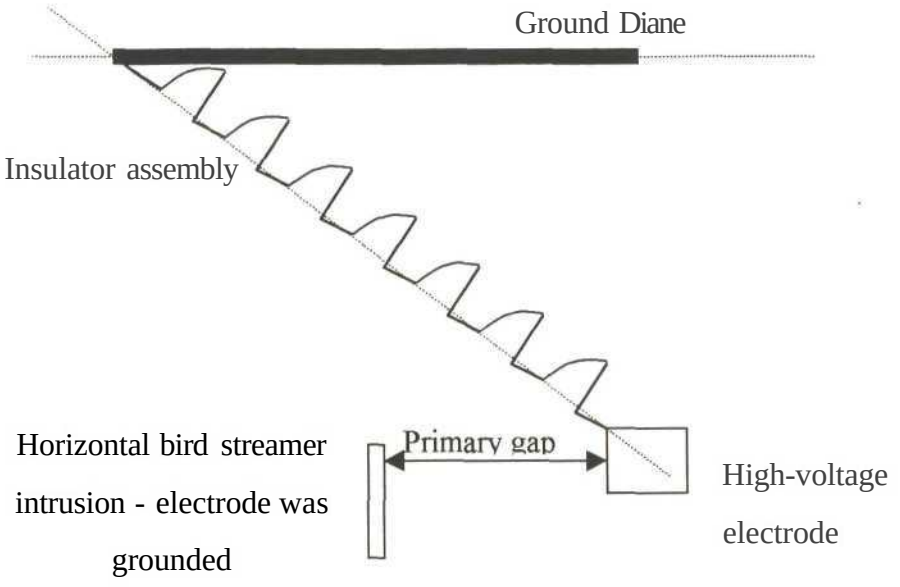

Figure 24. V string configuration indicating horizontal bird streamer intrusion

This experiment is of particular importance, as it will determine the critical distance where, if a bird streamer enters, flashover is likely. This distance is thought to be dependent on the insulator assembly type, as this will determine the electric field distribution at the live end hardware under nominal operating conditions.

4.4.2. Experimental results

The experimental results for the above configurations are summarised below. The average standard deviation for these results was less than 3%.

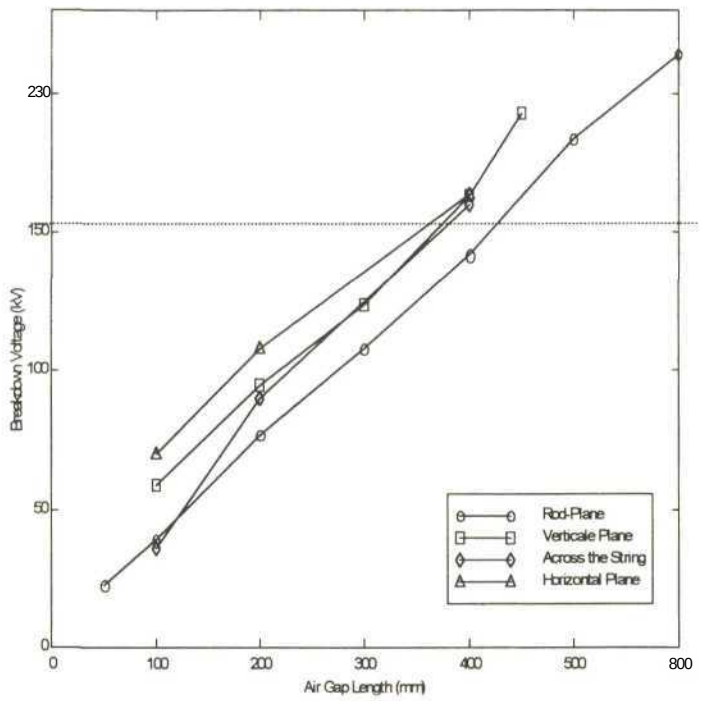

Figure 25. AC breakdown trends as a function of silicone composite insulation and electrode position - V string insulator configuration

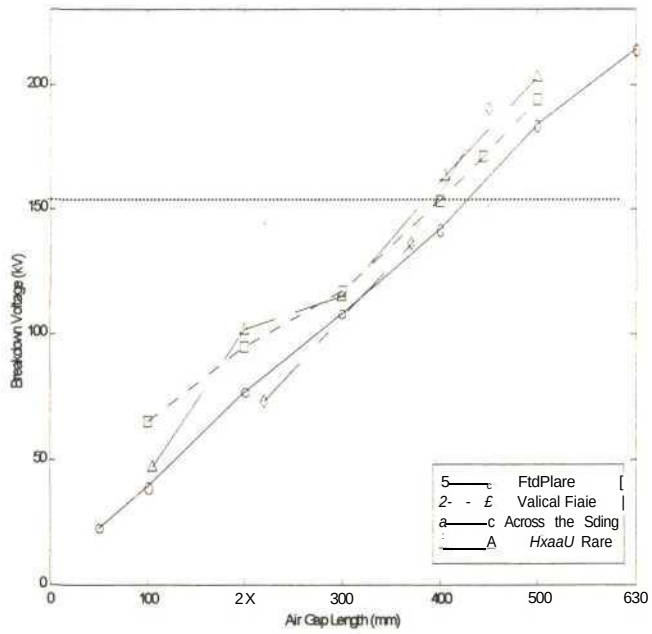

Figure 26. AC breakdown trends as a function of glass insulation and electrode position - V string insulator configuration

At 158 kV rms (on both glass and silicone V string assemblies) the air gap breakdown length is essentially the same for all electrode positions. This observation is interesting as the breakdown voltage appears to be a function of the primary gap length and not of the creepage path of the insulators (under dry conditions).

For an applied voltage of 158 kV the primary flashover gap for a brass earth electrode is 370 mm for silicone composite insulators and 390 mm for glass insulator assemblies (5%).

The probable reason why the Georgedale-Venus trip incidence doubled when silicone composite insulators replaced the glass string insulators is not easily quantified. It would appear that the former insulators do perform better than glass (5%) under bird streamer intrusion, but the corona rings decreased the air gap clearances by 100 mm. Assuming that the bird streamer lengths remained constant, the primary air gap for the silicone composite insulators was effectively reduced from 370 mm to 270 mm. This caused an effective decrease of 24% in the voltage withstand of the primary gap clearance. It is probable that the decrease of air gap clearance caused by the corona rings' intrusion into the air gap is the dominant factor.

These results indicate that it is reasonable to only record the air gap breakdown in the vertical plane when studying V string configurations.

4.5. Electrode position versus AC air gap breakdown for I string configurations

4.5.1. Experimental setup

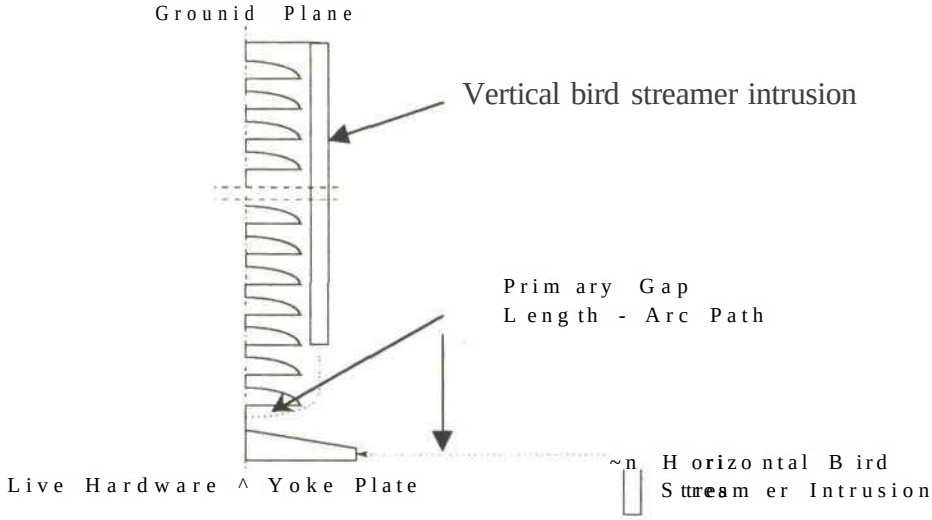

Figure 27. I string bird streamer simulations indicating vertical and horizontal intrusion positions

The purpose of this experiment was to investigate the breakdown characteristics of an I string insulator and explain why the I string insulators had not experienced many bird streamer related earth faults.

4.5.2. Experimental results

The silicone composite I string configuration had very different characteristics for bird streamer intrusion with respect to the horizontal and the vertical planes, the latter showing a 15% greater voltage withstand. The glass I string does not show this trend. For the latter scenario the breakdown strengths tend to be independent of electrode position.

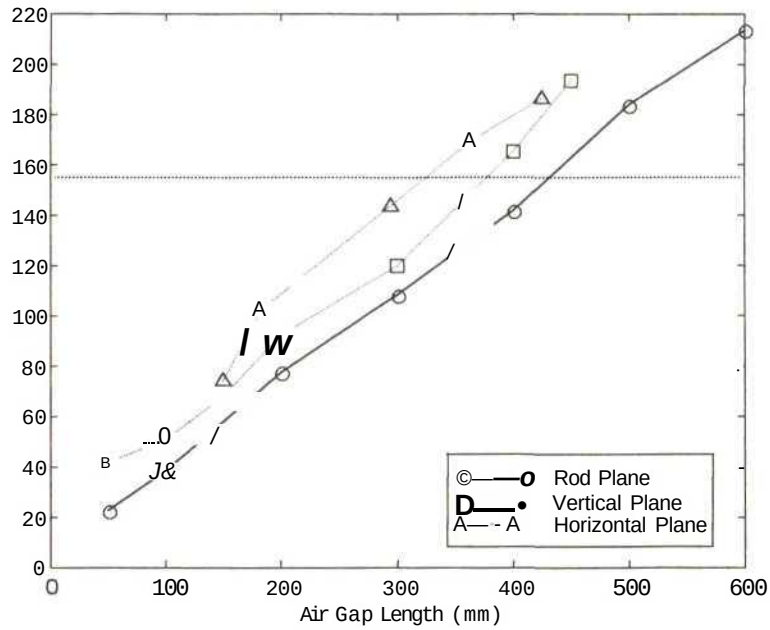

Figure 28. AC breakdown trends versus electrode position - silicone I string

The average standard deviation was < 3%.

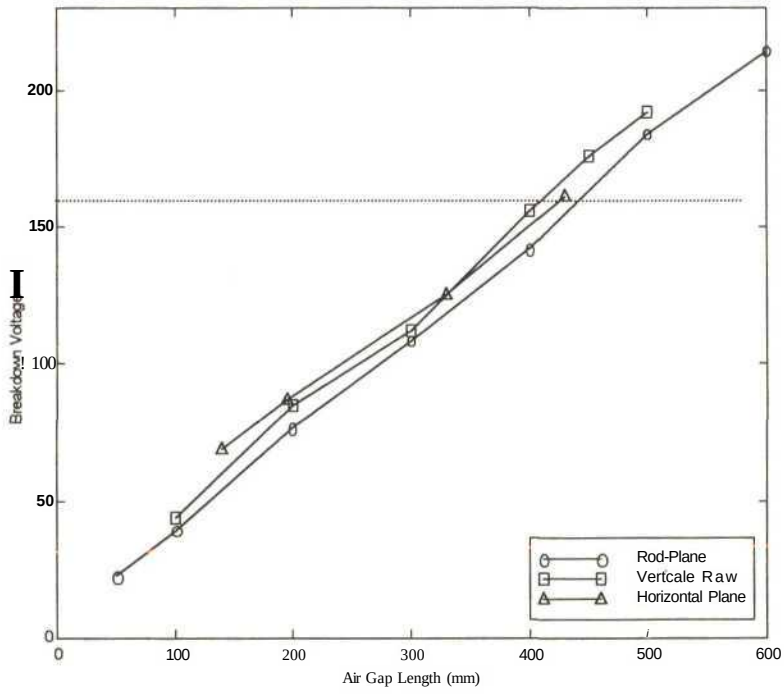

Figure 29. AC breakdown trends versus electrode position - glass I string

The average standard deviation was < 3%.

These results led to the conclusion that the voltage grading effect of the cap and pin glass insulators causes a more even distribution of electric field density in the air gap than that of the silicone composite insulators. The latter insulators would be expected to have a greater electric field concentration at the live hardware, but this would be expected to drop off more rapidly with distance than the field distribution obtained with the glass insulators.

For silicone composite insulators, the primary gap breakdown lengths at 158 kV are 330 mm and 380 mm for the horizontal and vertical configurations respectively. The glass insulator primary gap lengths are very similar at 158 kV for both the above configurations. The primary gap length is 390 mm.

For all future I string simulations, only the vertical air gap breakdowns will be implemented as these results will determine a worst-case scenario (for the composite 1 string) and will be representative for the glass I string case.

4.6. Effect of wet string resistivity on AC breakdowns

The previous experiments modelled the bird streamer as a brass rod. The purpose of this experiment was to determine the effects of a liquid streamer (stationary) on the primary gap breakdown characteristics.

The breakdown results are tabulated below:

Air gap length [mm]	Streamer resistivity [kQ.m^{-1}] NaCl solution	Breakdown voltage [kV]	Standard deviation [kV]	Corrected breakdown voltage [kV]	Corrected standard deviation [kV]
400	40	196.1	2.7	194.01	2.7
400	10 000	192	5.5	195.9	5.6

Table 10. Summary of AC breakdown voltage versus variation in streamer resistivity

Note: The average standard deviation was less than 5%.

The aim of the experiments using a wet string to simulate a bird streamer was to determine the effects of streamer resistivity with respect to the primary air gap voltage withstand. These experiments concluded that for a resistivity variation between 40 and 10 000 kf2.m"[1] there was no breakdown voltage variation for a gap spacing of 400 mm.

In Appendix 3, which contains the results tabulated for the AC voltage breakdown trend, the average resistivity of the wet string is tabulated as well.

4.7. Final summary of V string AC voltage trends for various electrodes

The experimental setup is the same as that of the previous V string simulations. This experiment correlated the AC voltage trend in the vertical plane only.

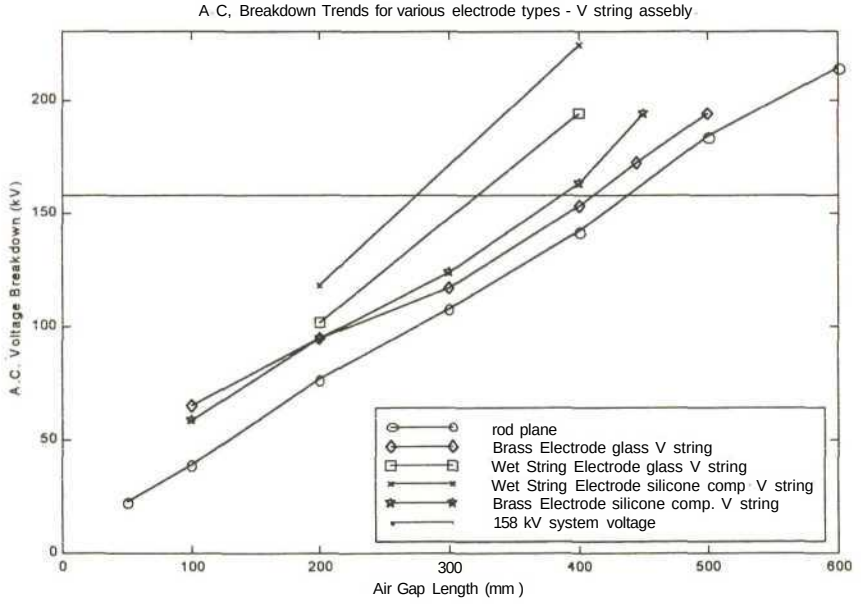

Figure 30. V string AC voltage trend summary

Intuitively it was expected that the electric field distortion under a liquid streamer intrusion in the air gap would be considerably less than in the case of a conducting brass rod. The results tend to support this reasoning; the wet string streamer yielded 24% and 18%

greater withstand characteristics than the brass electrodes for silicone composite and glass-insulated assemblies respectively. Table 11 summarises the primary gap distances for the various electrodes:

Electrode types	Air gap length (mm) to prevent breakdown at 158 kV (minimum)
Rod-plane	430
Brass electrode (12 mm point), glass V	390
Brass electrode (12 mm point), silicone V	370
Wet string electrode, glass V	320
Wet string electrode, silicone V	280

Table 11. Summary results of air gap breakdown clearances - V string

4.8. Final summary of I string AC voltage trends for various electrodes

The experimental setup of this experiment is the same as that shown in Figure 25. Like the V string experiment, this experiment correlates the AC voltage breakdown trends with bird streamers in the vertical planes.

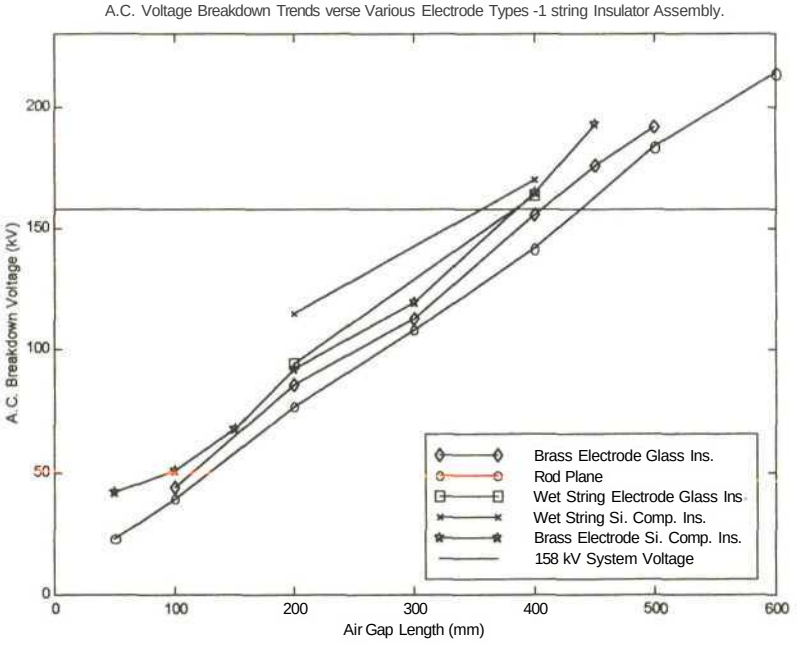

Figure 31. Summary of I string AC voltage trends for various electrodes

The I string simulations again yielded surprising results, in that the wetted string for the glass I string simulation yielded the same result as the brass rod of the silicone composite I string simulation. The results obtained are summarised below:

Electrode types	**Air gap length (mm) to prevent breakdown at 158 kV (minimum)**
Rod-plane	430
Brass electrode (12 mm point), glass I	405
Brass electrode (12 mm point), silicone I	380
Wet string electrode, glass I	380
Wet string electrode, for silicone I	355

Figure 32. Summary of air gap breakdown clearance results - I string

4.9. Conclusion and discussion of results

For large air gaps, space charge effects are dominant under AC voltage breakdowns. Consequently the breakdown voltage is independent of the electrode diameter and electrode tip shape. The rod-plane results compare favourably with Rizk's results. Rizk (Rizk, 1997) also correlated the effect of moisture in the air with AC voltages. These results show conclusively that for air gaps smaller than 1 m there is no significant reduction in breakdown voltage trends when mist is present.

The primary gap withstand results clearly illustrate that silicone composite insulators perform better than glass insulator assemblies under bird streamer intrusion, ie the streamer has to penetrate closer to the line hardware for a flashover to result. This is an important factor when reinsulating transmission lines, but the air gap clearances for the composite insulators must not be encroached upon by the corona rings on the live hardware side.

When comparing the actual primary gap lengths of glass and silicone composite insulator assemblies, and also considering the V and I insulator configurations, it is apparent that if the primary gap length is greater than 410 mm it will be sufficiently large to prevent

primary gap breakdown. Consequently a primary air gap of 410 mm was used as the design criterion for a 275 kV system voltage at standard temperature and pressure.

The length of the primary gap needs to be increased to accommodate the practicalities of transmission tower live hardware (eg that some lines may be fitted with corona rings in a horizontal plane) and the practicalities of bird excretion. The exact trajectory of a bird streamer after excretion is not known and has not been studied during this project. To accommodate the above factors, a safety factor of 2 was applied to the primary gap length. This thesis recommends that the bird streamers be moved at least 820 mm away from the live hardware for a 275 kV system operating voltage (at STP). This distance assumes that the conductor bundle width is 380 mm for the 275 kV transmission line. Consequently the critical distance a bird streamer would have to be moved on a 275 kV line would be 1 000 mm from the tower centre (the sum of 820 mm and 180 mm).

As stated above, a safety factor of 2 was used because the exact trajectory of the bird streamer, when excreted, is unknown. Furthermore, the effects of wind on the bird streamer trajectory were not considered. Considering performance where bird guards have been installed, this safety factor appears to be adequate.

Chapter 3

ELECTRIC FIELD MEASUREMENTS AT THE GROUND PLANE

The results discussed in Chapter 4 indicated that a bird streamer needs to be moved away from the live tower hardware by a relatively small distance - only 820 mm for a 275 kV system voltage. To confirm this finding, electric field measurements at the ground plane were implemented to determine the probability of air gap breakdown under these conditions.

Electrical streamers have been observed to propagate in air where the electric field exceeds 31 kV/cm and the streamers will stop propagating if the electric field falls below a value of 4-8 kV/cm. The objective of this chapter is to make use of electric field measurements at the ground plane to quantify the probability of air gap breakdown under intruding bird streamers.

5.1. Block diagram of a capacitive probe

The voltage (V_C2) is capacitively coupled to the source voltage via the capacitance of the external circuit. The magnitude of the external capacitance was determined as being in the order of 5 pF (Marode, 1975). The value of C_2 must be such that the circuit is not loaded and the probe measurements are therefore accurate. This signal is inputted into an oscilloscope via a high input impedance buffer amplifier. The experimental setup is illustrated below.

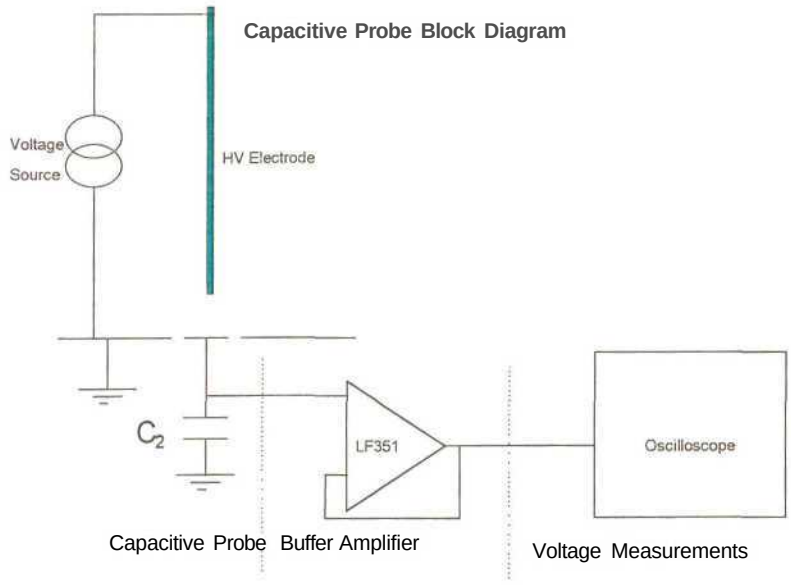

Figure 33. Capacitive probe block diagram

5.2. Introduction to electric field measurements

A capacitive probe may be used to measure the electric field at the ground plane under bird streamer intrusion. This measurement will be used to substantiate the finding that in order to prevent bird streamer faults the bird streamer should be moved away from the live hardware.

At an earthed plane, the charge (Q) induced on this plane is proportional to the electric field (E_n) at the plane. This relationship is known as Gauss's law.

$$\int_s E_n . ds = \frac{Q}{\varepsilon_0}$$ **Equation** 7

Consider an equipotential field distribution for a point-plane geometry. If it is assumed that for a small area at the ground plane (the area of the capacitive probe) the electric field distribution is uniform across this area, equation 6 (Chapter 2) simplifies to:

$E_{n} = Q/Aso$ **Equation 8**

Electric field at the plane can be measured by determining the charge induced on the surface. Using the definition of capacitance:

$C = Q/V$ **Equation 9**

Substituting 10 into 9, the following relationship is obtained:

$En = V.C/AEO$ **Equation 10**

This is known as a capacitive electric field probe. This probe has a limitation that has important practical implications. The total charge induced on the earth plane does not originate solely from the applied electric field but also, if any is present, from the conduction current.

$$Q = \varepsilon_0\left(\int_s E_n . ds + \int_0^t J . A dt\right)$$ **Equation 11**

Consequently this technique measures the total electric flux at the plane. Waters (Waters, 1968) has done research into this phenomenon and has developed field filter probes that are capable of filtering out this conduction current.

Equation 10 infers that the electric field is proportional to the voltage induced on the capacitive probe.

$E = V.C/Aeo$

$=$ kV kV/cm **Equation 12**

The capacitive probe used in this investigation had a surface area, $A = \% 0.01^2$ m^2.

Equation 10 may be simplified to equation 12 since both the capacitance and the surface area of the probe are constant. The accuracy of the probe is dependent on the measurement of charge in the air gap. The total charge in the air gap does not originate solely from the electric field in the air gap but also from the conduction current (caused by streamer activity in the air gap, equation 11). It is important to quantify the effect of the conduction current on the accuracy of the electric field measurement.

Equation 5 (Chapter 2) details the electric field and the point-plane relationship. Equation 5 will be used to determine the effect of the conduction current on the electric field measurements.

5.3. Experimental setup

Figure 33 illustrates the experimental setup for the electric field measurements. A variable supply voltage of 0-30 kV was used. The voltage was increased manually and the results were recorded at the respective voltages.

5.3.1. Capacitive probe calibration - parallel plane geometry

Using parallel plane electrode geometry, with an air gap of 250 mm, the following results were recorded:

V_{source} kVrms	$\bar{t}_{calculated}$ = V/d kV/cm	V_{out} Vrms	C = EsA/V PF
5.05	0.18	0.99	50.55
10.03	0.36	1.98	50.55
14.99	0.53	3.04	48.47
20.00	0.71	4.03	48.98
25.04	0.89	5.09	48.61
29.40	1.04	5.94	48.68
Average capacitance			49.31 ±2.1

Table 12. Calibration of capacitive probe

Table 12 shows that for an electric field of between 0.18 and 1.04 kV/cm the capacitive probe has a standard deviation of 4.3%. In subsequent experiments the input capacitance of the probe was taken as 49.31 pF. The above air gap was 250 mm, which resulted in low electric fields. Another experiment was implemented to determine when this capacitive probe saturated. This experiment had an air gap spacing of 84 mm.

V source kV rms	E calculated = V/d kV/cm	Vout V rms	E = CV/eA kV/cm, rms	% error	Comments
1.1	0.13	0.71	0.126	3.1	Okay
2.0	0.23	1.237	0.219	4.8	Okay
5.01	0.59	3.39	0.60	-1.7	Okay
7.07	0.84	4.738	0.84	0	Okay
10.07	1.20	6.789	1.20	0	Okay
15.11	1.80	10.18	1.80	0	Okay
20.58	2.45	14.65	2.60	-5.7	Okay
29.53	3.51	9.6	1.7	52	Probe saturated

Table 13. Results of capacitive probe saturation properties

Table 13 shows the results of the capacitive probe saturation characteristics. The probe appears to saturate when the input voltage becomes greater than 15V peak. The probe can measure electric fields up to 2.6 kV/cm rms. The percentage error versus applied electric field is illustrated below.

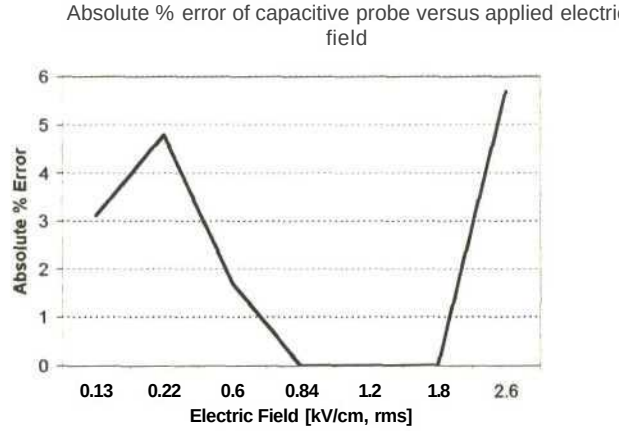

Figure 34. Absolute % error versus applied electric field of the capacitive probe

5.3.2. Capacitive probe calibration - sphere plane geometry

A sphere plane geometry was also used to calibrate the capacitive probe. The same experimental setup was used, as illustrated in Figure 33.

The radius of the sphere was 43.5 mm and the air gap length 250 mm. The results obtained are summarised in Table 14. These values were substituted into equation 5 (Chapter 2). Equation 5 then simplifies into:

$$E = \frac{2*V}{(0.0435 + 0.5)*\ln(^{a5435}/_{00}4_{35})}$$

$$= \frac{2*V}{1.372}$$

V ™ source kV rms	$\vec{E}$ calculated = 2V/1.372 kV/cm	V_{out} V rms	E = CV/eA KV/cm, rms	% error
2.02	0.029	0.148	0.026	10
3.98	0.058	0.31	0.055	5.1
8.06	0.117	0.65	0.115	1.7
9.97	0.145	0.79	0.14	3.4
15.10	0.220	1.20	0.21	1
20.04	0.292	1.626	0.288	1.3
25.02	0.365	2.05	0.363	0.5
29.53	0.430	2.475	0.439	-2

Table 14. Sphere plane electric field measurements

The results obtained show clearly that for an electric field greater than 0.05 kV/cm and smaller than 0.5 kV/cm (rms values) the capacitive probe has an accuracy of 2%.

5.4. Electric field measurement under bird streamer intrusion

On the 275 kV transmission grid the welded rod bird guards effectively moved the bird streamers 700 mm away from the nearest high-voltage line hardware. The purpose of this experiment was to quantify the likelihood of a primary air gap breakdown under bird streamer intrusion. It has been well documented that streamers will propagate into an air gap when the electric field is greater than 4 kV/cm (Hutzler, 1978). Should the electric field at the ground plane be close to 4 kV/cm, the bird streamers would have to be moved further away from the high-voltage transmission line hardware.

5.4.1. Experimental setup

Rod-plane electrode geometry was used as the HV test circuit. The rod electrode had a point tip. The experimental setup is illustrated below.

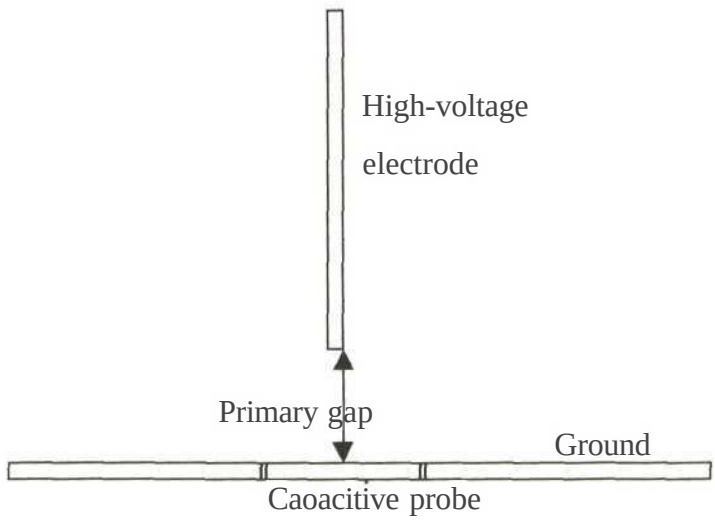

Figure 35. Electric field experimental setup

5.4.2. Experimental procedure

The applied voltage was increased manually and the electric field measurements were recorded at specific applied voltage magnitudes. The results were corrected to STP.

5.4.3. Results of electric field measurements under simulated bird streamer intrusion

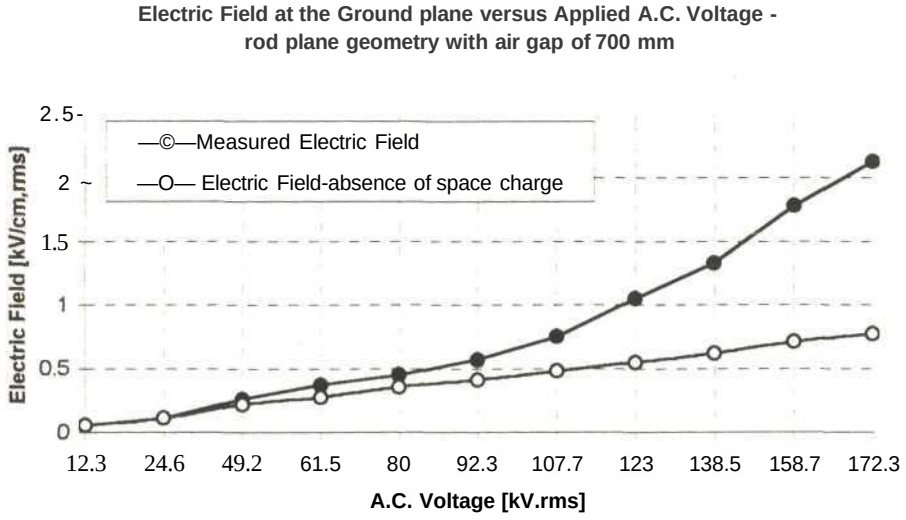

Figure 36. Results of electric field measurements under bird streamer intrusion

Figure 36 shows that at a 275 kV line voltage the electric field at the ground plane has a peak value of 2.5 kV/cm. This is significantly below the streamer propagation criteria of 4-5 kV/cm. If the gradient of the measured electric field in the absence of space charge is maintained, the second curve is derived. This curve has been titled "electric field - absence of space charge". The difference between this curve and the measured electric field at higher voltages indicates how the space charge in the air gap actually increases the electric field in the air gap at the ground plane at relatively large distances from the high-voltage electrode. For events of short duration, such as a falling bird streamer, it is postulated that

this lower curve may be a lower electric field limit and the measured electric field curve an upper limit. The most probable electric field enhancement caused by the falling bird streamer would be between these two limits.

These results have confirmed field experience that when the bird streamer is moved away from the transmission line hardware the probability of breakdown is greatly reduced.

Chapter 6

BIRD GUARD PROJECT IMPLEMENTATION

In order to prevent bird streamer earth faults, this thesis proposed to move the bird streamer away from the live-line hardware - such that the primary air gap would not break down. Chapters 4 and 5 determined that the critical distance to move the bird streamer is 1000 mm at 275 kV line voltage. To effect this solution, suitable bird guards needed to be designed and tested. This chapter documents this investigation. The chapter layout is presented below:

1. Suitable bird guards and test sites
2. Bird guard designs for field tests
3. Results of bird guard field tests
4. Discussion of field results, 1996-1997
5. Discussion of field results, 1998-1999

6.1. Identification of suitable bird guards and test sites

Initially three types of bird guards were identified:

1. Welded rod bird guards (WRBG); see Figure 34
2. Whirely Bird (WB, or rotating vane); see Figure 35
3. Crimped wire lug (CWL); (ABB, 1994)

In addition, three test sites were established on the Georgedale-Venus 275 kV lines:

1. Griffins Hill: Towers 338 to 355

Griffins Hill was identified as an active vulture restaurant. In the months of May, June and July of 1996, line 1 experienced seven and line 2 experienced five bird streamer faults.

2. Baynesfield: Towers 97 to 100

   Baynesfield was identified as an active ibis (hadedah) area. Line 1 had experienced one and line 2 had experienced two bird streamer faults. This was the area where most of the material for the bird guard video was recorded.

3. MidmarDam: Towers 168 to 178

   Line 1 experienced three trips and line 2 experienced one trip caused by bird streamers during 1996.

These tests commenced in August 1996 and terminated in December 1997. Because most of the faults occurred on the centre phase, bird guards were applied only on the centre phase. All faults occurring on these transmission lines were investigated with the aid of Hathaway travelling wave fault locators and correlated with the bird guard performance.

6.2. Bird guard designs for field test

Two welded rod bird guards were designed and tested:

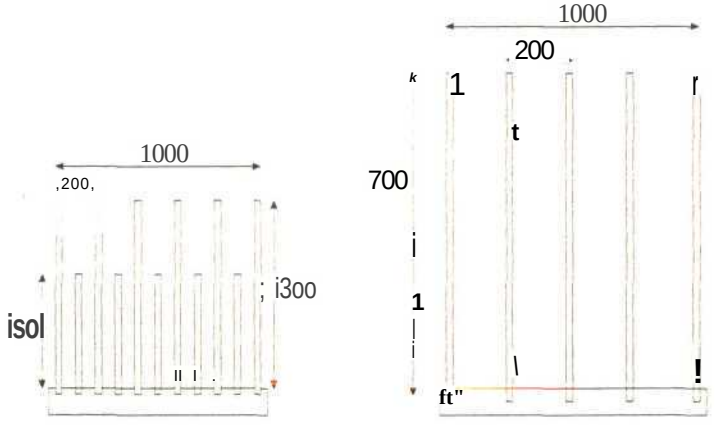

Figure 37. Welded rod bird guard design

EPRI (EPRI, 1988) used similar devices to deter bird activity on transmission towers and concluded that they were very effective. However, the application of these bird guards in the current experiment was different.

The application of the WRBG and the WB is illustrated below.

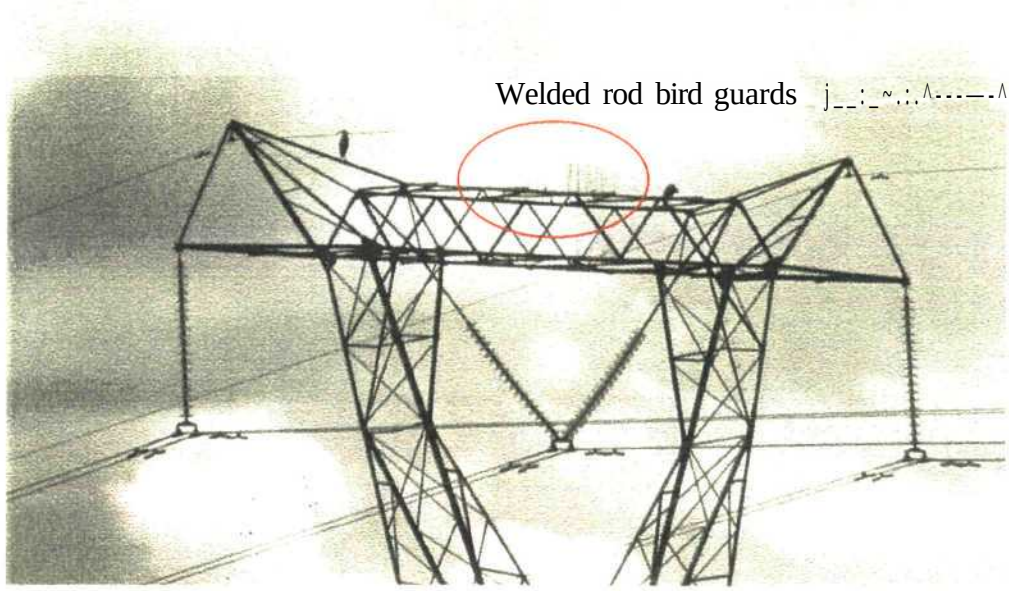

Figure 38. Application of welded rod bird guard

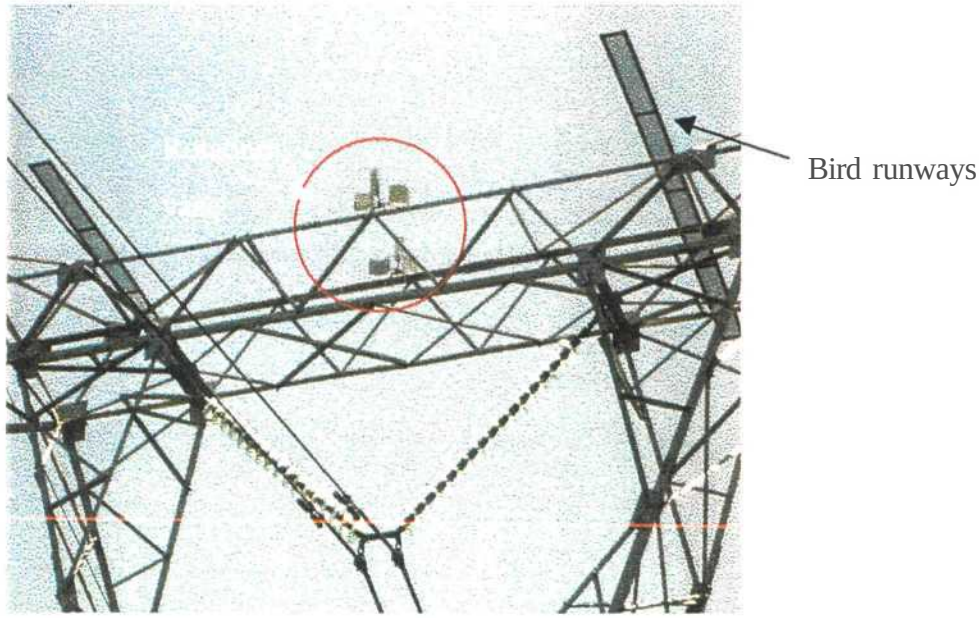

Figure 39. Application of rotating vane bird guard with bird runways

As illustrated in Figures 38 and 39, the bird guard application covers a relatively small area of the tower top. The intention of this design is not to eliminate bird activity on the transmission towers, nor to prevent the insulator assembly from being polluted. These diagrams also indicate possible areas where birds could still perch and could still cause a fault, eg the bottom of the tower boat, directly above the V string.

6.3. *Summary of bird guard field tests and results*

Most of the line faults experienced on the Georgedale-Venus lines were white phase earth faults. Consequently it was decided that bird guards would be installed only on the white phase, ie the centre phase. The hypothesis was raised that if the faults on the white phase decreased and the faults on the other two phases increased, then this would also indicate that bird streamers are a dominant fault mechanism. A summary of the field test results is tabulated below.

Georgedale-Venus 1 (275 kV) - line length 140 km			
Test site	**Date installed**	**BGtype**	**Results**
Griffins Hill, T 338-355: all towers and 2 WBs per tower	1 May 1997	WB	Mechanical failure of BG resulted in 2 trips: T 344 & 347. WBs were then replaced and no further trips occurred.
Baynesfield, T 95, 97 & 99: only IVI towers and 2 WBs per tower	1 Apr 1996	WB	No repeated trips.
Baynesfield, T 99	1 Dec 1997	PLP bird flight diverters suspended on wire	Mechanical failure of crimped wire lugs occurred. However, no repeated faults occurred.
Midmar, T 168-177: all IVI towers	1 Sept 1996	Shade cloth	No repeated trips, but the shade cloth was replaced with WRBGs at the end of 1997.
Baynesfield, T 50-80	1 May 1997	WB	Mechanical failure of units. No repeated trips. WBs were then replaced with WRBGs.

Table 15. Field test results on the Georgedale-Venus 1 line

Georgedale-Venus 2 (275 kV) - line length 140 km			
Test site	**Date installed**	**BGtype**	**Results**
Baynesfield, T 99	1 Apr 1996	Crimped wire lug	Birds (hadedah) were observed to land on the CWL BG and flatten it[21]. No repeated trips occurred.
Griffins Hill, T 338-355: all towers.	1 Aug 1996	WRBG typel	No repeated trips occurred on any phase at Griffins Hill. It must be noted that 4 towers at Griffins Hill do have bird runways.
Baynesfield, T 18-100: only IV! towers	1 Dec 1996	WRBG typel	No repeated trips. In February 1996 a crowned crane was found dead, hanging from a WRBG, type 1. Type 2 WRBG was designed and implemented on other portions of the line. There have been no further incidents or bird fatalities since using WRBGs.
Midmar Dam, T 173-176	1 Sept 1996	WB	No further trips and no mechanical failures. After the experiment these BGs were replaced with WRBGs.

Table 16. Field test results on the Georgedale-Venus 2 line

6.4. Discussion of field results, 1996-1997 (December)

With the exception of WRBG type 2, all bird guards tested experienced mechanical problems when exposed to the transmission line environment for a long time (six months). The bird guards also had limited success in preventing earth faults on the transmission lines.

1. Crimped wire lug BG: A hadedah landed on it and flattened it.
2. Shade cloth: This device got torn in the wind and it then tended to intrude into the electrical clearances of the power line.
3. Whirely Birds (WB, or rotating vane): The early designs had mechanical problems, which were later solved. However, experience gained on the Avon-Mersey and Avon-Durban North lines during 1997 showed that although these

bird guards were effective in preventing faults during daylight hours, there were three trips in the evenings.

4. Bird runways: These devices are mechanically very strong. Birds were observed using them, but the birds also tended, after landing on the runway, to migrate towards the centre of the tower. It is suggested that these be used when there are recurring trips where WRBGs have been fitted. The bird runways are illustrated in Figure 39.

Detailed summaries of faults experienced on the Georgedale-Venus 1 and 2 lines during 1997 are presented in Tables 17 and 18 respectively.

Georgedale-Venus 1 (275 kV) - performance summary 1997			
Month	**Number of faults**	**Fault description**	**Line fault locator reading from Georgedale**
January	Nil		
February	Nil		
March	Nil		
April	**1**	Blue phase, T 343, bird streamer	94 km
May	**2**	1. Blue phase, silicone composite I string bird streamer 2. White phase, unknown	1. 20 km 2. 130 km
June	**2**	1. Blue phase, T 359 (strain), bird streamer 2. White phase, T 344, bird streamer	1. 123 km 2. 110 km
July	**2**	1. White phase, T 37, bird streamer 2. White phase, T 347, bird streamer	1. 15km 2. 118 km
August	**1**	Lightning LPATS confirmed	1. 43 km
September	Nil		
October	Nil		
November	Nil		
December	**1**	Lightning LPATS confirmed	1. 90 km

Table 17. Line 1 performance summary, 1997

Georgedale-Venus 2 (275 kV) - performance summary 1997			
Month	**Number of faults**	**Fault description**	**Line fault locator reading from Georgedale**
January	Nil		
February	Nil		
March	**1**	White phase, T 130, bird streamer	**40 km**
April	Nil		
May	Nil		
June	**1**	White phase, T 241, bird streamer	**79 km**
July	**3**	1. Blue phase, unknown 2. White phase, unknown 3. White phase, T 361, bird streamer	**1. 80 km** **2.** 125 **km** **3.** 126 **km**
August	**2**	1 Lighting LPATS confirmed 2 White phase, T 24, III tower bird streamer	**2. 7.6 km**
September	**1**	White phase, T i l, bird streamer	**3.5 km**
October	Nil		
November	**1**	Lightning LPATS confirmed	
December	Nil		

Table 18. Line 2 performance summary, 1997

The performance data of the fault trips clearly indicates that the welded rod bird guards installed on line 2 were more effective than the rotating vane bird guards installed on line 1. Most of the bird streamer faults occurred outside the identified bird corridors, consequently bird guards will be installed along the entire length of the line in all future bird guard projects.

The improvements in the trip incidence appear to be a direct result of the bird guards installed. These results gave the investigator the confidence to conclude that the bird streamer fault mechanism is a significant cause of earth faults on the high-voltage transmission system.

As a result of the above data, welded rod bird guards were installed on a further sixteen 275 kV lines in KwaZulu-Natal. The 275 kV transmission network is illustrated below.

Figure 40. Map of 275 kV network in KwaZuIu-Natal

Bird guards were installed on the centre phase of the following power lines:

Line Name	KM.	% installed bird guards of line length - installed on centre phase
Bloukrans/Danskraal 1	24.5	100
Bloukrans Tugela 1	61.4	100
Bloukrans Tugela 3	62.3	100
Bloukrans Venus 1	20	100
Bloukrans Venus 2	21.1	100
Hector Mersey 1	55.49	**90**
Georgedale Mersey 2	50.2	**90**
Georgedale Venus 1	140	100
Georgedale Venus 2	140	100
Avon Durban North 1	22.2	100
Avon Durban North 2	23.1	100
Avon Mersey 1	68.7	**30**
Avon Mersey 2	68.8	**30**
Georgedale Illovo 2	49.3	100
Georgedale Klaarwater 2	27.5	100
Hector Illovo 1	54.4	100
Hector Klaarwater 2	22	100
Hector Klaarwater 3	22	100

Table 19. 275 kV, KZN power lines with bird guards

6.5. *Discussion of field results, 1998-1999*

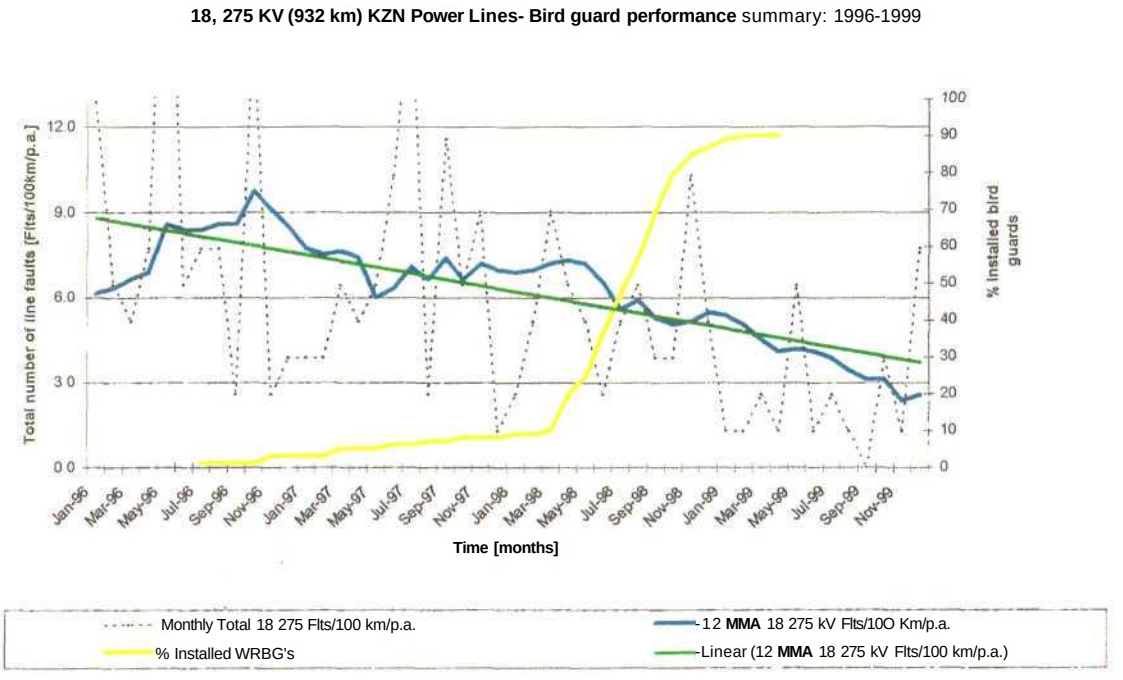

Figure 41. KwaZulu-Natal bird guard project results

Figure 41 shows the total number of faults experienced by the above transmission network of eighteen 275 kV transmission lines. The cumulative length of this network is 932 km. Since the application of bird guards, there has been a reduction in the total number of line faults experienced on this 275 kV network, from 9.8 faults/100 km/pa in October 1996 to 2.6 faults/100 km/pa in December 1999. This represents a 73.4% reduction in the total number of line faults experienced.

The twelve-month moving average performance statistics of the individual power lines are presented below.

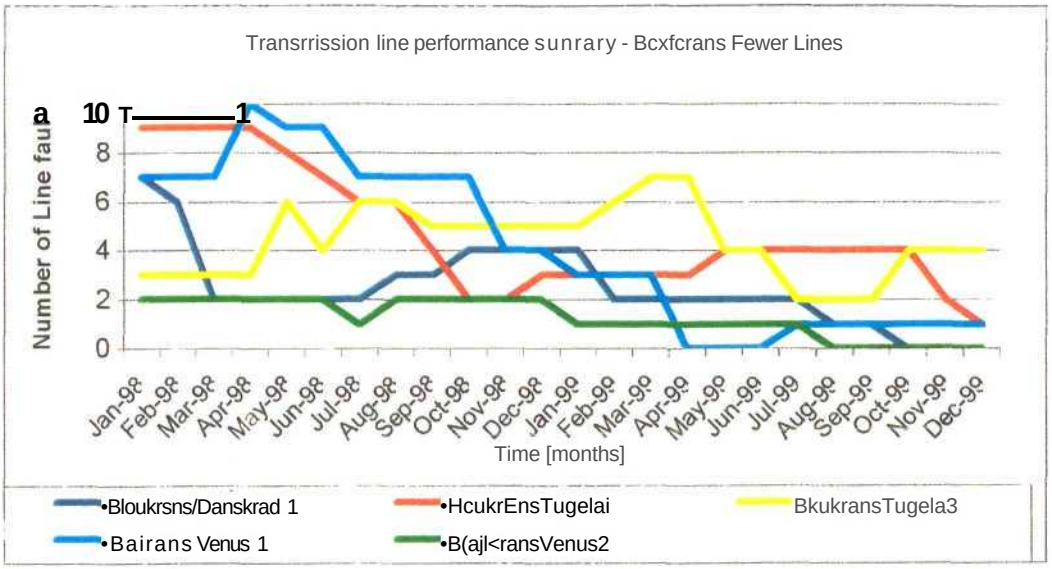

Figure 42. Bird guard performance summary of the Bloukrans lines

Note: 18 transmission lines have had welded rod bird guards installed since 1996. Sixteen of the 275 kV transmission lines are presented in Figures 36, 37 and 38. This is because two transmission lines (Hector-Klaarwater 2 and 3) that had WRBGs installed on them were recently commissioned. These transmission lines have never faulted and as a result they have not been included in the above performance summary.

All of the 18 transmission lines except Georgedale-Venus 2 and Bloukrans-Danskraal 1 had welded rod bird guards installed on them during the period from May to November 1998. The other power lines had bird guards installed on them by January 1998. All the power lines at Bloukrans have experienced a reduction in the number of line faults.

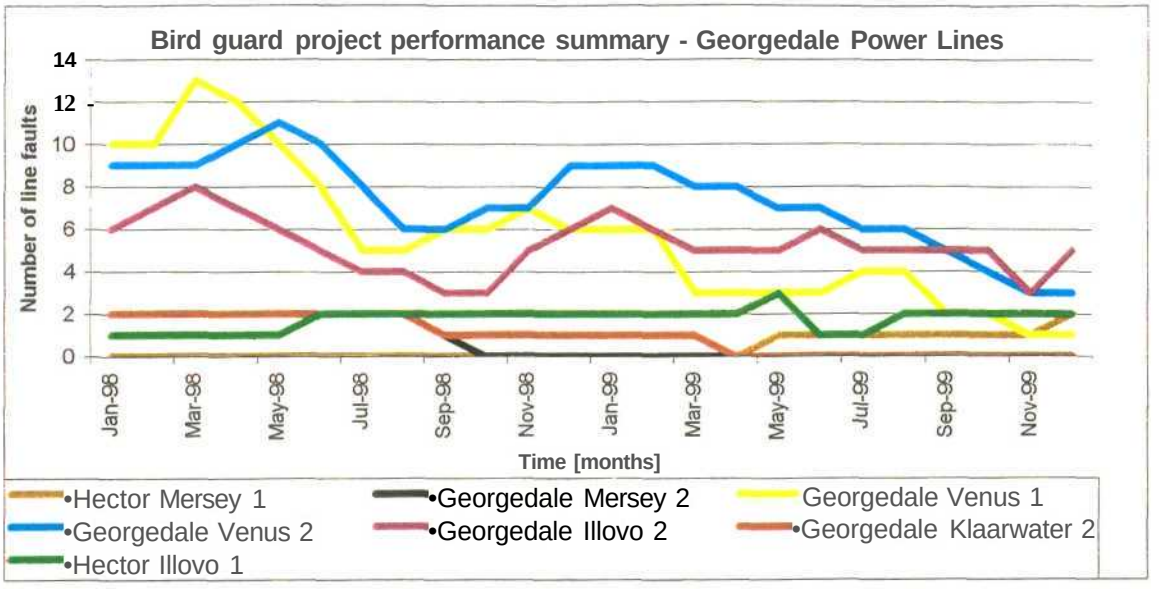

Figure 43. Bird guard performance summary of the Georgedale lines, 1998-1999

All these power lines, except Hector-Mersey 1, whose only line fault was caused by a cane fire, experienced a decrease in the number of line faults following the 1998 bird guard project. The most noticeable is the Georgedale-Venus 1 power line - from 13 line faults (March 1998) to only one line fault (December 1999).

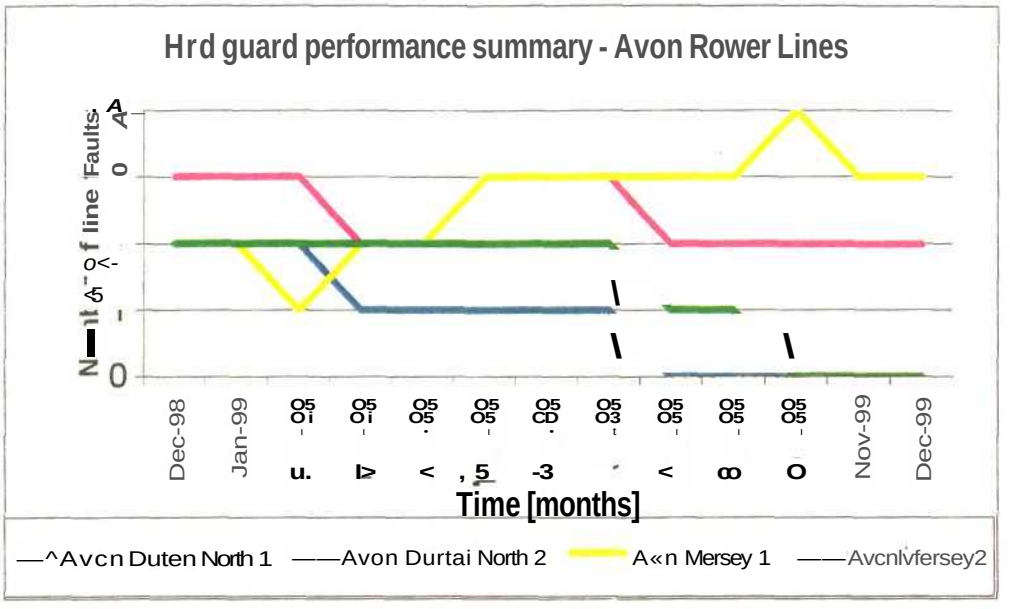

Figure 44. Bird guard performance summary of the Avon lines, 1998-1999

This network has relatively few line trips and most of the line faults are associated with cane fires. However, Figure 44 does show the success of the bird guard project on the Avon-Durban North 1 power line - the number of line faults was reduced from 4 to 0 faults per annum.

Bird guards were installed only on the first 22 towers outside Avon, on the Avon-Mersey 1 line. However, during 1999 two bird streamer line faults occurred on this power line on two separate strain towers. This type of experience shows that bird guards should be fitted to the entire power line and not selectively to certain corridors.

6.6. Conclusion

The poor performance of the 275 kV Georgedale-Venus 1 and 2 lines was investigated. Numerous solutions had previously been implemented but limited success was achieved in curbing transient earth faults. These actions included reinsulation with silicone composite insulators and glass insulators respectively. Various bird guards, including saw tooth, crimped wire lugs, shade cloth and bird landing platforms, had also been implemented with limited success.

Historically the unknown faults were attributed to a pollution mechanism breakdown. This investigation determined that the majority of the earth faults were caused by bird streamer air gap breakdown.

Welded rod bird guards were designed and installed and they have had tremendous success in reducing the number of transient earth faults on the greater 275 kV transmission network in KwaZulu-Natal. The total number of line faults has been reduced from 9.8 to 2.6 faults per 100 kilometres per annum. This represents a percentage reduction of 74%.

Chapter 7

CONCLUSION

This investigation was initiated to determine the root cause of the increasing fault trend of transient earth faults on the 275 kV transmission grid in KwaZulu-Natal. The following conclusions have been reached:

- Post-line-fault patrols revealed that the faults on the Georgedale-Venus 1 and 2 lines were characterised by an apparent air gap breakdown, ie the tower burn mark was located vertically above the live end burn mark. This indicates a bird streamer mechanism and is further supported by evidence of bird activity in the power line servitude.
- Time-of-day analysis appears to indicate that bird streamer faults can occur over the entire 24 hour period.
- Bird streamer faults can occur in both dry and wet climates. No conclusive trends are evident when these faults are correlated with relative humidity and rainfall.
- Bird streamer faults have been observed to occur on V string, I string and strain tower jumpers on the 275 kV network. However, on the 400 kV network bird streamer faults have only been observed on V strings.
- This thesis recommends that to prevent bird streamer faults the bird streamers should be moved a minimum distance of 1 000 mm away from the centre of the tower at 275 kV.
- Welded rod bird guards have been identified as the most effective bird guards in KwaZulu-Natal.
- When reinsulating power lines with silicone composite insulators the insulator connecting length should be increased to prevent air gap clearance infringement caused by the installation of corona rings.
- The primary gap breakdown strength is not sensitive to variation of liquid streamer resistivities between 40 and 10 000 kQ/m.

apter 8

RECOMMENDATIONS FOR FURTHER WORK

On the basis of this investigation the following recommendations are made:

1. Time-of-day models as proposed by Burnham appear to be a successful tool in determining the cause of transmission line outages. However, this method needs to be refined to accommodate the South African characteristics of pollution, lightning and fire-related outages.
2. Welded rod bird guards should be installed on other poorly performing transmission lines where there appear to be air gap breakdown phenomena as determined by line patrols.
3. Further work needs to be done on the possibility of this fault mechanism occurring at 132 kV, 88 kV, 66 kV and 33 kV system voltages.
4. Bird interaction with power lines needs to be reviewed and streamer excreta characteristics of birds need to be documented.
5. Other bird guard types need to be developed to accommodate live-line maintenance activities.

References

ABB Feralin Pty **(Ltd), High Voltage Fittings catalogue.** Guard Devices - Bird, February 1994, pages 99-100.

Bell, **R, Transmission monthly performance report,** Eskom Transmission, August 1999.

Boulet, L and Jakubezyk, **B,** J, **Alternating current corona in foul weather: 1 - above freezing point,** IEEE transactions on power apparatus and systems Volume PSA-83, May 1964, pages 508 - 512.

Boulet, L, Cahill, L and Jakubezyk, **B,** J, **Alternating current corona in foul weather: II - below freezing point,** IEEE transactions on power apparatus and systemsVolume PSA-85, June 1966, pages 649 - 656.

Britten, A, C, **Investigation into light pollution of glass disc insulator as a cause of unexplained flashovers.** Technology Services International (TSI), Eskom, TRR/CONS6/98, P99-000867, 1998.

Burger, A, A and Sadurski, K, **J. Experimental investigation of bird initiated AC flashover mechanisms.** CIGRE SC 33-95 (WG07), 1995.

Burnham, J, **Bird streamer flashovers on FP&L transmission lines,** IEEE transactions on power delivery Volume 10 Number 2, April 1995, pages 970-977'.

Carrara, G & Thione, L, **Switching surge strength of large air gaps: a physical approach,** IEEE transactions on power apparatus and systems Volume PAS-95, 1976, pages 512-524.

Diesendorf, W, **Insulation co-ordination in high voltage electric power systems,** London: Butterworth & Co, 1974.

EPRI, **Transmission line reference book 345 kV and above.** Second edition, EL-2500, 1987, pages 472-473.

EPRI, **A joint power utility investigation of unexplained transmission line outages,** EL5735, 1998.

Evert, C, **R, The detection of fires under high voltage transmission lines,** T.S.I., Eskom, TRR/E/93/PL017, Project number 7755P009R, 1993.

Gallet, G and Leroy, G, **Expression for switching impulse strength suggesting the highest permissible voltages for AC systems,** IEEE transactions on power delivery, Summer Power Meeting, 1973.

Gallimberti, I, **A computer model for streamer propagation.** Journal of Applied Physics D Volume 5, 1972, pages 2179-2189.

Gallimberti, I, Goldin, M and Poli, E, **A computer model of leader - streamer propagation in long spark.** Fourth International symposium on HV engineering. Athens, September 1983.

Geldenhuys, H, **Positive streamer voltage gradient as a function of atmospheric parameters.** Masters dissertation, University of Pretoria, Novemberl986.

Goldman, M, **Corona discharges and their applications.** IEE proceedings Volume 128 Number 4, May 1981.

Hepworth, J, K, Klewe, R, C and Tozer, **B,** A, **A model of impulse breakdown in divergent field geometries.** Journal of applied physics D Volume 5, 1972, pages 730-740.

Hirsh, Merle, N and Oskam, H, **Gaseous electronics. Volume 1. Electrical discharges.** Academic Press, Corona discharges: Chapter 4, 1978, page 225.

Hutzler, B and Hutzler-Barre, **D, Leader model for predetermined of switching surge flashover voltage of large air gaps.** IEEE transactions on power apparatus and system Volume PAS-97 Number 4, 1978, pages 1087-1096.

EEC 815, **Guide for the selection of insulators in respect of polluted conditions.** First edition, 1986.

Jones, B and Waters, R, T, **Air insulation at large spacing,** IEE proceedings Volume 125 Number 11, 1978, pages 1153-1176.

Kachler, A, La Forest, **J** and Zaffanella, L, **Switching surge flashover of UHV transmission line insulation,** IEEE transactions of power apparatus and systems Volume PAS-90, 1971, page 1598.

Kline, L, E, **Corona cloud model predictions of switching surge flashover voltages versus electrode geometry,** IEEE transactions on power systems Volume PAS-96, 1977, pages 543-549.

Kuffel, E, and Zaengl, W, S, **High voltage engineering - fundamentals,** Pergamon Publishers, 1984.

Les Renardienes Group, **Research on large air gap discharges at Les Renardienes,** Electra Number 23, 1972.

Les Renardienes Group, **Research on large air gap discharges at Les Renardienes,** Electra Number 35, 1974.

Les Renardienes Group, **Research on large air gap discharges at Les Renardienes,** Electra Number 53, 1977.

Lloyd, K, J and Zaffanella, L, E, **Switching impulse tests at project UHV using long wave fronts,** IEEE transactions on power apparatus and systems Volume PAS-100 Number 2, February 1981, pages 510-517.

Loeb, L and Meek, J, **The mechanism of electric spark.** Stanford: Stanford University **Press,** 1940.

Los, E, J, **New studies of the transient glow discharge in parallel electrode gaps.** IEEE transactions on power apparatus and systems Volume PAS-99 Number 2, 1980, pages 720-728.

Marode, E, **The mechanism of spark breakdown in air at atmospheric pressure between a positive point and a plane. 1. Experimental: Nature of the streamer track.** Journal of applied physics D Volume 46 Number 5. May 1975, pages 2005-2015.

Meek, J and Craggs, **J, Electrical breakdown of gasses.** New York, Wiley publishers, 1978.

Paris, **L** and Cortina, **R, Switching and lightning impulse discharge characteristics of large air gaps and long insulator strings,** IEEE transactions on power apparatus and systems Volume PAS-87, 1968, page 947.

Raether, H, **Electron avalanches and breakdown in gases.** Butterworth & Co., London, 1964.

Rizk, F, A, M, **An overview of recent high voltage engineering research in Canada,** International symposium of high voltage (ISH), 1997.

Rizk, F, A, M, **A model for switching impulse leader inception.** EEEE Transactions on Power Delivery, Volume 4 Number 1, 1989, pages 596-606.

Steynberg, B and Gouws, T, **Performance study on Georgedale Venus 275 kV lines.** Eskom Transmission Line Engineering, Technology Services International, November 1993.

Schneider, H, M and Nicholls, C, W, **Contamination flashover performance of insulators for UHV..** IEEE transaction on power apparatus and systems Volume PAS-97 Number 4, July 1978, pages 1411-1420.

Schneider, H, M and Los, E, J, **Switching surge breakdown development in large conductor-tower air gaps.** IEEE transactions on power apparatus and systems Volume PAS-97 Number 3, 1978, pages 866-873.

Schneider, K and Week, K, H, **Parameters influencing the gap factor.** Electra. Number 35, 1974, pages 25-45.

Takasu, K, Arai, N, Imano, Y, Shindo, T and Seta, T, **AC flashover characteristics of long air gaps and insulator strings under fog conditions,** IEEE transactions on power apparatus and systems Volume PAS-100 Number 2, 1981, pages 639-645.

Trinth, G, N and Jordan, J, B, **Modes of corona discharges in air,** IEEE transactions on power apparatus and systems Volume PSA-87 Number 5, May 1981, Pages 1207-1215.

Uman, M, A, **Lightning.** Dover Publication Inc. New York, 1968.

Waters, R, Rickard, T and Stark, W, **Electric field and current density in the impulse corona discharge in a rod-plane gap.** Proceedings Royal Society. A 304, 1968, pages 187-210.

Waters, R, **Diagnostic techniques for discharges and plasmas,** Electrical breakdown and discharges in gasses, Part B: Macroscopic processes and discharges, New York, Plenumu, 1983.

West, H, Brown, J and Kinyon, A, **Simulation of EHV transmission line flashover initiated by bird excretion,** IEEE PES winter meeting, Paper 71, Tp 145-pwr, February 1971.

APPENDIX 1: All KwaZulu-Natal 275 kV Line Faults of 1996

	DATE	TIME OFF	LINE NAME	KV	R	REASON	PHASE	LFLR	REMARKS
1	02.01.96	10.00	Georgedale-Venus 2	275	B	Birds	White	34.6	Nothing visual found
2	11.01.96	08.56	Georgedale-Venus 1	275	B	Birds	Blue	64	T 174/75 & 176: flash marks visible
3	15.01.96	10.28	Ingagane-Bloukrans 2	275	B	Birds	White	66	Between T 195 & 238: crows' nests found
4	19.01.96	08.24	Georgedale-Venus 2	275	B	Birds	White	6	T 23, W phase: corona ring to structure flashover
5	19.01.96	18.16	Ingagare-Danskraal 1	275	B	Birds	White	72	T 212: flashed over; between T 195 & 238: crows' nests found
6	19.01.96	23.55	Ingagane-Danskraal 1	275	B	Birds	White	0	Between T 195 & 238: crows' nests found
7	20.01.96	09.54	Georgedale-Venus 1	275	B	Birds		61.31	T 174/75 & 176: flash marks visible
8	25.01.96	12.44	Georgedale-Venus 1	275	B	Birds	White	10	T 37: white phase flashed over
9	25.01.96	16.56	Georgedale-Venus 1	275	B	Birds	White	18	T 58: white phase flashed over
10	02.02.96	01.50	Bloukrans-Tugela 3	275	B	Birds	White	33	T 24: bottom disc white phase flashed over
11	12.02.96	16.39	Ingagane-Danskraal 1	275	B	Birds	White	70	T 197-238: crows' nests found
12	22.02.96	22.39	Georgedale-Venus 2	275	B	Birds	White	26.49	Patrolled, Nov 96 - T 85: flashed over due to bird streamer
13	25.02.96	09.09	Georgedale-Venus 2	275	B	Birds	White	55	New flash mark, T 175: badly bird-polluted
14	21.03.96	09.43	Avon-Durban North 1	275	B	Birds	White	6	T 21: flashed over
15	22.03.96	21.20	Avon-Mersey 2	275	B	Birds	White	16	T 56: flashed over due to bird streamer
16	04.04.96	21.22	Bloukrans-Tugela 1	275	B	Birds	White	0	LFL faulty / T 84-86: top disc W PH flashed over
17	10.04.96	06.30	Ingagane-Bloedrivier 4	275	B	Birds	White	18	T 51 & 53: flashed over due to bird pollution and crows' nests
18	11.04.96	09.39	Georgedale-Venus 2	275	B	Birds	White	28.23	T 97: flashed to top cross member (hadedah)
19	11.04.96	19.38	Bloukrans-Tugela 3	275	B	Birds	White	6	Vultures in the area. No flash marks found
20	15.04.96	09.16	Avon-Mersey 2	275	**B**	Birds	White	**1**	T 6: flashed over due to bird streamer

21	17.04.96	01.53	Ingagane-Bloedrivier 4	275	B	Birds	White	21	T 54 & 55: badly polluted and have been replaced
22	28.04.96	10.14	Ingagane-Danskraal 1	275	B	Birds	White	64	T 164: W & R phase flashed over
23	01.05.96	00.01	Bloukrans-Tugela 3	275	B	Birds	White	0	T 124: bottom disc flashed over
24	01.05.96	00.26	Bloukrans-Danskraal 1	275	B	Birds	White	5	T 9: flashed over to steel, disc not flashed
25	01.05.96	23.59	Bloukra is-Tugela 3	275	B	Birds	White	0	T 124: bottom disc flashed over
26	02.05.96	01.50	Bloukrans-Tugela 3	275	B	Birds	White	0	T 124: bottom disc flashed over
27	06.05.96	01.16	Georgedale-Venus 2	275	B	Birds	White	115.8	T 346-355 /T 347: two discs flashed over, one broken
28	06.05.96	04.59	Georgedale-Venus 1	275	B	Birds	White	94	T 346-355 /T 343: flashed over
29	09.05.96	01.55	Georgedale-Venus 1	275	B	Birds	White	100.4	T 346-355 *K* 344: flashed over
30	09.05.96	03.25	Georgedale-Venus 1	275	B	Birds	White	101.3	T 346-355 /T 348: bottom three discs flashed over
31	09.05.96	04.41	Georgedale-Venus 1	275	B	Birds	White	103	T 346-355 /Tower 350: flashed over
32	16.05.96	10.35	Ingagane-Danskraal 1	275	B	Birds	White	69	T 231: badly flashed over - to be replaced
33	22.05.96	17.56	Georgedale-Venus 2	275	B	Birds	White	103	T 343, 344 & 347: badly polluted
34	22.05.96	22.46	Georgedale-Venus 2	275	B	Birds	White	98.3	T 343, 344 & 347: badly polluted
35	23.05.96	06.51	Georgedale-Venus 2	275	B	Birds	White	103	Flashed on S/Tower 345 from jumper-tower
36	27.05.96	10.04	Avon-Durban North 1	275	B	Birds	White	7	T 27: flashed over due to bird pollution
37	27.05.96	20.42	Georgedale-Venus 2	275	B	Birds	White	100	Flashed on S/Tower 345 from jumper tower
38	28.05.96	08.55	Avon-Mersey 2	275	B	Birds	White	1	T 5: badly polluted
39	28.05.96	18.51	Bloukrems-Tugela 3	275	B	Birds	White	44	T 115, 114: possible flash marks
40	06.06.96	18.19	Georgedale-Venus 1	275	B	Birds	White	94	T 344: flashover from conductor to tower / vultures
41	07.06.96	02.47	Georgedale-Venus 2	275	B	Birds	White	94.11	T 344: flashover from conductor to tower / vultures
42	07.06.96	07.31	Georgedale-Venus 2	275	B	Birds	White	83	T 344: flashover from conductor to tower / vultures
43	14.07.96	16.50	Avon-Durban North 1	275	B	Birds	White	7	T 26: flash mark
44	28.07.96	22.12	Georgedale-Venus 1	275	B	Birds	White	107.7	T 347: flash marks visible on steelwork
45	29.07.96	05.51	Georgedale-Venus 1	275	B	Birds	White	106.2	T 343: flash marks visible on steelwork

46	30.07.96	12.08	Georgedale-Venus 2	275	B	Birds	White	14	T 49: steelwork flashed over / composite rubber (281 kV)
47	30.07.96	13.30	Ingagane-Chivelston 1	275	B	Birds	White	0	T 2: flashed over / suspect bird streamer
48	31.07.96	04.18	Ingagane-Bloukrans 2	275	B	Birds	White	19	T 68: flashed over / T 64-74 birds' nests
49	20.08.96	00.51	Georgedale-Venus 1	275	B	Birds	White	53.74	T 173: flashed over
50	22.08.96	06.33	Georgedale-Venus 1	275	B	Birds	White	101.4	Patrolled T 345-329: T 333 flashed over
51	23.08.96	10.28	Ingagane-Danskraal 1	275	B	Birds	White	70	T 211: flashed over
52	28.08.96	17.44	Ingagane-Danskraal 1	275	B	Birds	White	71	T 208: possible flash damper to tower
53	29.08.96	07.31	Georgedale-Mersey 2	275	B	Birds	White	12.9	T 45: flashed from jumper to tower/next to waterhole
54	28.09.96	19.24	Bloukrans-Tugela 1	275	B	Birds	White	5	T 18: wire hanging down from bird's nest
55	01.10.96	10.24	Bloukrans-Tugela 1	275	B	Birds	White	5	T 18: bird's nest collapsed onto jumper
56	06.10.96	06.38	Ingagane-Danskraal 1	275	B	Birds	White	21	T 30-90: dead birds found under T 75
57	08.10.96	10.15	Georgedale-Venus 2	275	B	Birds	White	18.36	T 59: bird streamer (found 20/11/96)
58	21.10.96	09.32	Georgedale-Venus 2	275	B	Birds	Red	46	Crows' nests: T 136-139 / T 136, 138, 139 flashed over
59	22.10.96	06.10	Avon-Mersey 2	275	B	Birds	White	48	T 145: flashed over due to bird pollution
60	02.11.96	06.30	Ingagane-Danskraal 1	275	B	Birds	White	70	T 227: flashed over due to bird pollution
61	10.11.96	22.56	Avon-Mersey 2	275	B	Birds	White	16	T 56: flashover jumper to steelwork due to bird streamer
62	17.11.96	10.58	Ingagane-Danskraal 1	275	B	Birds	White	71	T 220: flashover due to bird streamer
63	19.11.96	07.12	Georgedale-Venus 2	275	B	Birds	White	17.19	T 61: bird streamer TWS = 19.4
64	19.12.96	23.39	Georgedale-Venus 2	275	B	Birds	Red	30.6	T 92: flashed over due to bird pollution
65	05.01.96	12.12	Klaarwater-Mersey 1	275	C	Cane fire	Three	55.13	T 41-42: Hullet's Shongweni Estates
66	17.05.96	16.00	Avon-Irnpala 2	275	C	Cane fire	W-B	54	Unreported, T 165-166 (farmer unknown)
67	18.05.96	05.40	Avon-Impala 2	275	C	Cane fire	White	81	Unreported, T 229-230, Manyana Farm
68	03.06.96	13.02	Avon-Durban North 1	275	C	Cane fire	Blue	11	T 22-23: runaway fire, Redwoods Farm (J Hullet or J Laatz)

69	08.06.96	06.11	Avon-Impala 2	275	C	Cane fire	Blue	60	T 142-143: contractor burned close to line (windy)
70	21.06.96	04.15	Georgedale-Illovo 2	275	C	Cane fire	Blue	24.64	T 73-74: runaway fire, Klipspruit Farm (Linley Gonlag)
71	24.06.96	05.11	Avon-Impala 2	275	C	Cane fire	White	79	T 204-205: runaway fire, Emoyini Farm (Mr MS Dunne)
72	24.06.96	05.14	Avon-Durban North 1	275	C	Cane fire	Blue	0	T 204-205: runaway fire, Emoyini Farm (Mr MS Dunne)
73	30.06.96	00.30	Avon-Durban North 1	275	C	Cane fire	Red	30	T 86-95: runaway veld fire started cane fire
74	16.08.96	05.11	Avon-Impala 2	275	C	Cane fire	White	46	T 211: farm, Emoyeni area (Mr Johan Mncwango)
75	16.08.96	08.41	Avon-Mersey 1	275	C	Cane fire	Blue	41	T 176-177: unreported, Krommedraai Farm (C Teddar)
76	16.09.96	17.45	Avon-Durban North 1	275	C	Cane fire	W-B	107	T 302-303: unreported, Marsabit Farm (Mr Pretorius)
77	15.10.96	10.23	Avon-Durban North 1	275	C	Cane fire	Blue	7.8	T 221 -222, Obanjeni Estates, unreported
78	24.10.96	14.48	Avon-Durban North 1	275	C	Cane fire	R-B	8.3	T 23-24: runaway fire, Redwood Estates (B Hulet)
79	24.10.96	14.50	Avon-Durban North 1	275	C	Cane fire	R-B	8.3	T 23-24: runaway fire, Redwood Estates (B Hulet)
80	24.10.96	14.51	Avon-Durban North 1	275	C	Cane fire	R-B	8.3	T 23-24: runaway fire, Redwood Estates (B Hulet)
81	24.10.96	14.51	Avon-Durban North 1	275	C	Cane fire	R-B	8.3	T 23-24: runaway fire, Redwood Estates (B Hulet)
82	04.01.96	07.51	Ingagane-Bloukrans 2	275	W	Foreign	White	66	T 196: pieces of wire on conductor
83	11.04.96	00.49	Ingagane-Danskraal 1	275	I	Hardware	White	66	T 165: bottom two discs flashed over
84	20.11.96	18.06	Hector-Illovo 1	275	I	Hardware		0	T 113: line switched out for parted e/wire
85	15.05.96	18.50	Impala-Invubu 2	275	H	Human	White	0	T 10: contractor painting tower's left cover on ins
86	16.05.96	07.09	Impala-Invubu 2	275	H	Human	White	0	T 10: contractor painting tower's left cover on ins

87	03.02.96	13.45	Georgedale-Venus 1	275	A	Pollution	Blue	108	T 318 & 329: flashed over / agripollution
88	05.02.96	02.48	Avon-Durban North 1	275	A	Pollution	Blue	68	T 185: marine pollution / not reinsulated yet
89	24.01.96	00.42	Georgedale-Illovo 1	275	Z	Storm	Three	27.92	LPATS confirmed
90	26.01.96	17.39	Georgedale-Venus 2	275	z	Storm	Blue	45.53	LPATS confirmed
91	26.01.96	18.35	Georgedale-Illovo 1	275	z	Storm	White	45.45	LPATS confirmed
92	12.03.96	20.06	Georgedale-Venus 2	275	z	Storm	Red	72.74	LPATS confirmed
93	25.06.96	21.10	Georgedale-Venus 2	275	z	Storm	Red	71	LPATS confirmed - 43 kA
94	08.07.96	21.04	Georgedale-Venus 2	275	z	Storm	Red	99.94	LPATS confirmed
95	24.09.96	17.50	Georgedale-Illovo 2	275	z	Storm	Blue	2.4	LPATS confirmed -23 kA
96	08.10.96	16.47	Avon-Durban North 1	275	z	Storm	Red	37	LPATS confirmed
97	08.10.96	18.22	Georgedale-Venus 2	275	z	Storm	B-R	58	LPATS confirmed
98	19.10.96	15.11	Georgedale-Venus 2	275	z	Storm	Red	33	LPATS confirmed
99	26.10.96	21.46	Georgedale-Venus 2	275	z	Storm	White	44.14	LPATS confirmed
100	02.12.96	18.20	Hector-Klaarwater 1	275	z	Storm	Red	10.1	LPATS confirmed
101	23.12.96	18.23	Ingagane-Danskraal 1	275	z	Storm	White	72	LPATS confirmed
102	01.01.96	01.40	Avon-Impala 2	275	u	Unknown	White	21	No fault found
103	26.01.96	07.10	Bloukrans-Danskraal 1	275	u	Unknown	White	14	Nothing visual found
104	27.01.96	12.36	Ingagane-Bloukrans 2	275	u	Unknown	White	21	T 37, 74, 75 & 77: crows' nests; T 36 & 70: one disc broken
105	16.02.96	18.23	Ingagane-Bloukrans 2	275	u	Unknown	White	71	Patrolled from T 185 to T 244: nothing visual found
106	18.02.96	20.16	Avon-Mersey 1	275	u	Unknown	Blue	41	LPATS negative
107	03.03.96	08.57	Ingagane-Danskraal 1	275	u	Unknown	White	95	T 204-216: T 205 - one broken disc; T 212-old flash marks
108	19.03.96	02.38	Bloukrans-Tugela 3	275	u	Unknown	White	2	T 6: ground and members polluted / no flash marks
109	24.03.96	21.29	Ingagane-Bloukrans 2	275	u	Unknown	White	19	T 16-80: nothing visual found
110	02.04.96	00.58	Bloukrans-Tugela 1	275	u	Unknown	White	0	LFL faulty / LPATS negative
111	06.04.96	09.33	Ingagane-Bloukrans 2	275	u	Unknown	White	60	Lads did patrol: no report received
112	13.04.96	05.45	Georgedale-Venus 2	275	u	Unknown	White	44	Patrolled T 135-167/168-178: nothing visual found

113	18.05.96	22.17	Ingagane-Bloedrivier 4	275	U	Unknown	White	21	LPATS negative. LFL suspect. Tienie to confirm
114	24.05.96	20.57	Georgedale-Venus 2	275	U	Unknown	White	27	Nothing visual found
115	26.05.96	02.23	Georgedale-Illovo 1	275	**u**	Unknown	White	4.4	T 107 back to s/station: nothing visual found
116	18.07.96	18.52	Ingagane-Danskraal 1	275	**u**	Unknown	White	19	Patrolled T 16-60: nothing found
117	19.07.96	02.31	Bloukrans-Tugela 1	275	**u**	Unknown	Red	25	No report received; requested again on 24/7
118	01.08.96	17.07	Georgedale-Venus 2	275	**u**	Unknown	White	18	LPATS negative, no patrol done
119	12.09.96	01.25	Klaarwater-Mersey 1	275	**u**	Unknown	Blue	73.16	Patrolled T 45-79: nothing visual found
120	03.10.96	14.10	Georgedale-Venus 2	275	**u**	Unknown	White	16	Patrolled by Brian Peachey: nothing visual found
121	01.12.96	06.03	Georgedale-Illovo 2	275	**u**	Unknown	White	0	Patrolled from Georgedale - T 40: nothing visual **found**
122	01.12.96	06.08	Georgedale-Illovo 2	275	**u**	Unknown	White	7.4	Patrolled from Georgedale - T 40: nothing visual found
123	01.12.96	20.17	Ingagane-Danskraal 1	275	**u**	Unknown	White	70	Neville patrolled T 204-215: nothing visual found
124	14.08.96	17.04	Georgedale-Venus 2	275	F	Veld fire	R-W	56	Between T 167 and 168: Mpopomeni Township area
125	14.08.96	17.07	Georgedale-Venus 1	275	F	Veld fire	White	57	Between T 167 and 168: Mpopomeni Township area

APPENDIX 2: - Georgedale-Venus Performance Summary 1996-1998

	Date	Time	Line name	Cause	Phase	Line fault locators [Georgedale-Venus] km
1	20.08.96	0.51	Georgedale-Venus 1	Birds	White	53.74
2	11.01.96	08.56	Georgedale-Venus 1	Birds	Blue	64
3	11.07.97	0.54	Georgedale-Venus 1	Birds	White	117.7/23.3
4	09.05.96	1.55	Georgedale-Venus 1	Birds	White	100.4
5	09.05.96	3.25	Georgedale-Venus 1	Birds	White	101.3
6	09.05.96	4.41	Georgedale-Venus 1	Birds	White	103
7	06.05.96	4.59	Georgedale-Venus 1	Birds	White	94
8	20.01.96	09.54	Georgedale-Venus 1	Birds	White	61
9	22.04.97	5.07	Georgedale-Venus 1	Birds	Blue	94/18.56
10	29.07.96	5.51	Georgedale-Venus 1	Birds	White	106.2
11	22.08.96	6.33	Georgedale-Venus 1	Birds	White	101.4
12	04.05.97	10.35	Georgedale-Venus 1	Birds	Blue	20/121
13	10.07.97	10.55	Georgedale-Venus 1	Birds	White	16.8/124.2
14	25.01.96	12.44	Georgedale-Venus 1	Birds	White	10
15	21.06.97	16.43	Georgedale-Venus 1	Birds	White	110/18.26
16	25.01.96	16.56	Georgedale-Venus 1	Birds	White	18
17	06.06.96	18.19	Georgedale-Venus 1	Birds	White	94
18	28.07.96	22.12	Georgedale-Venus 1	Birds	White	107.7
19	20.06.97	22.25	Georgedale-Venus 1	Birds	Blue	112/14.47
20	05.03.98	9.21	Georgedale-Venus 1	Pollution	White	11
21	03.02.96	13.45	Georgedale-Venus 1	Pollution	Blue	108
22	03.09.97	20.1	Georgedale-Venus 1	Storm	R-N	45.7/95.3
23	06.03.98	20.37	Georgedale-Venus 1	Storm		
24	28.12.97	17	Georgedale-Venus 1	Storm	Blue	80/30
25	31.05.97	8.21	Georgedale-Venus 1	Unknown	White	131.6/8.8
26	08.03.98	12.01	Georgedale-Venus 1	Unknown	White	
27	14.08.96	17.07	Georgedale-Venus 1	Veld fire	White	57
28	06.05.96	1.16	Georgedale-Venus 2	Birds	White	115.8

29	07.06.96	2.47	Georgedale-Venus 2	Birds	White	94.11
30	28.05.98	3.47	Georgedale-Venus 2	Birds	White	70
31	23.05.96	6.51	Georgedale-Venus 2	Birds	White	103
32	19.11.96	7.12	Georgedale-Venus 2	Birds	White	17.19
33	07.06.96	7.31	Georgedale-Venus 2	Birds	White	83
34	15.08.97	7.36	Georgedale-Venus 2	Birds	White	7.6/133.7
35	22.03.97	8.1	Georgedale-Venus 2	Birds	White	40.07/91.5
36	19.01.96	8.24	Georgedale-Venus 2	Birds	White	6
37	21.09.97	8.59	Georgedale-Venus 2	Birds	White	3.45/137
38	25.02.96	9.09	Georgedale-Venus 2	Birds	White	55
39	21.10.96	9.32	Georgedale-Venus 2	Birds	Red	46
40	11.04.96	9.39	Georgedale-Venus 2	Birds	White	28.23
41	02.01.96	10	Georgedale-Venus 2	Birds	White	34.6
42	08.10.96	10.15	Georgedale-Venus 2	Birds	White	18.36
43	18.07.97	10.25	Georgedale-Venus 2	Birds	White	126.1/15.2
44	30.07.96	12.08	Georgedale-Venus 2	Birds	White	14
45	10.06.97	14.39	Georgedale-Venus 2	Birds	White	78.8/62.5
46	22.05.96	17.56	Georgedale-Venus 2	Birds	White	103
47	27.05.96	20.42	Georgedale-Venus 2	Birds	White	100
48	22.02.96	22.39	Georgedale-Venus 2	Birds	White	26.49
49	22.05.96	22.46	Georgedale-Venus 2	Birds	White	98.3
50	19.12.96	23.39	Georgedale-Venus 2	Birds	Red	30.6
51	19.10.96	15.11	Georgedale-Venus 2	Storm	Red	33
52	01.04.98	16.53	Georgedale-Venus 2	Storm		
53	26.01.96	17.39	Georgedale-Venus 2	Storm	Blue	45.53
54	06.11.97	18.22	Georgedale-Venus 2	Storm	Blue	45.4/91.8
55	08.10.96	18.22	Georgedale-Venus 2	Storm	B-R	58
56	31.08.97	19.1	Georgedale-Venus 2	Storm	Red	48.1/93.1
57	12.03.96	20.06	Georgedale-Venus 2	Storm	Red	72.74
58	06.03.98	20.21	Georgedale-Venus 2	Storm		
59	08.07.96	21.04	Georgedale-Venus 2	Storm	Red	99.94
60	25.06.96	21.1	Georgedale-Venus 2	Storm	Red	71
61	26.10.96	21.46	Georgedale-Venus 2	Storm	White	44.14
62	13.04.96	5.45	Georgedale-Venus 2	Unknown	White	44
63	22.07.97	11.09	Georgedale-Venus 2	Unknown	White	124/16

64	03.10.96	14.1	Georgedale-Venus 2	Unknown	White	16
65	09.07.97	15.32	Georgedale-Venus 2	Unknown	Blue	84/?
66	01.08.96	17.07	Georgedale-Venus 2	Unknown	White	18
67	24.05.96	20.57	Georgedale-Venus 2	Unknown	White	27
68	14.08.96	17.04	Georgedale-Venus 2	Veld fire	R-W	56

	Jan	Feb	Mar	Apr	May	Jun	Jul	Aug	Sep	Oct	Nov	Dec
Number of trips	6	3	3	3	13	6	8	4	1	3	1	1
Ave min temperature ^{U}C - Cedara	15.5	15.5	13.8	10.5	6.8	3.7	3	5.8	9.1	11.6	12.5	14.3
Ave max temperature ^{U}C - Cedara	24.5	25.3	24	22.3	20	19	17	20	22	21.9	22.8	25.4
	Jan	Feb	Mar	Apr	May	Jun	Jul	Aug	Sep	Oct	Nov	Dec
Number of trips	6	3	3	3	13	6	8	4	1	3	1	1
Ave min. temperature ^{U}C - Estcourt	15.9	16.1	14.3	10.3	6	2.3	2.5	5.2	9.4	11.7	12.8	14.9
Ave max temperature ^{U}C - Estcourt	26.7	26.8	25	22.7	20	19	17	21	24	23.6	24.7	27.1
	Jan	Feb	Mar	Apr	May	Jun	Jul	Aug	Sep	Oct	Nov	Dec
Number of trips	6	3	3	3	13	6	8	4	1	3	1	1
Rainfall mm - Cedara	161	132	113	63	64	34	78	17	18	91	99	97
Rainfall mm - Estcourt	226	135	151	47	30	29	48	20	34	101	99	170
	Jan	Feb	Mar	Apr	May	Jun	Jul	Aug	Sep	Oct	Nov	Dec
Number of trips	6	3	3	3	13	6	8	4	1	3	1	1
Average humidity % - Cedara - 08:00	83	86	87	85	80	74	81	75	77	77	77	80
Average humidity % - Cedara - 20:00	93	92	91	89	91	72	80	78	81	89	89	92
Average humidity % - Cedara -14:00	71	68	66	58	49	40	47	41	50	63	68	65

Table 2: Weather data correlated with fault performance

APPENDIX 3: Suspected Bird Streamer Faults 1993-1998

1	19.06.93	0.04	Georgedale-Venus 1	Pollution		
2	28.07.95	0.28	Georgedale-Venus 2	Birds		105
3	20.08.96	0.51	Georgedale-Venus 1	Birds	White	53.74
4	11.07.97	0.54	Georgedale-Venus 1	Birds	White	117.7/23.3
5	19.06.94	1.06	Georgedale-Venus 2	Unknown		95
6	06.05.96	1.16	Georgedale-Venus 2	Birds	White	115.8
7	17.09.93	1.23	Georgedale-Venus 1	Birds		7
8	09.05.96	1.55	Georgedale-Venus 1	Birds	White	100.4
9	07.06.96	2.47	Georgedale-Venus 2	Birds	White	94.11
10	16.04.93	3.12	Georgedale-Venus 2	Pollution		50
11	09.05.96	3.25	Georgedale-Venus 1	Birds	White	101.3
12	20.06.94	3.57	Georgedale-Venus 1	Unknown		0
13	13.12.94	4.22	Georgedale-Venus 1	Unknown		28
14	27.12.95	4.25	Georgedale-Venus 2	Birds		22.14
15	03.05.93	4.3	Georgedale-Venus 1	Birds		
16	01.08.94	4.3	Georgedale-Venus 2	Birds		0
17	26.11.95	4.31	Georgedale-Venus 1	Pollution		44.1
18	02.08.94	4.36	Georgedale-Venus 1	Birds		21
19	09.05.96	4.41	Georgedale-Venus 1	Birds	White	103
20	09.05.93	4.48	Georgedale-Venus 1	Pollution		
21	06.05.96	4.59	Georgedale-Venus 1	Birds	White	94
22	22.04.97	5.07	Georgedale-Venus 1	Birds	Blue	
23	01.08.94	5.11	Georgedale-Venus 2	Birds		96
24	21.11.95	5.4	Georgedale-Venus 2	Pollution		5.3
25	13.04.96	5.45	Georgedale-Venus 2	Unknown	White	44
26	29.07.96	5.51	Georgedale-Venus 1	Birds	White	106.2
27	20.06.94	6.07	Georgedale-Venus 1	Unknown		94
28	22.08.96	6.33	Georgedale-Venus 1	Birds	White	101.4
29	18.04.94	6.43	Georgedale-Venus 1	Birds		44
30	11.09.94	6.47	Georgedale-Venus 2	Birds		102
31	23.05.96	6.51	Georgedale-Venus 2	Birds	White	103
32	19.11.96	7.12	Georgedale-Venus 2	Birds	White	17.19

33	07.06.96	7.31	Georgedale-Venus 2	Birds	White	83
34	15.08.97	7.36	Georgedale-Venus 2	Birds	White	7.6/133.7
35	27.12.95	7.45	Georgedale-Venus 2	Birds		53.05
36	22.03.97	8.1	Georgedale-Venus 2	Birds	White	40.07/91.5
37	31.05.97	8.21	Georgedale-Venus 1	Unknown	White	131.6/8.8
38	06.02.94	8.23	Georgedale-Venus 1	Pollution		40
39	19.01.96	8.24	Georgedale-Venus 2	Birds	White	6
40	16.12.95	8.44	Georgedale-Venus 2	Birds		25.19
41	21.09.97	8.59	Georgedale-Venus 2	Birds	White	3.45/137
42	25.02.96	9.09	Georgedale-Venus 2	Birds	White	55
43	21.10.96	9.32	Georgedale-Venus 2	Birds	Red	46
44	10.10.94	9.34	Georgedale-Venus 2	Birds		67
45	11.04.96	9.39	Georgedale-Venus 2	Birds	White	28.23
46	02.01.96	10	Georgedale-Venus 2	Birds	White	34.6
47	08.10.96	10.15	Georgedale-Venus 2	Birds	White	18.36
48	18.07.97	10.25	Georgedale-Venus 2	Birds	White	126.1/15.2
49	04.05.97	10.35	Georgedale-Venus 1	Birds	Blue	20/121
50	10.07.97	10.55	Georgedale-Venus 1	Birds	White	16.8/124.2
51	22.07.97	11.09	Georgedale-Venus 2	Unknown	White	124/16
52	30.07.96	12.08	Georgedale-Venus 2	Birds	White	14
53	09.08.95	12.25	Georgedale-Venus 2	Birds		12
54	25.01.96	12.44	Georgedale-Venus 1	Birds	White	10
55	03.02.96	13.45	Georgedale-Venus 1	Pollution	Blue	108
56	03.10.96	14.1	Georgedale-Venus 2	Unknown	White	16
57	24.11.95	14.14	Georgedale-Venus 2	Pollution		6.53
58	10.06.97	14.39	Georgedale-Venus 2	Birds	White	78.8/62.5
59	09.07.97	15.32	Georgedale-Venus 2	Unknown	Blue	84/?
60	04.08.94	16.29	Georgedale-Venus 2	Birds		97
61	21.06.97	16.43	Georgedale-Venus 1	Birds	White	110/18.26
62	25.01.96	16.56	Georgedale-Venus 1	Birds	White	18
63	01.08.96	17.07	Georgedale-Venus 2	Unknown	White	18
64	16.12.95	17.36	Georgedale-Venus 2	Pollution		44.43
65	19.09.95	17.56	Georgedale-Venus 2	Birds		134.3
66	22.05.96	17.56	Georgedale-Venus 2	Birds	White	103
67	02.05.93	18.13	Georgedale-Venus 1	Pollution		

68	06.06.96	18.19	Georgedale-Venus 1	Birds	White	94
69	14.04.95	18.22	Georgedale-Venus 2	Unknown		10
70	19.12.95	18.53	Georgedale-Venus 1	Birds		91.52
71	03.09.93	19.29	Georgedale-Venus 2	Birds		0
72	19.06.94	19.49	Georgedale-Venus 1	Unknown		0
73	26.04.94	20.19	Georgedale-Venus 2	Birds		98
74	06.06.95	20.42	Georgedale-Venus 1	Birds		2
75	27.05.96	20.42	Georgedale-Venus 2	Birds	White	100
76	24.05.96	20.57	Georgedale-Venus 2	Unknown	White	27
77	17.11.95	21.04	Georgedale-Venus 1	Pollution		25.43
78	18.04.94	21.17	Georgedale-Venus 2	Birds		51
79	24.05.94	21.18	Georgedale-Venus 2	Unknown		96
80	21.12.95	21.3	Georgedale-Venus 2	Birds		38
81	26.04.93	21.44	Georgedale-Venus 1	Pollution		101
82	28.07.96	22.12	Georgedale-Venus 1	Birds	White	107.7
83	20.06.97	22.25	Georgedale-Venus 1	Birds	Blue	112/14.47
84	22.02.96	22.39	Georgedale-Venus 2	Birds	White	26.49
85	22.05.96	22.46	Georgedale-Venus 2	Birds	White	98.3
86	10.10.93	23.26	Georgedale-Venus 1	Pollution		39
87	09.10.94	23.35	Georgedale-Venus 2	Birds		42
88	19.12.96	23.39	Georgedale-Venus 2	Birds	Red	30.6
89	11.01.96	08.56	Georgedale-Venus 1	Birds	Blue	64
90	20.01.96	09.54	Georgedale-Venus 1	Birds	White	61

APPENDIX 4: AC Voltage Flashover Results

1. Rod-plane breakdown characteristics - effects of electrode tip and rod diameter

3 mm rod diameter, with a flat cut electrode tip

Air gap length [mm]	Breakdown voltage [kV]	Standard deviation [kV]	Corrected breakdown voltage [kV]
50	31.48	0.86	31.59
100	50.82	0.16	51.05
150	76.89	0.86	77.23
200	97.23	1.78	97.67
250	108.72	1.74	109.06
300	118.24	4.85	118.51
350	124.43	0.81	124.68
400	139.08	0.71	139.36
450	157.42	1.66	157.73
500	180.68	1.3	181.04
600	210.04	1.67	210.46

T = 20.7°C; P = 754 mmHg, RH = 66.7%; source resistance = 300 kfi

3 mm rod diameter, point electrode tip

Air gap length [mm]	Breakdown voltage [kV]	Standard deviation [kV]	Corrected breakdown voltage [kV]
50	25.08	0.13	25.25
100	41.86	0.21	42.06
200	74.97	0.89	75.17
300	106.77	0.37	107.06
400	137.96	0.96	138.33
500	178.28	1.33	178.76
*600	354.29	3.77	218.62

T = 20.7 °C; RH = 67.2%; P = 756 mmHg; *T = 20.5 °C; RH = 70.5%; P = 756 mmHg

3 mm rod diameter, parabola electrode tip

Air gap length [mm]	Breakdown voltage [kV]	Standard deviation [kV]	Corrected breakdown voltage [kV]
50	45.43	1.06	45.42
100	59.57	0.74	60
200	77.85	0.49	78.11
300	110.01	0.73	110.3
400	144.8	0.65	145.2
500	183.3	0.79	183.8
600	217.91	2.1	218.5

T = 20.5 °C; RH = 70.5%; P = 756 mmHg

12 mm rod diameter, sharp point electrode tip

Air gap length [mm]	Breakdown voltage [kV]	Standard deviation [kV]	Corrected breakdown voltage [kV]
50	22.67	0.54	22.72
100	38.85	0.34	38.91
200	77.24	0.66	77.36
300	107.94	0.87	108.09
400	142.05	0.82	142.23
500	183.90	1.48	184.14
600	213.24	1.43	213.52

T = 20.7 °C; RH = 67.1%; P = 753 mmHg

12 mm rod diameter, flat cut electrode tip

Air gap length [mm]	Breakdown voltage [kV]	Standard deviation [kV]	Corrected breakdown voltage [kV]
50	33.99	0.59	34.04
100	56.76	0.96	56.90
150	91.29	0.79	91.51
200	126.4	1.66	126.58
250	174.72	10.17	174.36
300	228.19	10.34	227.32

T = 20.7 °C; RH = 67.1%; P = 753 mmHg

12 mm rod diameter, parabola electrode tip

Air gap length [mm]	Breakdown voltage [kV]	Standard deviation [kV]	Corrected breakdown voltage [kV]
50	25.62	0.68	25.67
100	51.51	1.1	51.59
200	77.03	0.76	78.94
300	107.94	0.31	108.02
400	141.63	0.66	141.74
500	183.04	0.93	183.17
600	211.96	1.32	212.1

T = 20.6 °C; RH = 67.2%, P = 752 mmHg

6 mm rod diameter, point electrode

Air gap length [mm]	Breakdown voltage [kV]	Standard deviation [kV]	Corrected breakdown voltage [kV]
50	23.47	0.42	23.49
100	39.82	0.58	39.84
200	77.36	0.68	77.39
300	108.72	1.14	108.75
400	140.93	0.87	140.97
600	209.65	1.49	209.71

T = 20.7 °C; RH = 67.5%; P = 751 mmHg

6 mm rod diameter, parabola electrode tip

Air gap length [mm]	Breakdown voltage [kV]	Standard deviation [kV]	Corrected breakdown voltage [kV]
50	37.72	1.87	37.50
100	51.61	1.09	51.65
200	77.81	0.78	77.84
400	142.07	1.35	142.11
600	210.03	1.36	210.09

T = 20.7 °C; RH = 67.5%; P = 751 mmHg

2. Effects of corona rings on breakdown characteristics

275 kV silicone composite insulator, I string with corona ring

Air gap length [mm]	Breakdown voltage [kV]	Standard deviation [kV]	Corrected breakdown voltage [kVJ
50	42.95	1.6	42.37
100	52.43	5.9	51.20
150	68.92	2.5	67.72
200	93.05	3.0	92.17
300	121.05	2.4	119.84
400	166.90	2.0	165.23
450	195.20	1.6	193.25

T = 21.7°C; RH = 55.7%, P = 754mmHg

275 kV silicone composite insulator, I string with no corona ring

Air gap length [mm]	Breakdown voltage [kV]	Standard deviation [kV]	Corrected breakdown voltage [kV]
50	33.05	2.5	32.52
100	63.82	4.5	63.18
150	80.82	0.7	80.01
200	90.36	0.8	89.45
300	116.62	0.5	115.45
400	156.2	1.5	154.64
450	176.72	1.5	174.95

T = 21.7 °C; RH = 55.7%; P = 754 mmHg

3. Effect of electrode position on air gap breakdown, using a V string silicone composite insulator assembly with corona rings

Brass electrode centre of V string, vertical plane air gap breakdown

Air gap length [mm]	Breakdown voltage [kV]	Standard deviation [kV]	Corrected breakdown voltage [kV]
100	58.46	2.4	59.01
200	94.46	1.4	95.26
300	123.90	2.7	124.60
400	162.26	1.4	163.10
450	192.53	7.4	193.61

T = 23.9 °C; RH = 55.7%; P = 755 mmHg

Brass electrode placed across string 2, composite insulators with corona rings

Air gap length [mm]	Breakdown voltage [kV]	Standard deviation [kV]	Corrected breakdown voltage [kV]
100	36.10	1.3	36.24
200	89.15	2.5	89.74
400	159.28	1.4	160.03

T = 23.9 °C; RH = 55.7%; P = 755 mmHg

Brass electrode moved horizontally away from V string configuration (silicone composite insulators) level with corona rings

Air gap length [mm]	Breakdown voltage [kV]	Standard deviation [kV]	Corrected breakdown voltage [kV]
100	70.57	0.8	70.40
200	107.18	0.9	108.19
400	163.49	1.8	164.31

T = 23.9 °C; RH = 55.7%; P = 755 mmHg

4. Effect of electrode position on air gap breakdown, using glass I string, with 16 U120 BS insulator assembly

Brass electrode, in the vertical plane, with a glass I string

Air gap length [mm]	Breakdown voltage [kV]	Standard deviation [kV]	Corrected breakdown voltage [kV]
100	44.06	2.3	44.39
200	85.23	1.8	85.71
300	111.57	1.8	112.62
400	155.39	2.3	156.12
450	175.39	2.6	176.21
500	191.28	1.3	192.18

T = 21.6 °C; RH = 60.3%; P = 749 mmHg

Brass electrode, in the horizontal plane, glass I string insulator assembly

Air gap length [mm]	Breakdown voltage [kV]	Standard deviation [kV]	Corrected breakdown voltage [kV]
140	68.56	1.9	69.20
195	86.77	2.5	87.42
330	124.68	1.5	125.15
430	160.37	1.9	160.96

T = 21.6°C; RH = 60.3%; P = 749 mmHg

5. Effect of electrode position on air gap breakdown, using an I string silicone composite insulator assembly with corona rings

Brass electrode moved away in the horizontal plane

Air gap length [mm]	Breakdown voltage [kV]	Standard deviation [kV]	Corrected breakdown voltage [kV]
150	73.29	10.64	73.98
183	101.85	1.3	102.81
295	142.47	1.1	143.67
365	168.19	1.9	169.45
425	185.36	1.3	186.40

T = 21.6°C; RH = 60.3%; P - 749 mmHg

275 kV silicone composite insulator, I string with corona ring, brass electrode moved in the vertical plane

Air gap length [mm]	Breakdown voltage [kV]	Standard deviation [kV]	Corrected breakdown voltage [kV]
50	42.95	1.6	42.37
100	52.43	5.9	51.20
150	68.92	2.5	67.72
200	93.05	3.0	92.17
300	121.05	2.4	119.84
400	166.90	2.0	165.23
450	195.20	1.6	193.25

T = 21.7°C; RH = 55.7%; P = 754 mmHg

6. Effect of electrode position on air gap breakdown, using a V string glass insulator assembly with 16 discs per string

Brass electrode, air gap breakdown in centre of V string, in the vertical plane - no corona rings

Air gap length [mm]	Breakdown voltage [kV]	Standard deviation [kV]	Corrected breakdown voltage [kV]
100	63.26	2.8	64.51
200	92.93	0.6	94.58
300	115.88	0.8	117.02
400	'152.43	2.4	153.14
445	*170.99	4.2	171.63
500	193.23	1.2	193.9

*T = 22.0 °C; RH = 55.0%; P = 749 mmHg
T - 21.6 °C, RH = 64.9%; P = 755 mmHg

Brass electrode, air gap breakdown in the horizontal plane

Air gap length [mm]	Breakdown voltage [kV]	Standard deviation [kV]	Corrected breakdown voltage [kV]
105	46.56	0.3	47.29
200	100.49	1.8	102.47
300	114.03	2.8	114.92
405	161.75	4.2	163.01
500	201.30	2.0	202.87

T = 21.6 °C; RH = 64.9%; P = 755 mmHg

Brass electrode placed on the metal end caps of the V string

Air gap length [mm]	Breakdown voltage [kV]	Standard deviation [kV]	Corrected breakdown voltage [kV]
220 - 1 disc	72.49	3.1	72.92
370-2 disc	134.46	0.6	135.51
450 - 3 disc	189.11	1.4	189.99

T = 21.6 °C; RH = 64.9%; P = 755 mmHg

Brass electrode moved horizontally away, but air gap is now between the electrode and the side of the yoke plate

Air gap length [mm]	Breakdown voltage [kV]	Standard deviation [kV]	Corrected breakdown voltage [kV]
120	61.54	0.8	62.75
240	100.93	0.7	101.92
480	163.08	2.3	163.68

T = 21.6 °C; RH = 64.9%; P = 755 mmHg

7. Effect of wet string resistivity on air gap breakdown, using a V string glass insulator assembly

Air gap length [mm]	Streamer resistivity [kQ.m^{-1}] NaCl solution	Breakdown voltage [kV]	Standard deviation [kV]	Corrected breakdown voltage [kV]
400	40	196.1	2.7	194.01
400	10 000	*192	5.5	195.9

*T = 19.7 °C; RH = 85.3%; P = 755 mmHg
T = 21.8 °C; RH = 62.7%; P = 755 mmHg

8. Effects of wet string electrode on air gap breakdown, using a V string glass assembly

Air gap length [mm]	Streamer resistivity [kQ.m^{-1}] NaCl solution	Breakdown voltage [kV]	Standard deviation [kV]	Corrected breakdown voltage [kV]
200	100	101.5	3.8	101.6
400	40	196.1	2.7	194.0

T = 21.8 °C; RH = 62.7%; P = 755 mmHg

9. Effects of wet string electrode on air gap breakdown, using a V string silicone composite insulator assembly with corona rings

Air gap length [mm]	Streamer resistivity [kQ.m^{-1}] NaCl solution	Breakdown voltage [kV]	Standard deviation [kV]	Corrected breakdown voltage [kV]
200	200	114.98	5.7	118.2
400	400	217.7	2.3	223.8

T = 20.3°C; RH = 81.1%, P = 752 mmHg

10. Effects of wet string electrode on air gap breakdown, using an I string silicone composite insulator assembly with corona ring

Air gap length [mm]	Streamer resistivity [kQ.m^{-1}] NaCl solution	Breakdown voltage [kV]	Standard deviation [kV]	Corrected breakdown voltage [kV]
200	500	113.3	10.1	114.9
400	200	169.03	5.2	170.2

T - 19.8 °C; RH = 68.4%; P = 756 mmHg

11. Effect of wet string electrode on air gap breakdown, using an I string glass insulator assembly

Air gap length [mm]	Streamer resistivity [kQ.m"^{1}] NaCl solution.	Breakdown voltage [kV]		Corrected breakdown voltage [kV]
200	350	93.23	2.3	94.4
400	350	162.03	5.8	163.5

T = 19.8 °C; RH = 68.4%; P = 756 mmHg

BIRD STREAMERS

IMPACT QUALITY OF SUPPLY

Immalure Martial Cagb

Tawny Eagle

What is a Bird Streamer and how does it cause Line Faults?

White Stork

Tonowbiiwd Sforic

Bird streamers is a continuous conductive excretement.

Active Vulture Restaurant

Photograi phi Johon Kn-sbel

Bald Ibis

Experiments at the CSIR have confirmed that if a bird streamer bridges power line air gap clearances. fkuhoversda result.

Grey Heron

Hadnjalbl.ontow.rloa

Lappetfaced Vulture

Martiol Eagh

Burn mark analysis

Bird slfeamer **faults** can be identified by bum **mark** analysis.

Flashover on strain tower

1. Burn marks on strain jumper

2. Bum marks on strain tower

Whitebacked Vulture

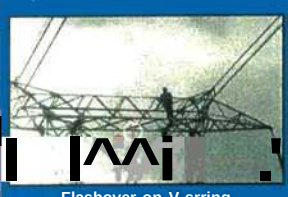

Flashover on V-srring

1. Burn marks on corona ring

2. Burn marks on tower

Vulture perched next to welded rod bird guards

Flashover on glass **V-string**

1. Burn marks on glass disc

2. Burn marks on tower

Spurwinged Goose

Egyptian Geese

Flashover on I-string

Burn mark on tower top of I-string, suspension tower

Burn mark on I-string

VuUurMonlmMr

ESKOM

POWiH POOL * STS-

TtMOK

VBkV

TSI

•OOUIUNI

wornnNo

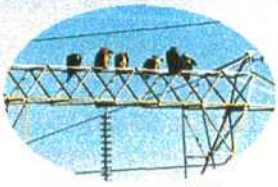

VJhjrM pvdml on tower

Crowmd Crnrx

tlaclc Eogl.

FOR SOLUTIONS TO BIRD STREAMERS PHONE TOLLFREE: 0800 111 535